ÖAW AUSTRIAN ACADEMY OF SCIENCES

SMI – STEFAN MEYER INSTITUTE

X-RAY AND (GAMMA-RAY) DETECTOR SYSTEMS FOR HIGH PRECISION MEASUREMENTS

- Motivation
- Silicon Drift Detectors – Kaonic hydrogen mesurement
- Transition Edge Sensors – Kaonic helium, charged kaon mass

Johann Zmeskal
SMI, ÖAW
Vienna, Austria

LNGS SEMINARS
November 23, 2016

WWW.OEAW.AC.AT/SMI

Motivation

Exotic (kaonic) atoms – probes for strong interaction

- hadronic shift ε_{1s} and width Γ_{1s} directly observable
- experimental study of low energy QCD
- testing chiral symmetry breaking in systems with strangeness

Kaonic hydrogen

- <u>scattering lengths</u>, no extrapolation to zero energy
- precise experimental data:

K^-p (K^-He) → SIDDHARTA

K^-d measurement is urgently needed

- **determination of the isospin dependent $\bar{K}N$ scattering lengths**

Low-energy $\bar{K}$-N systems

- Chiral perturbation theory, which was developed for πp, ππ is **not** applicable for $\bar{K}$-N systems

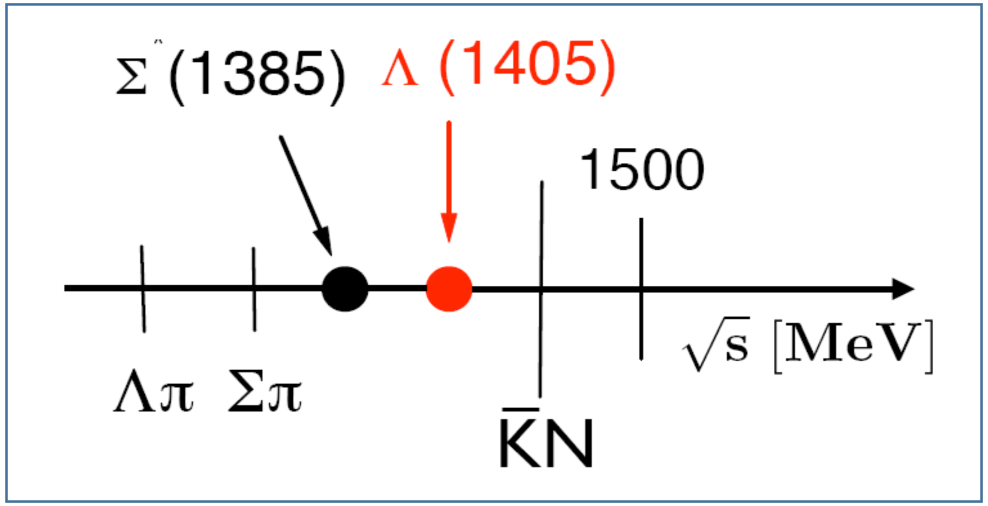

Non-perturbative coupled channels approach based on **chiral SU(3) dynamics**

Forming "exotic" atoms

"normal" hydrogen

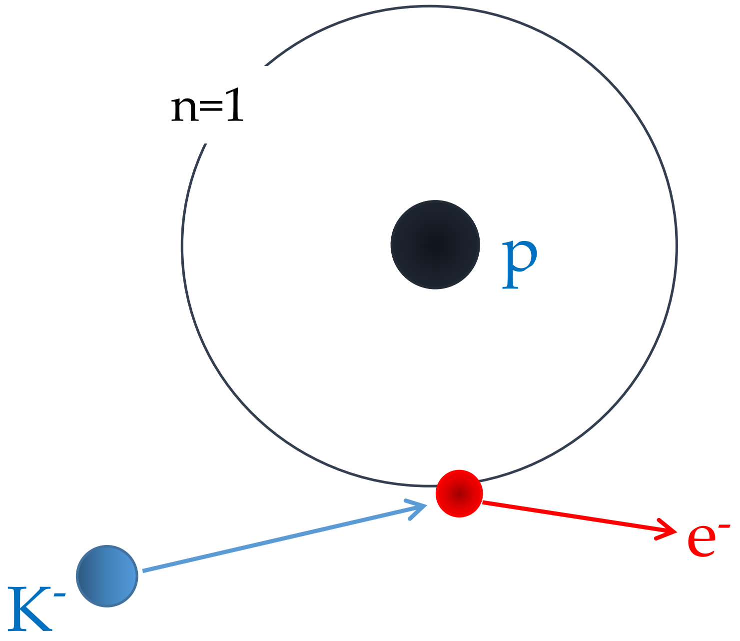

"exotic" (kaonic) hydrogen

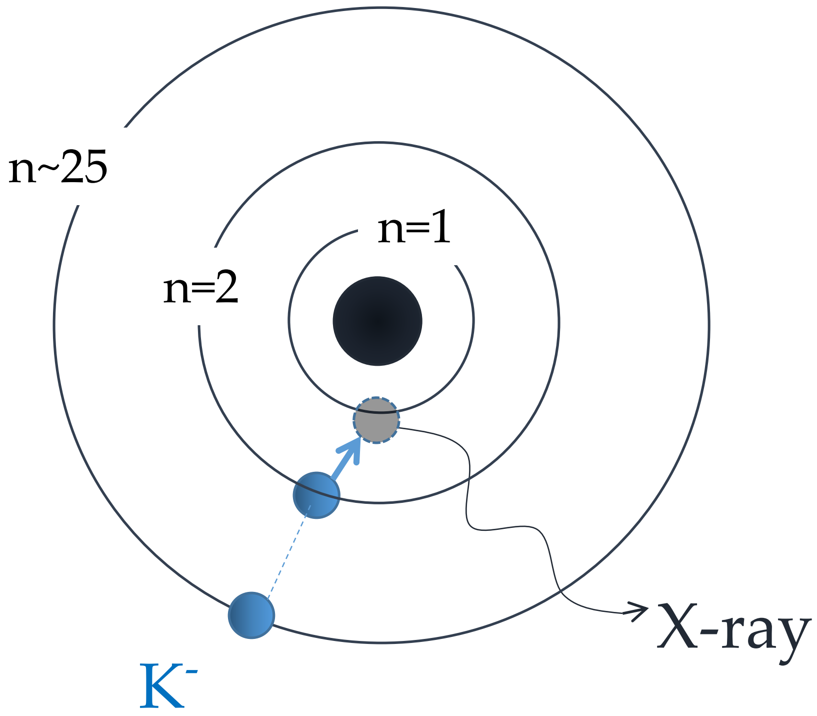

$$n \approx \sqrt{\frac{m_{\text{red}}}{m_e}} \cdot n_e$$

$2p \rightarrow 1s$
K_α transition

X-ray transitions to the 1s state

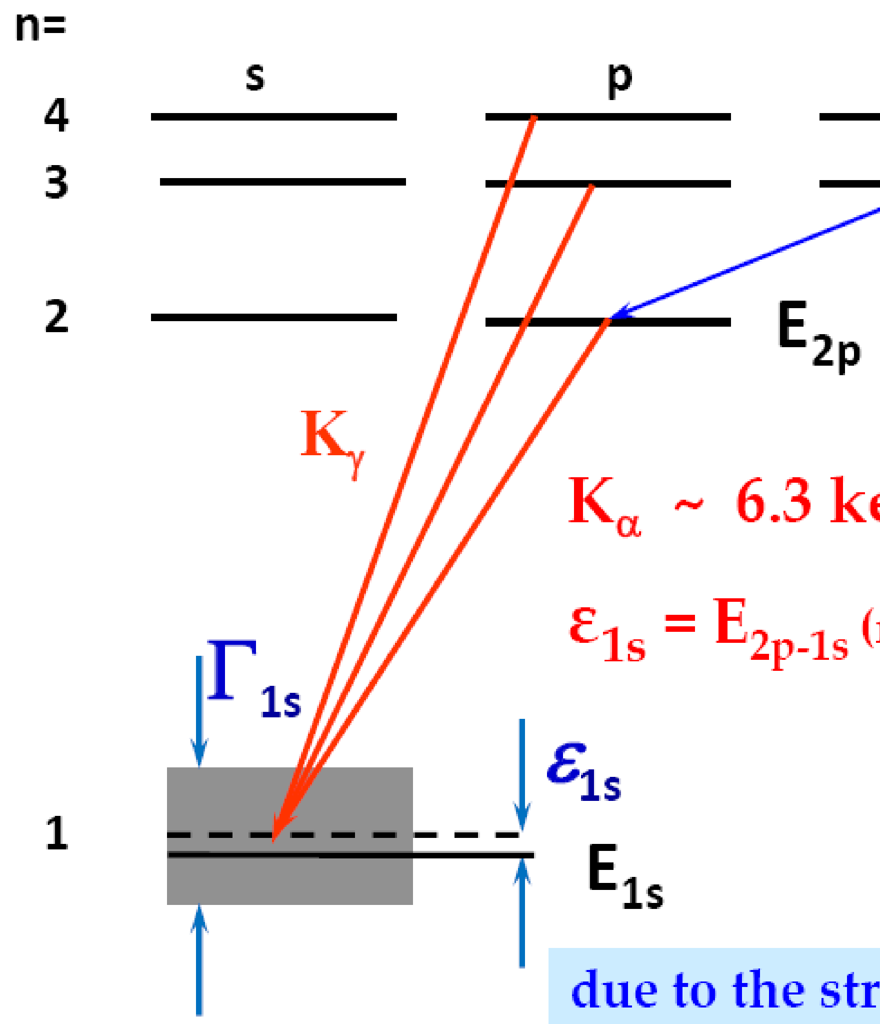

shift and width of states $n > 1$ are negligible

K_α ~ 6.3 keV

$\varepsilon_{1s} = E_{2p\text{-}1s}\,(\text{meas.}) - E_{2p\text{-}1s}\,(\text{e.m.})$

due to the strong interaction kaon-proton the 1s level is shifted and broadened

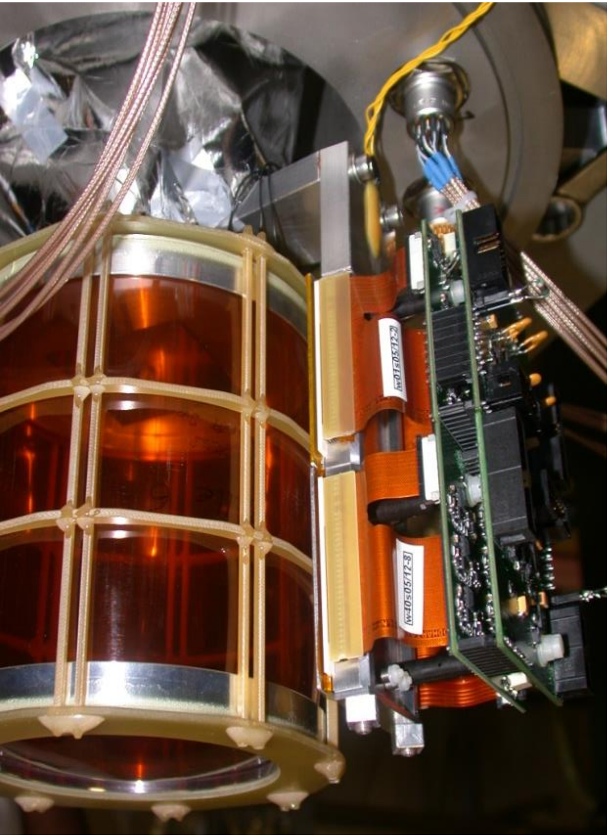

Development of large area Silicon Drift Detectors

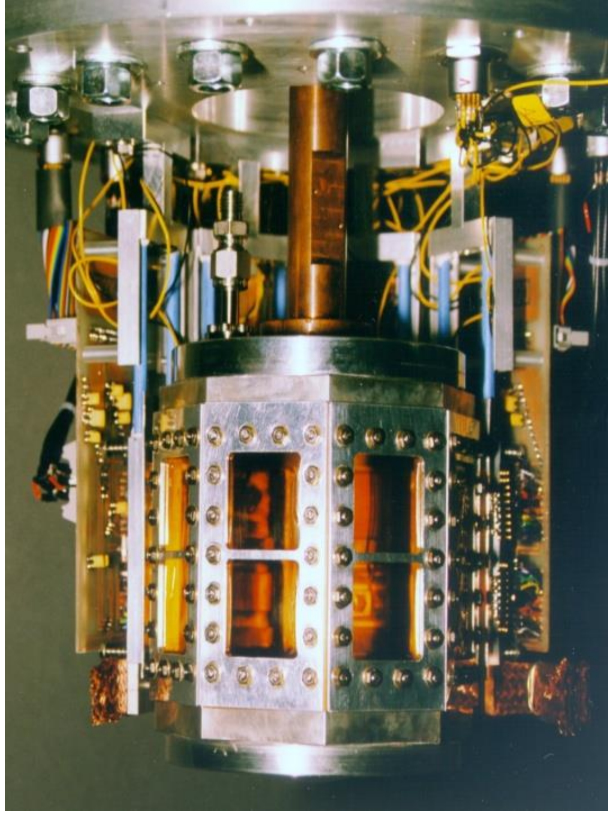

for precision X-ray spectroscopy

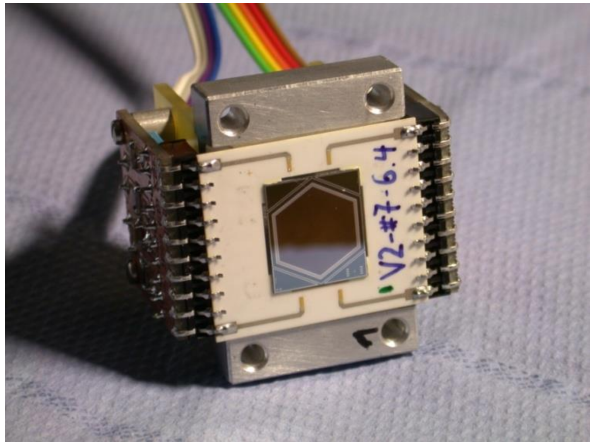

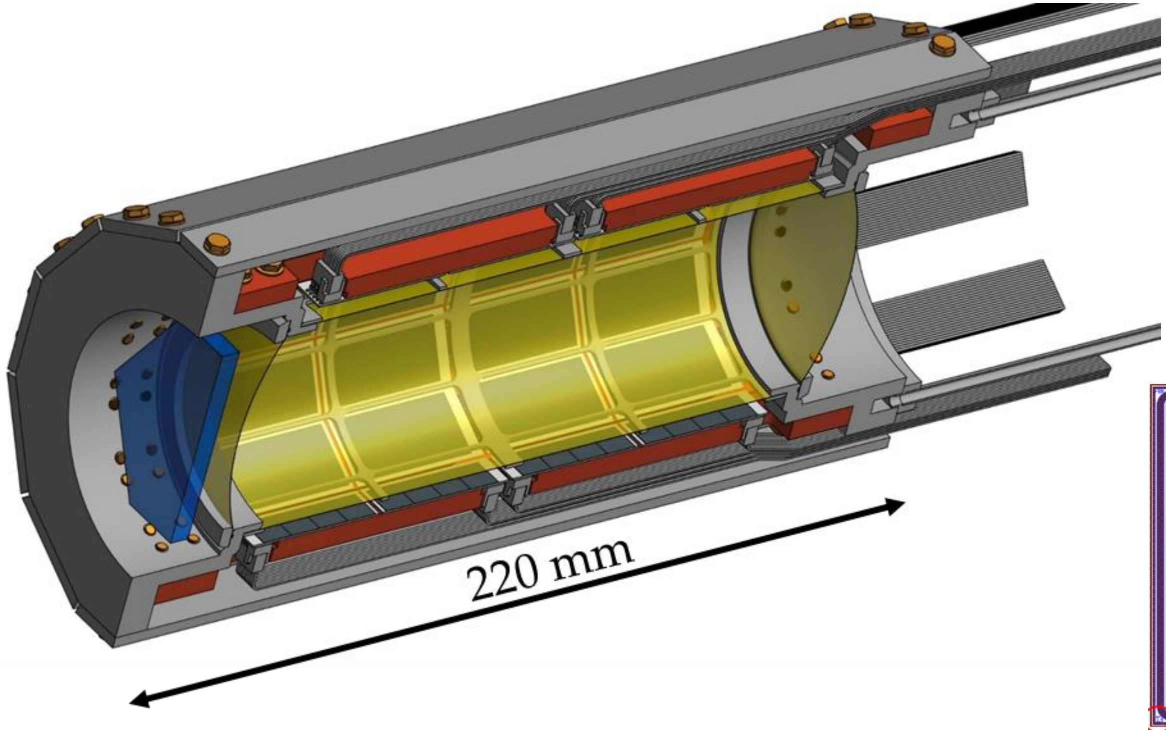

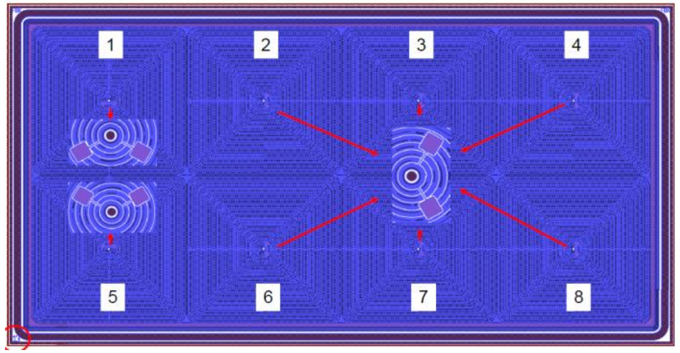

Sideward depletion structure

Emilio Gatti and Pavel Rehak, 1983

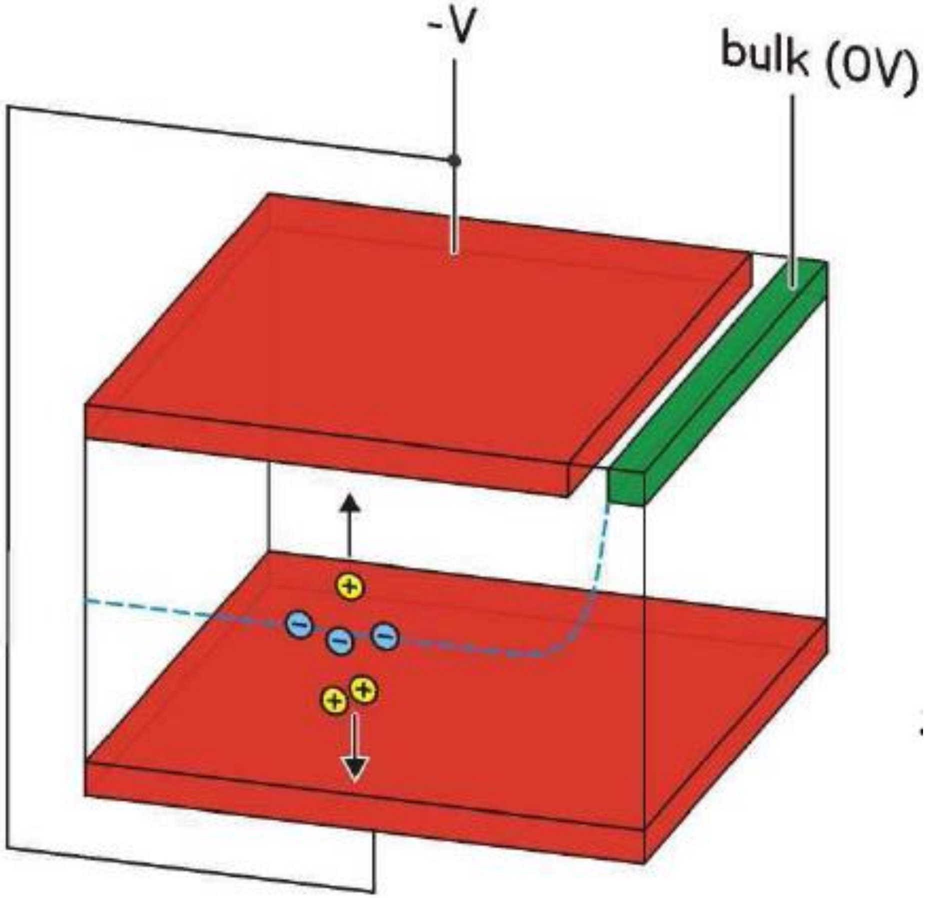

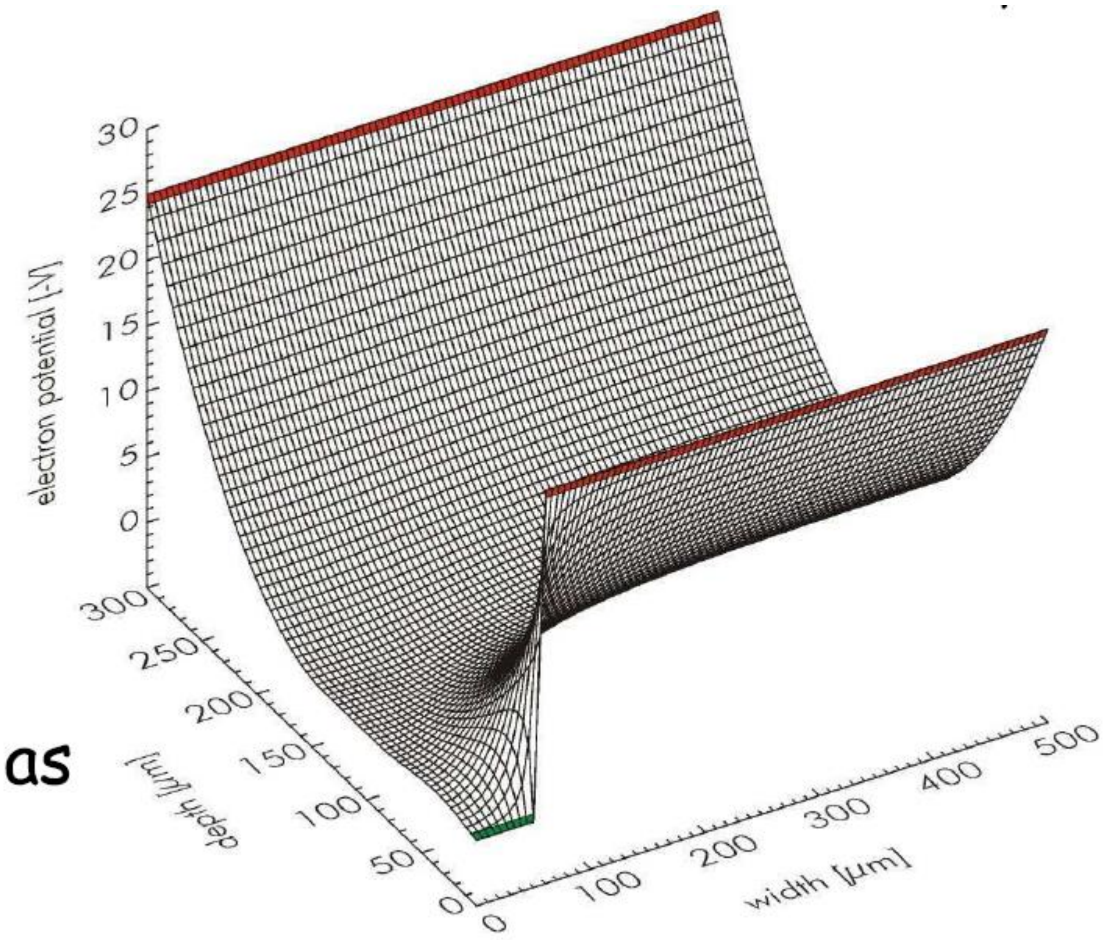

as

Silicon Drift Detector for X-rays

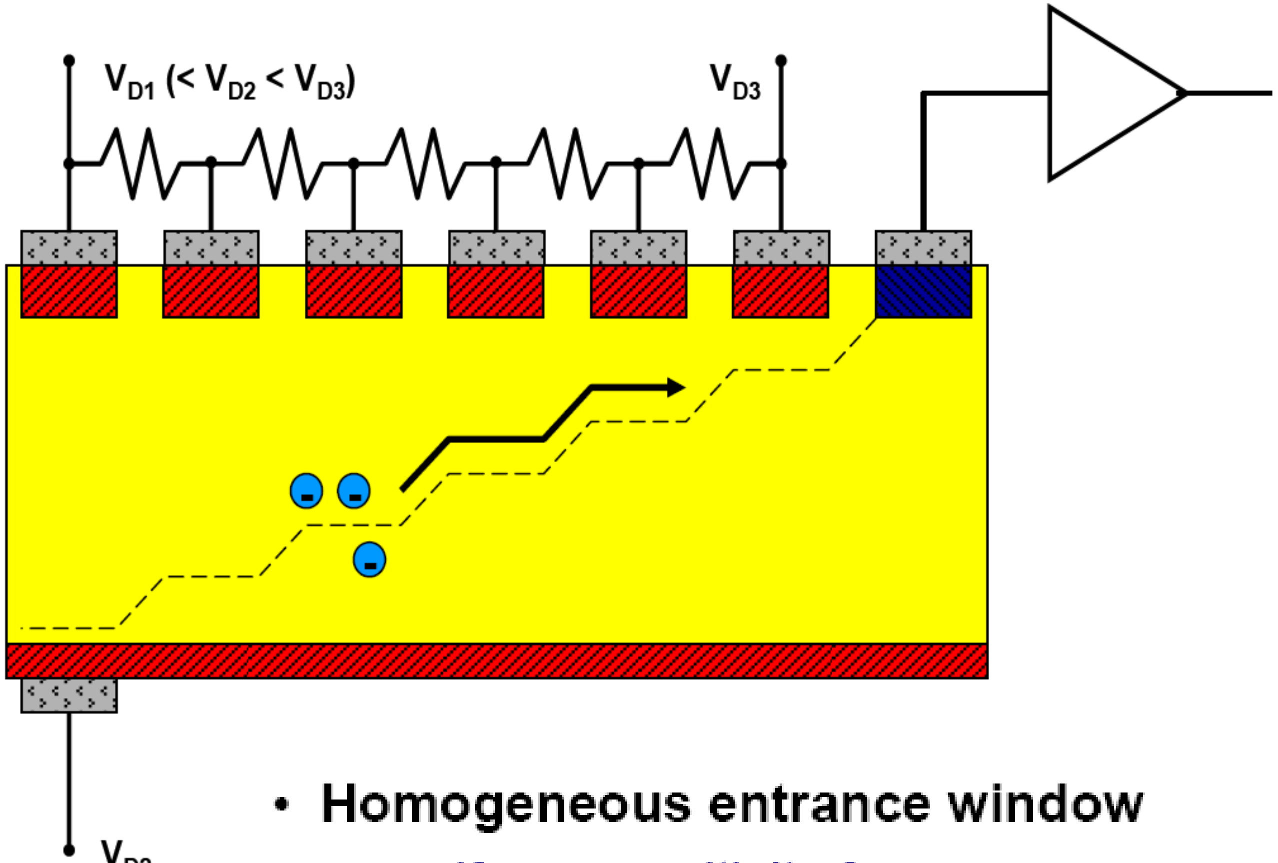

Electron potential

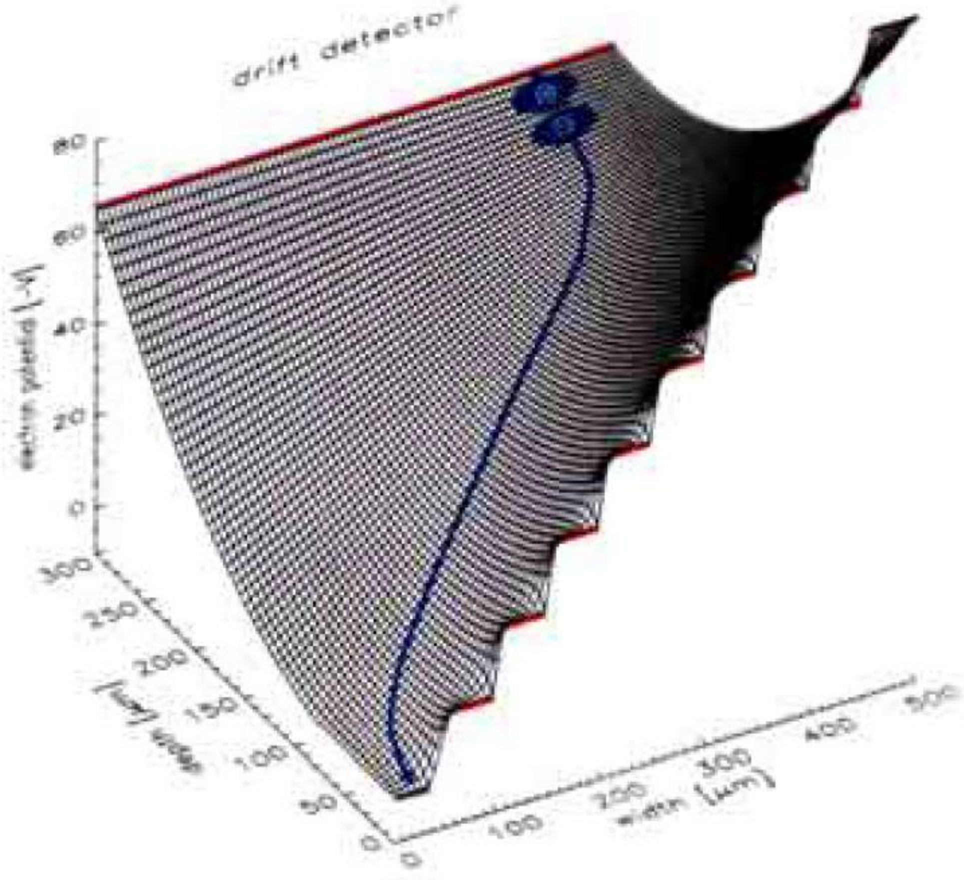

- **Homogeneous entrance window**

  uniform sensitivity for x-rays
- **Drift electrodes only at one side**

  simpler technology
- **Sloped potential valley**

Silicon Drift Detector (SDD)

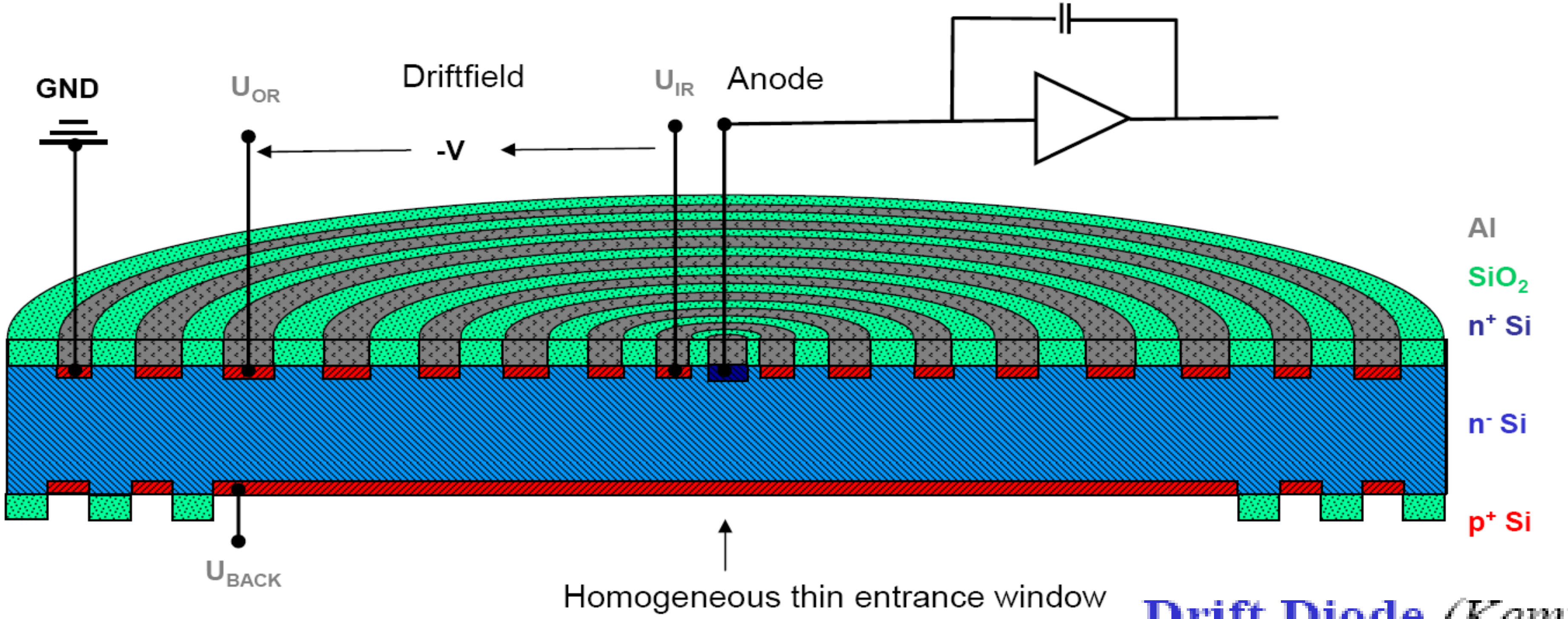

Drift Diode *(Kemmer+Lutz 1987)*

- **Single sided structured**
- **Point anode ⇒ small capacitance, small electronic noise**
- **Thin, homogeneous radiation entrance window**

Silicon Drift Detector (SDD) with integrated FET

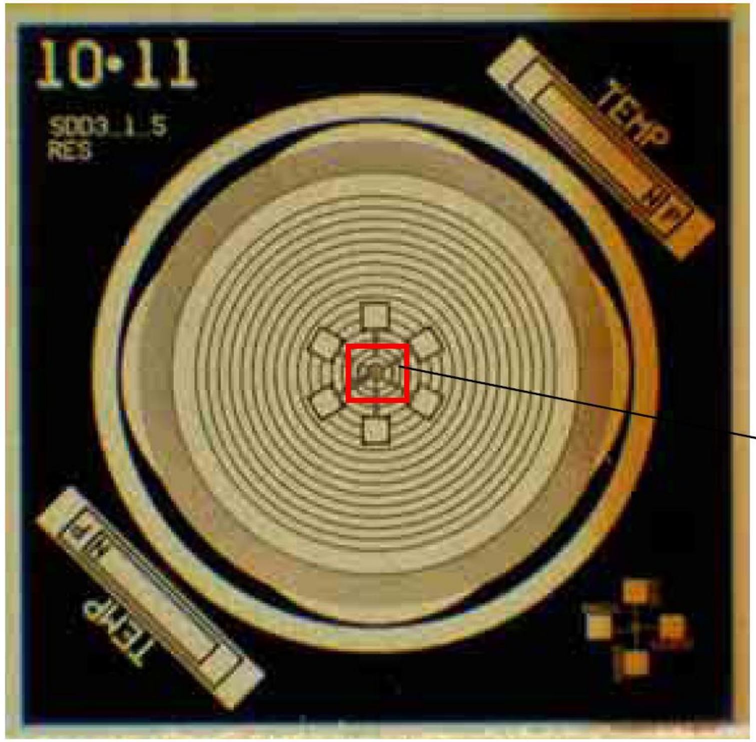

Center part of SDD

Development of large area SDDs
EU-programme HadronPhysics

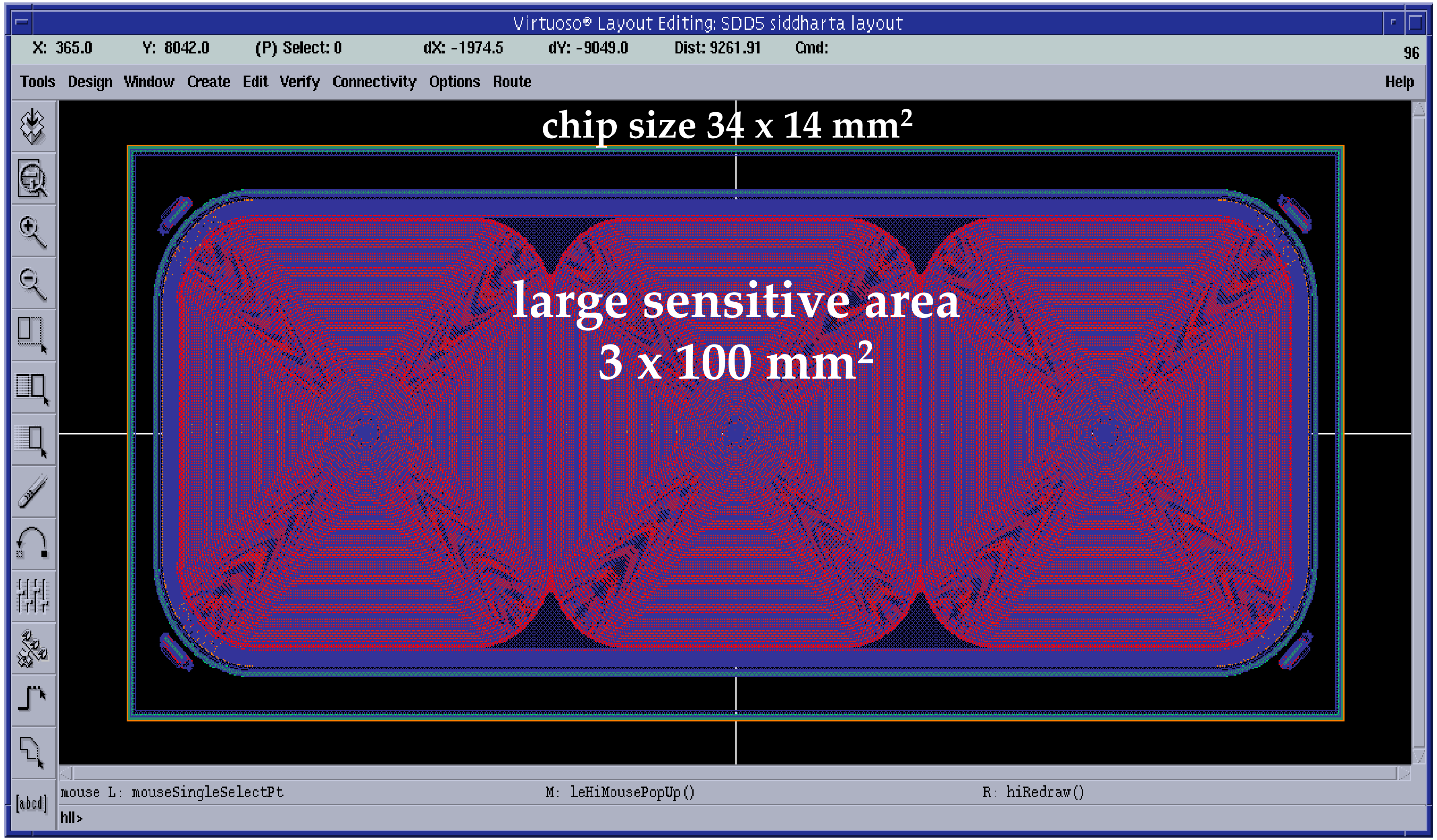

3x1 cm^2 SDD setup

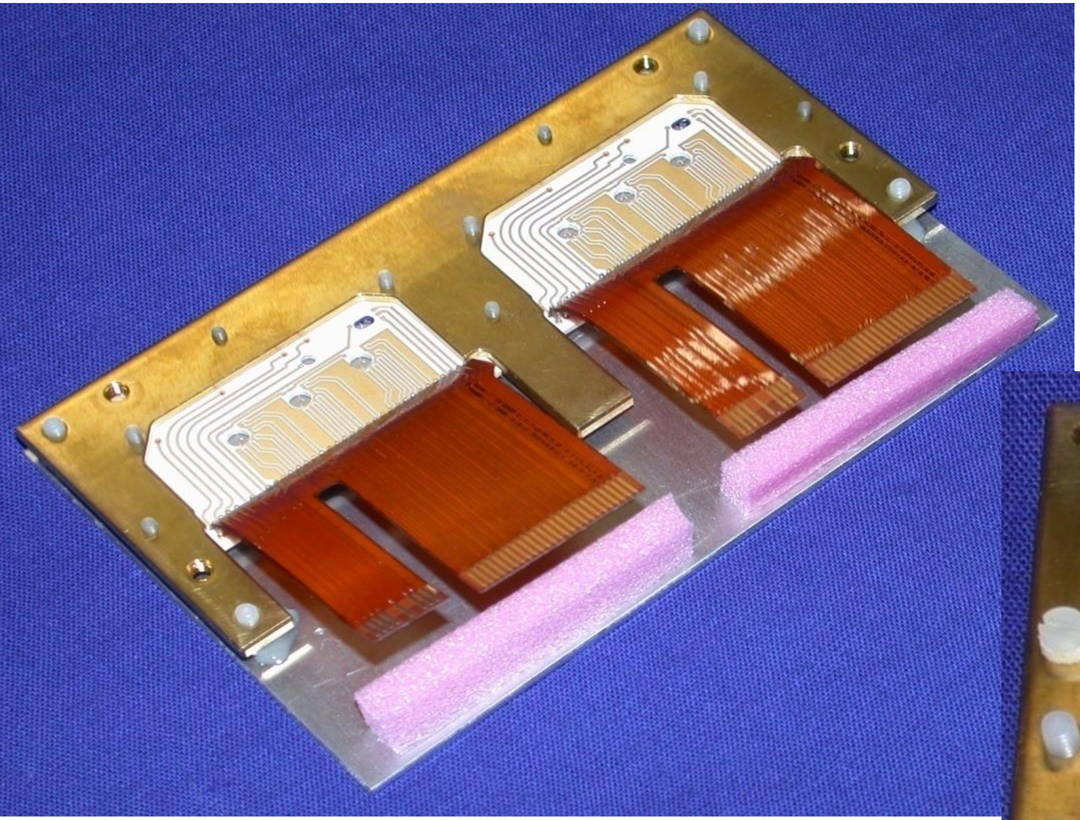

SDD-chip glued into ceramic frame and bonded.
SDD are connected with flexible Kapton boards.

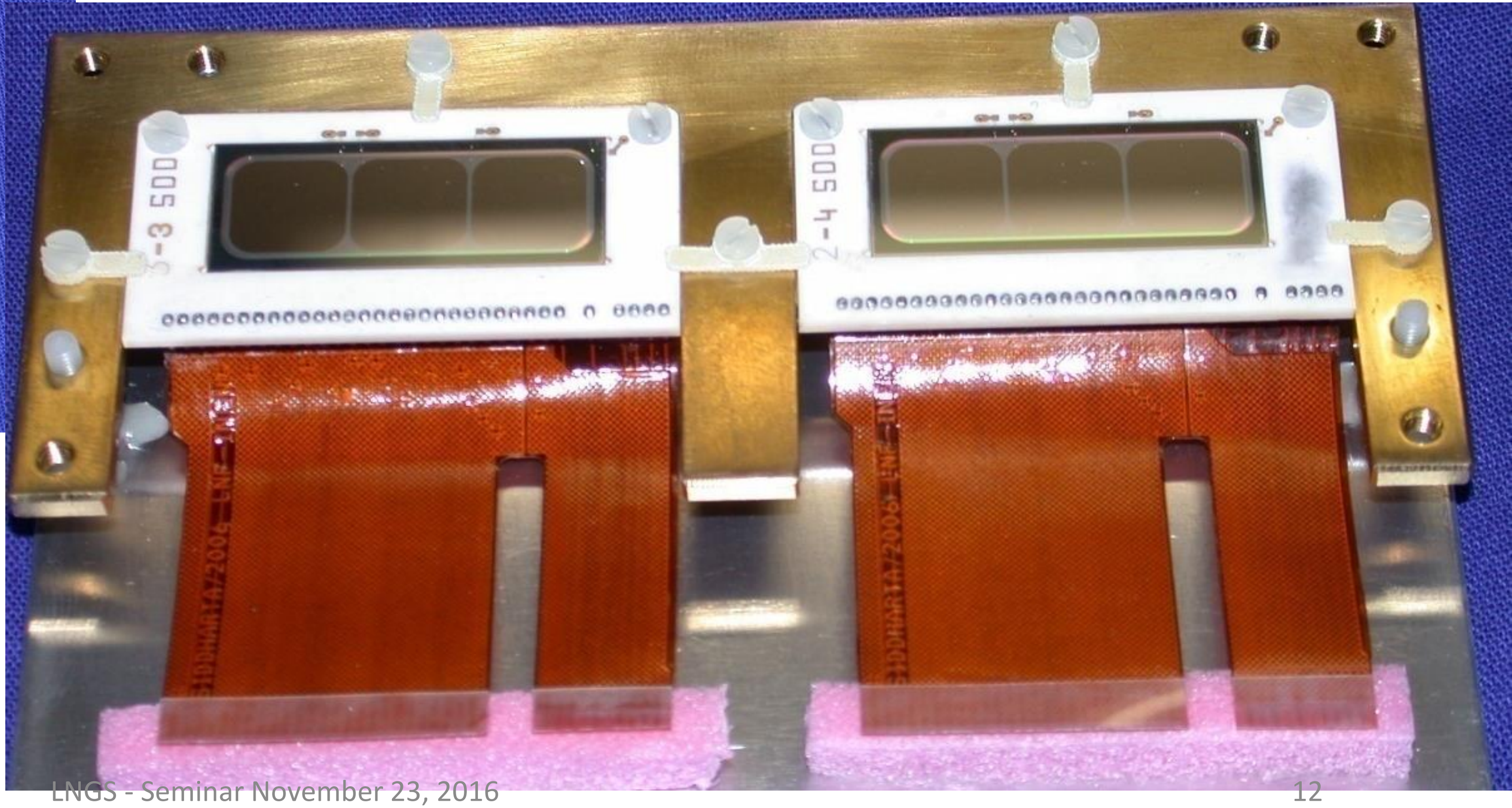

Bonding - optical inspection

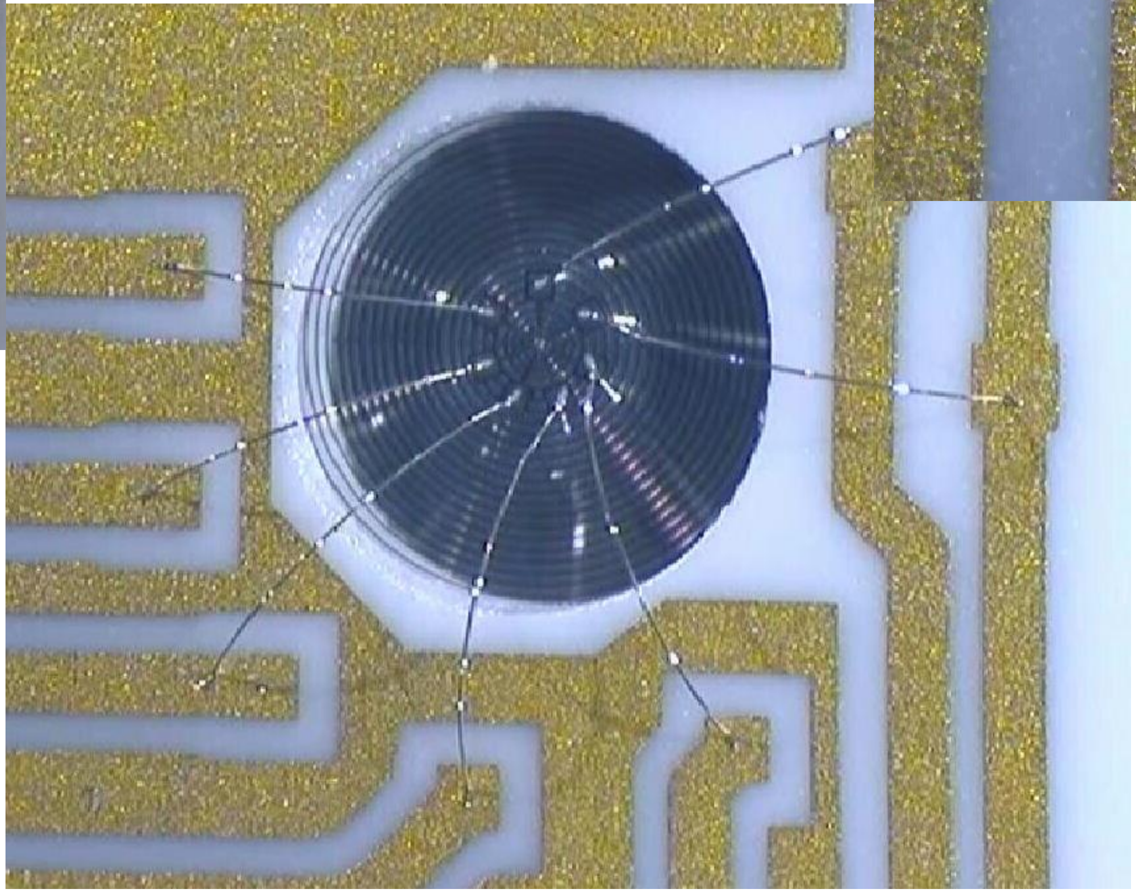

problems with “dirty” surface, most probable due to the soldering flux $\rightarrow$ solved: using Kapton tape to cover the remaining surface during soldering process

SDD – mounting device

unit for 2 CDD-chips with cooling

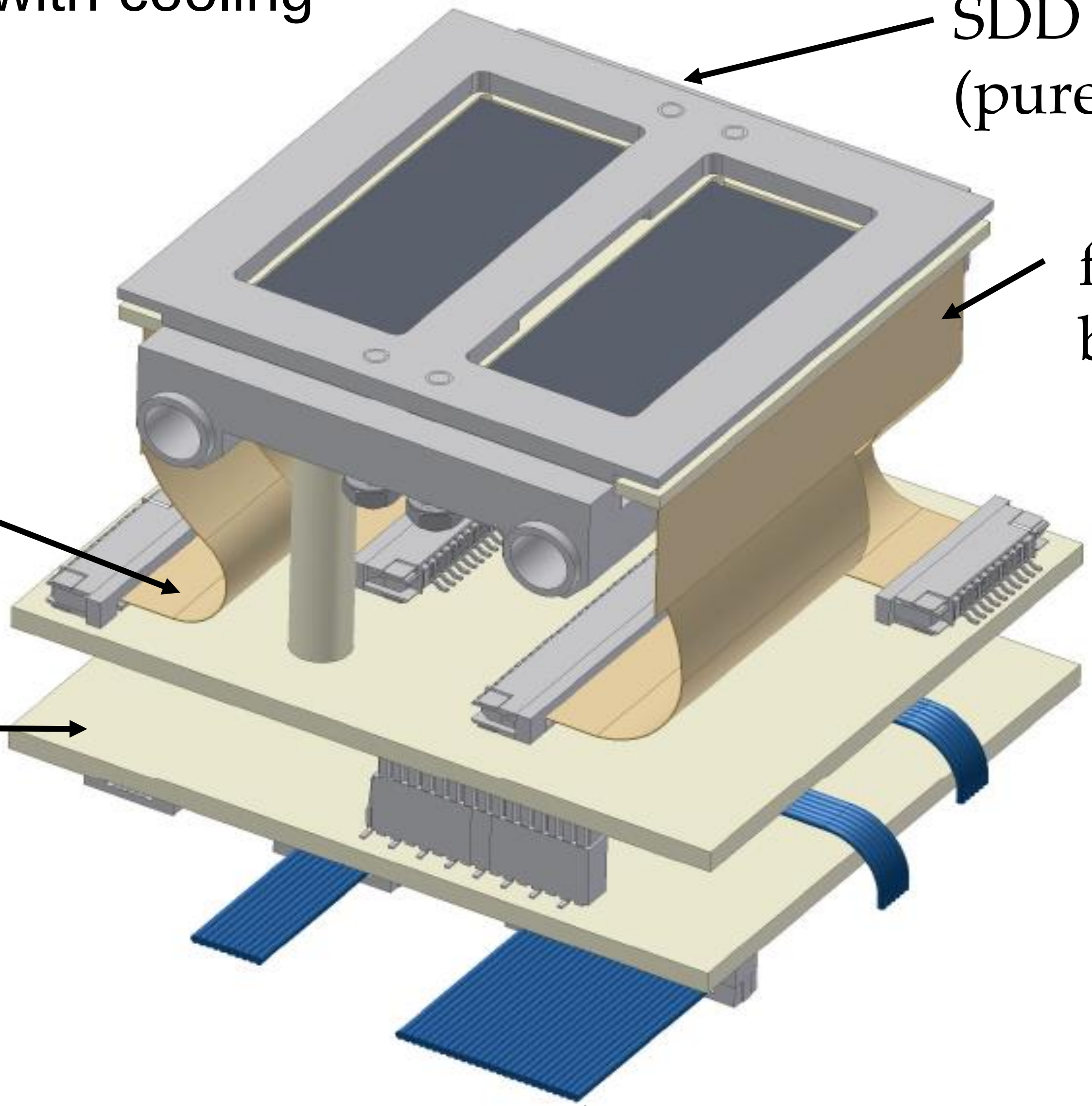

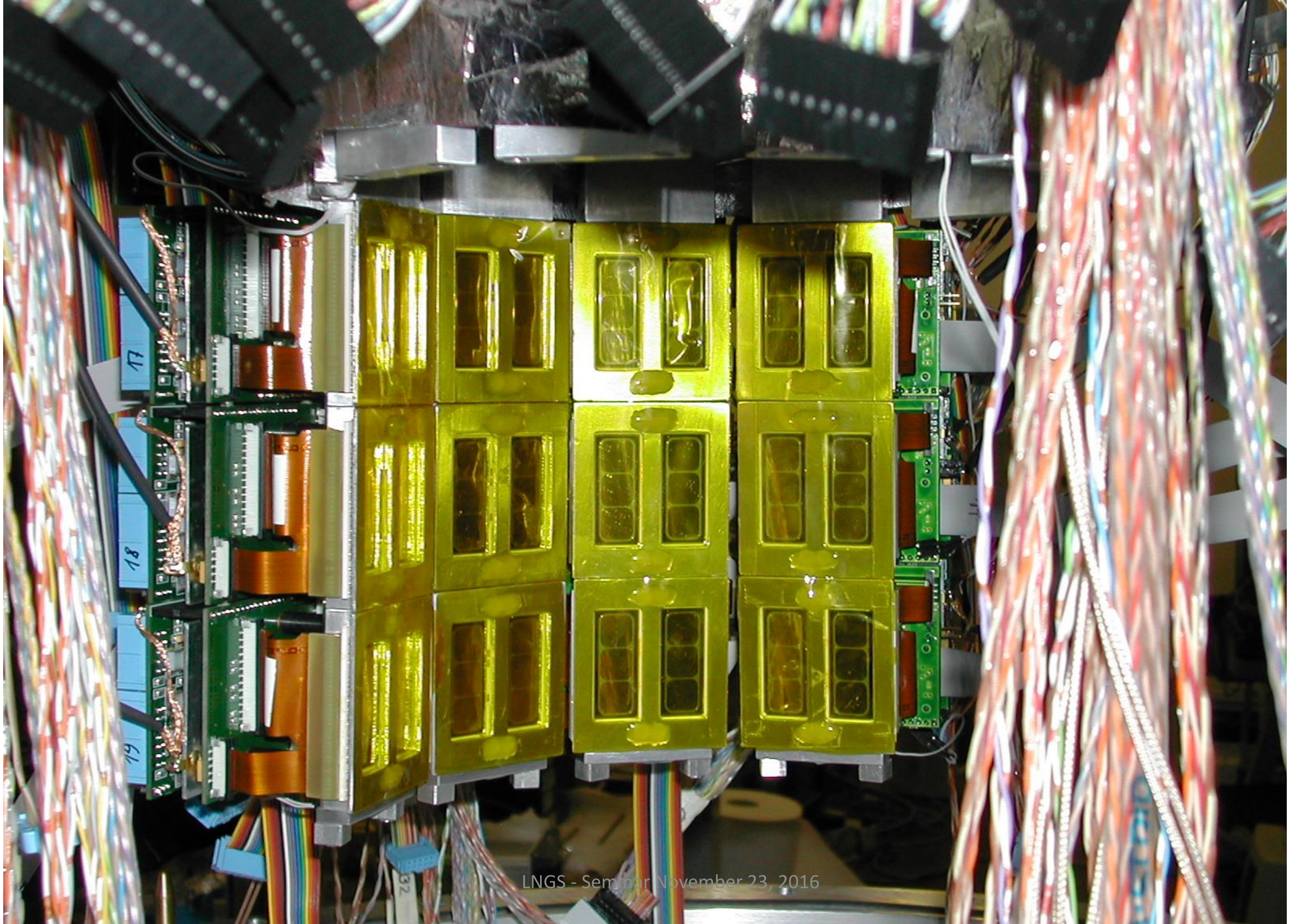
17
18
19

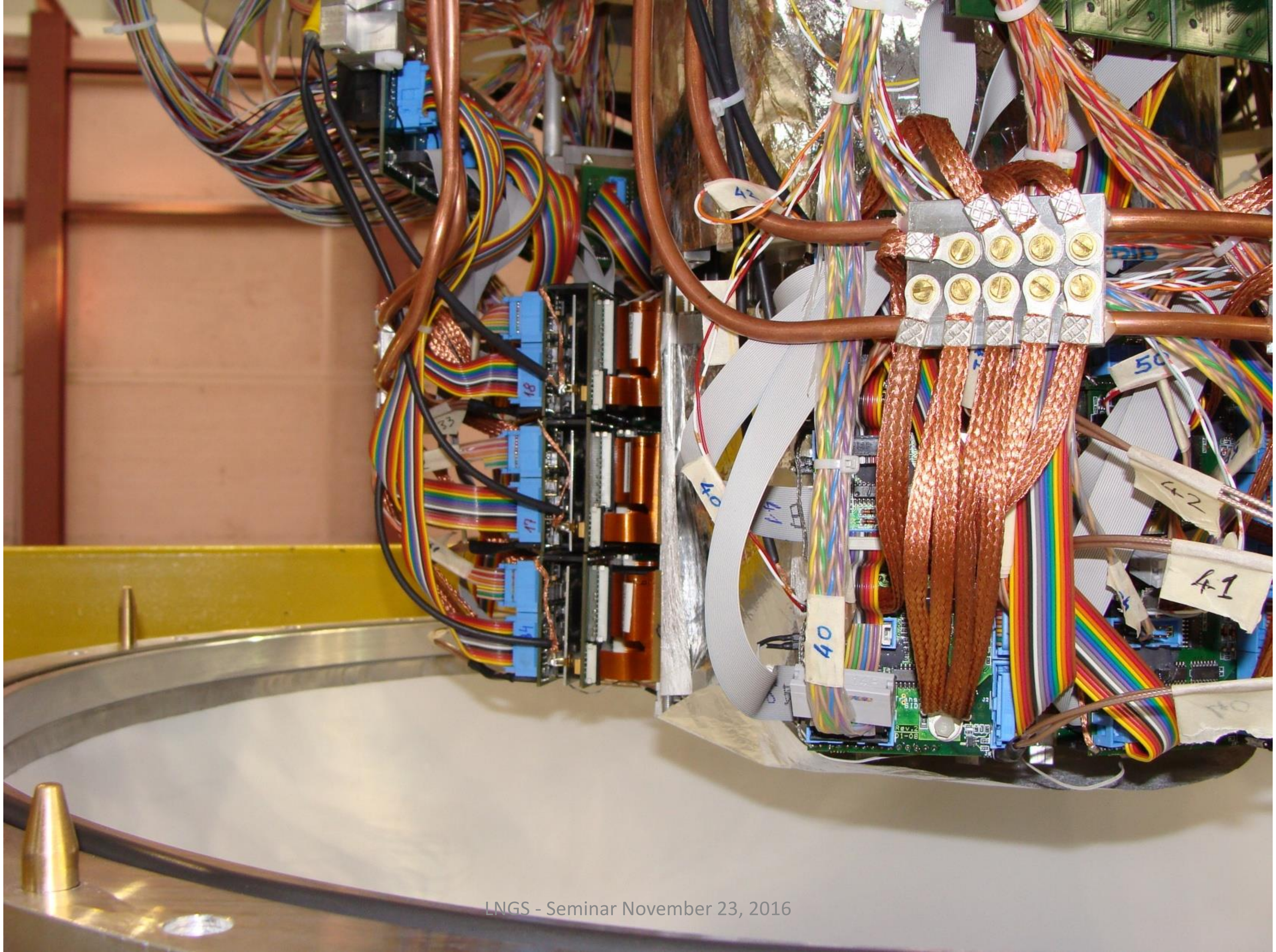
18
17
40
41

Kaonic hydrogen atoms at DAΦNE

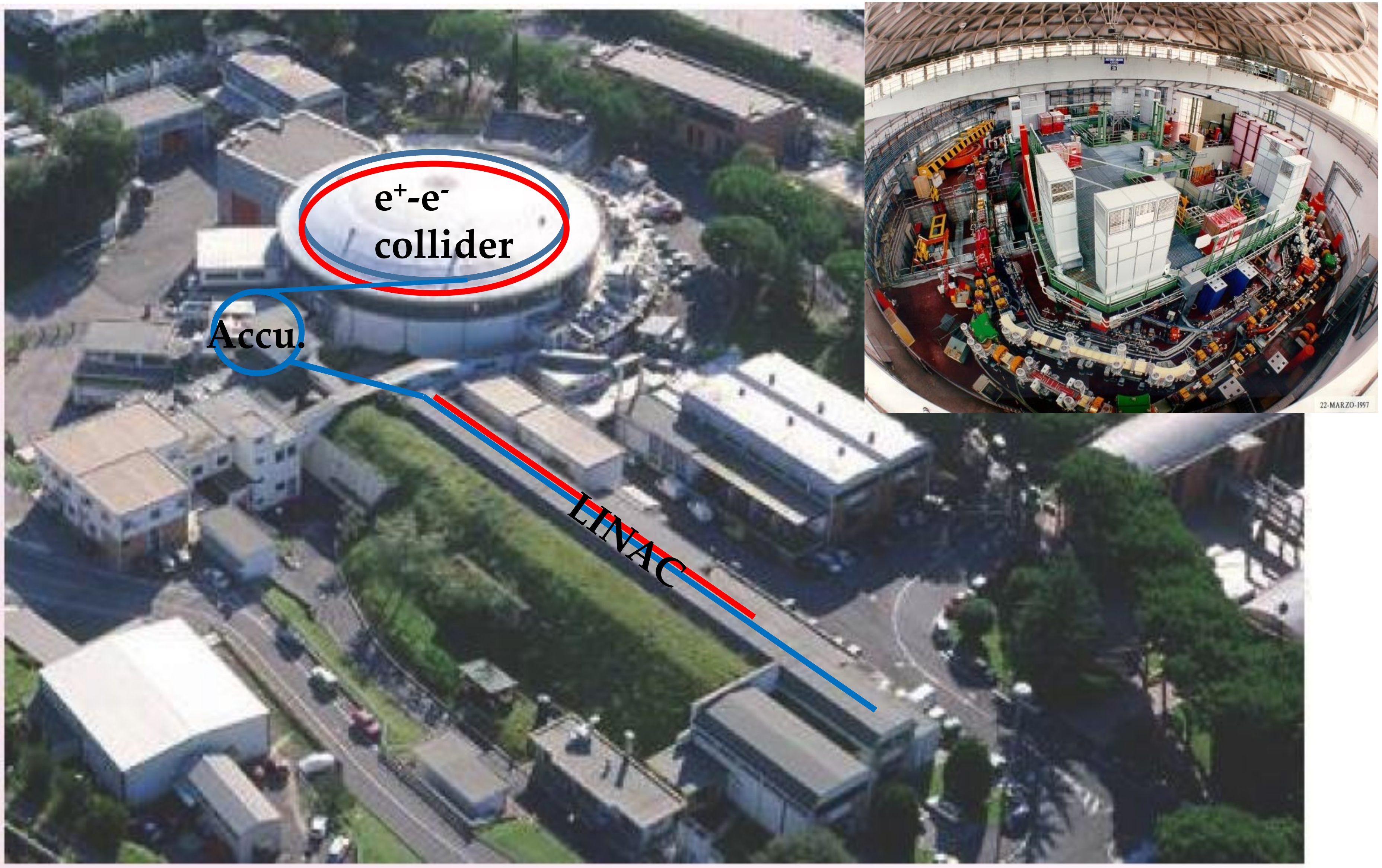

DAΦNE principle

- operates at the centre-of-mass energy of the Φ meson

  mass m = 1019.413 ± .008 MeV

  width Γ = 4.43 ± .06 MeV

- Φ produced via e^+e^- collision with

  $\sigma(e^+e^- \rightarrow \Phi) \sim 5\ \mu b$

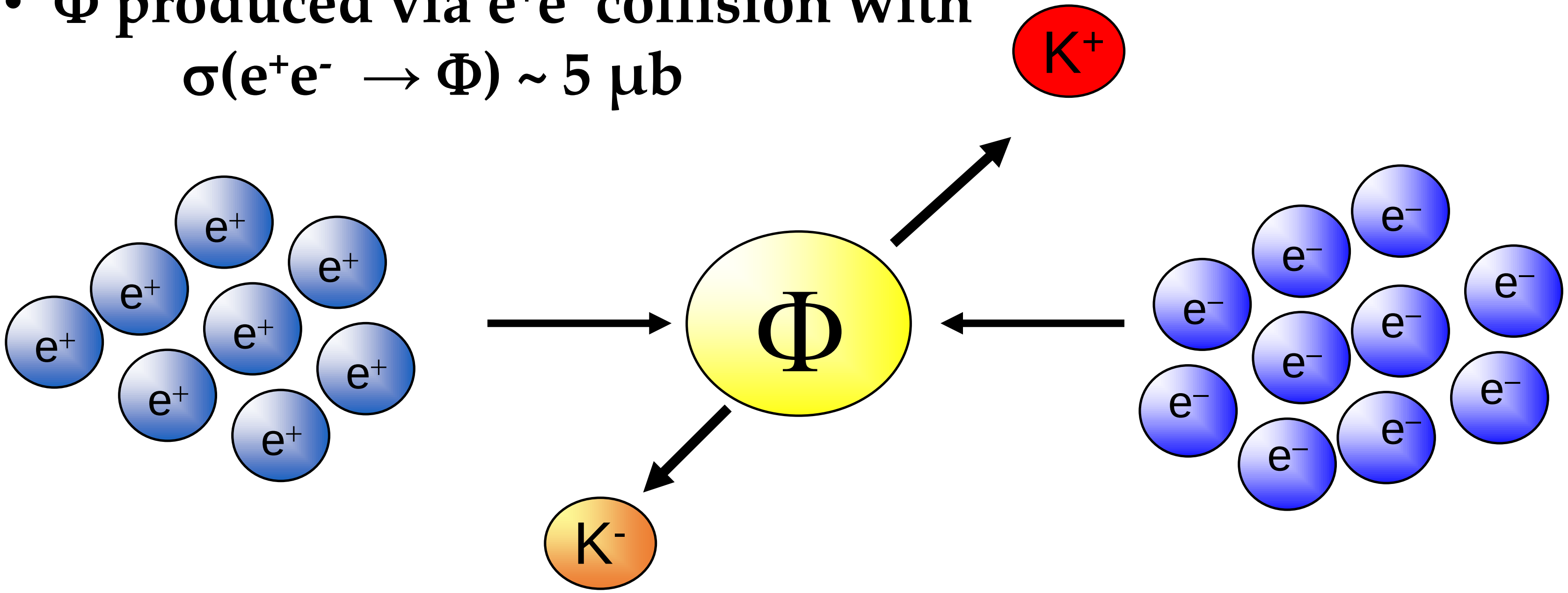

→ Φ production rate 2.5 x $10^3\ s^{-1}$

→ monochromatic kaon beam (127 MeV/c)

Data taking scheme at DAΦNE

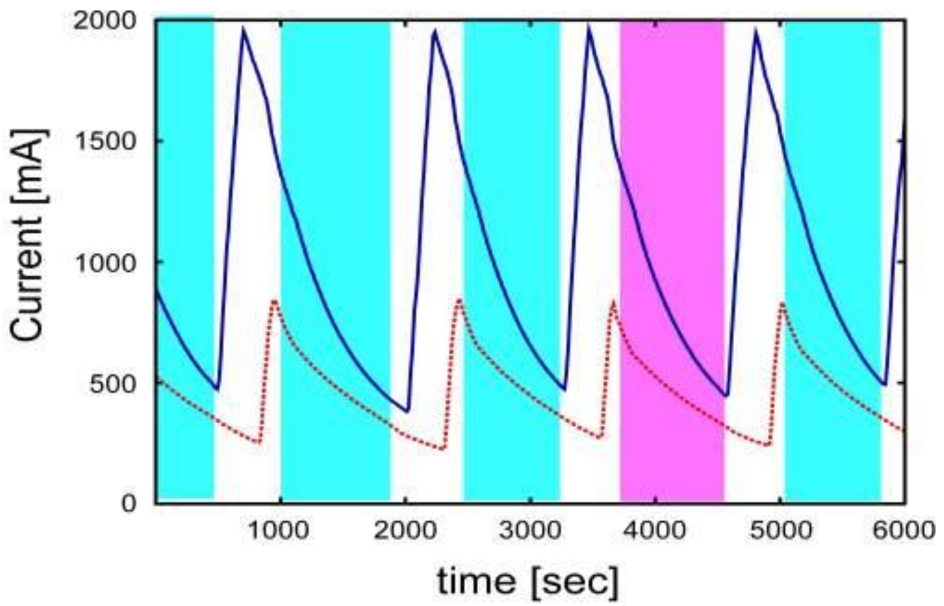

"X-ray tube" data taken with "beam" ON

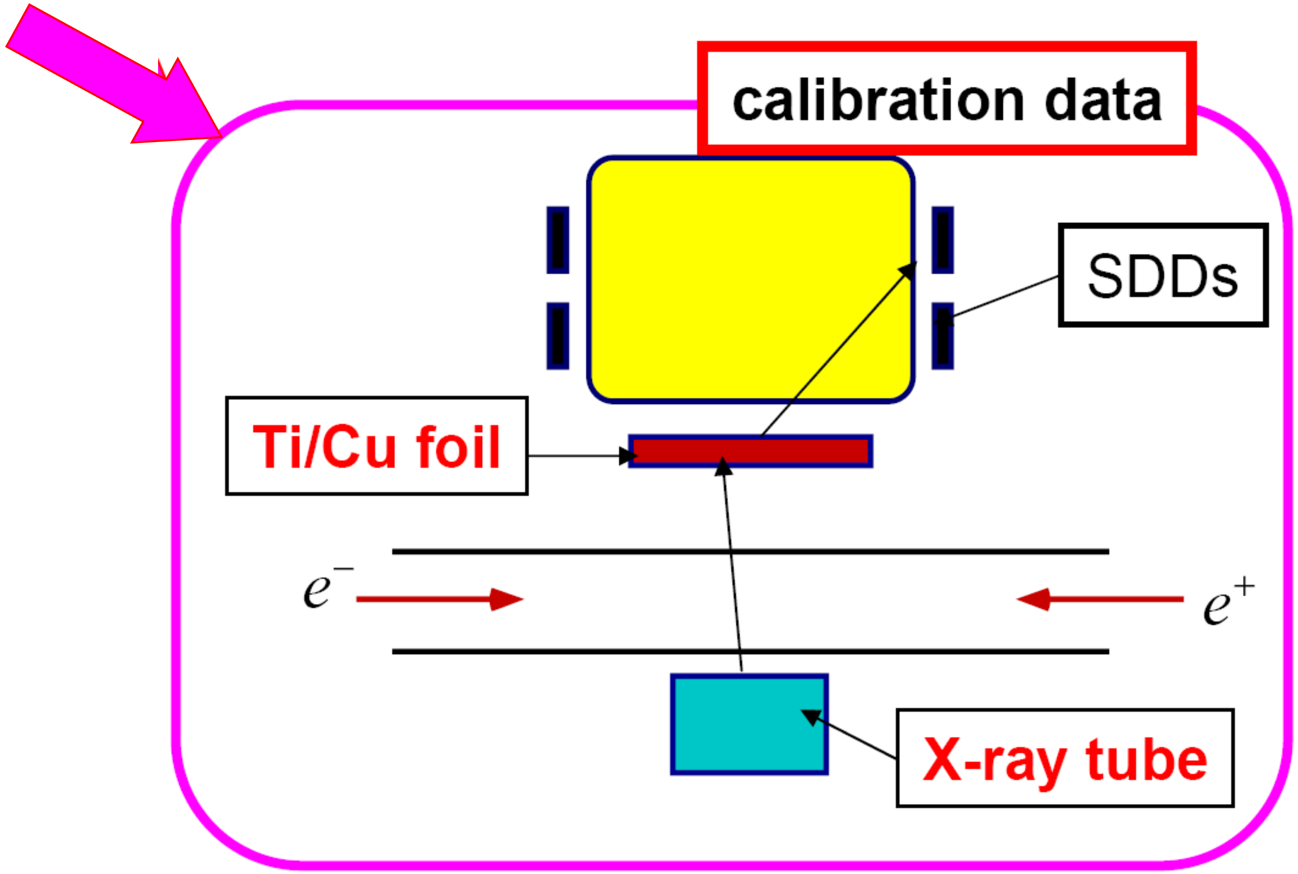

SDD X-ray energy spectra

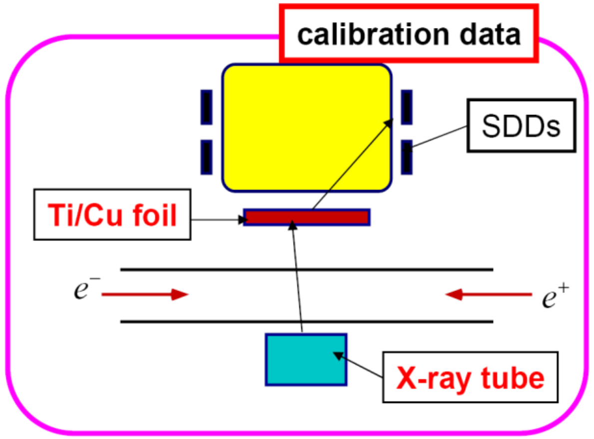

“X-ray tube” data taken

estimated systematic error ~ 3-4 eV

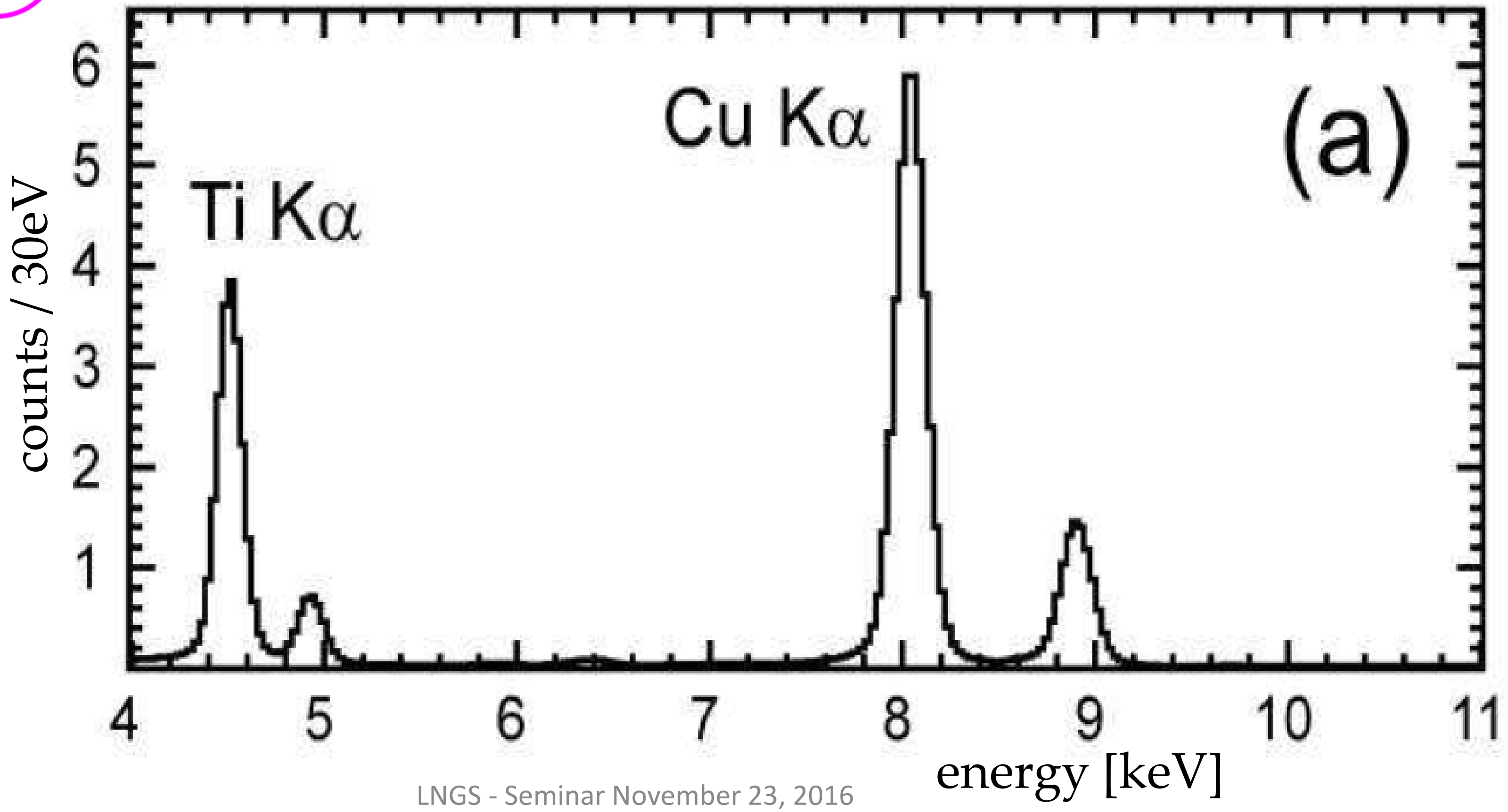

Data taking scheme at DAΦNE

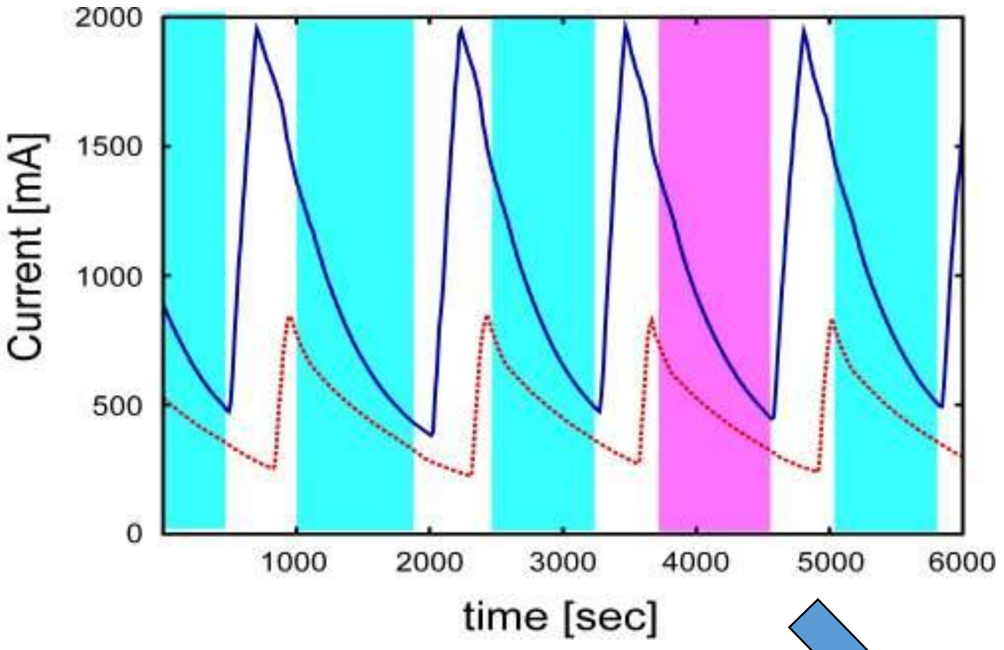

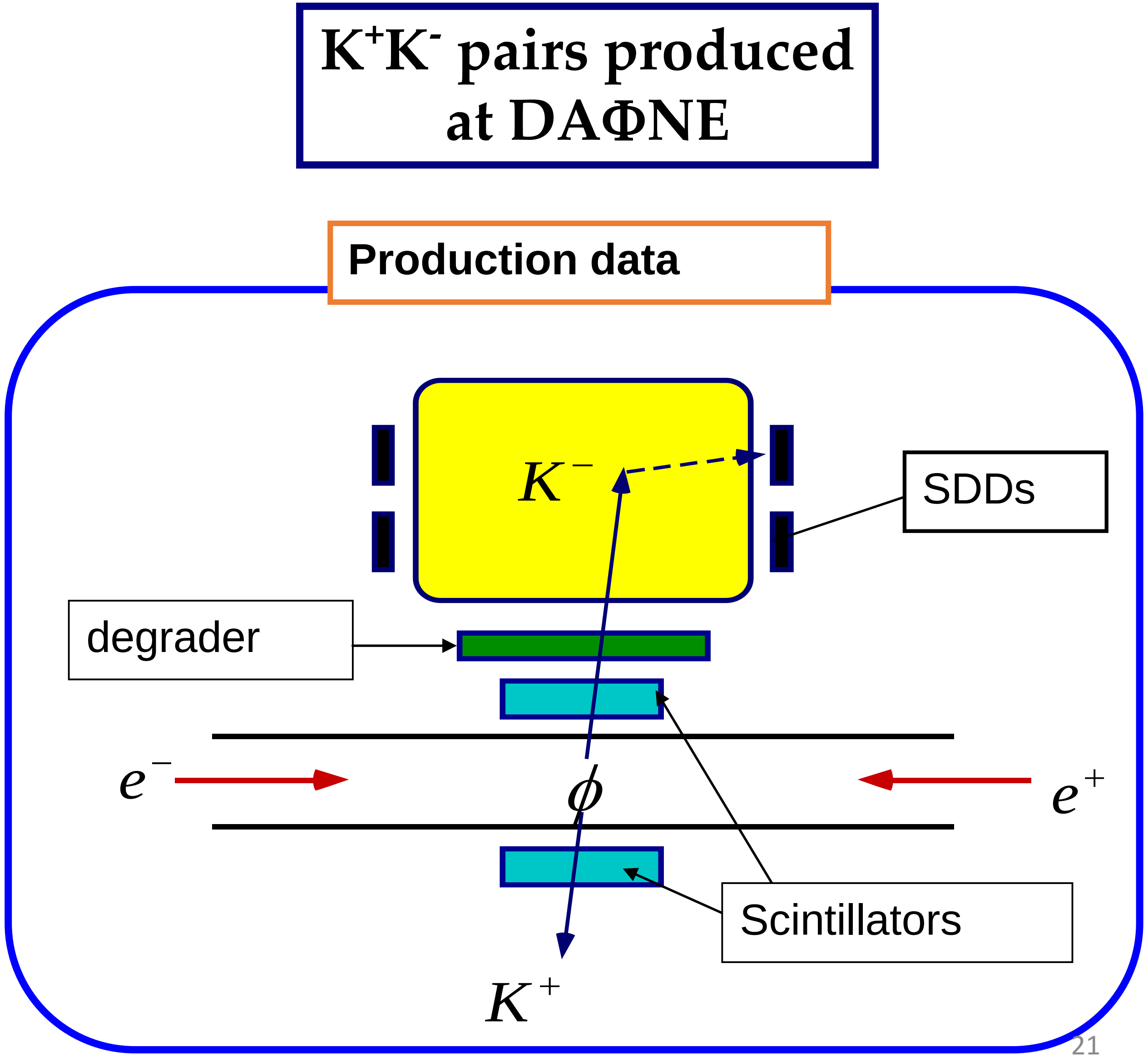

KAONIC HYDROGEN DATA ANALYSIS

Calibration data with X-ray tube

All events ("self trigger")

Coincidence: K^+K^- and SDD timing

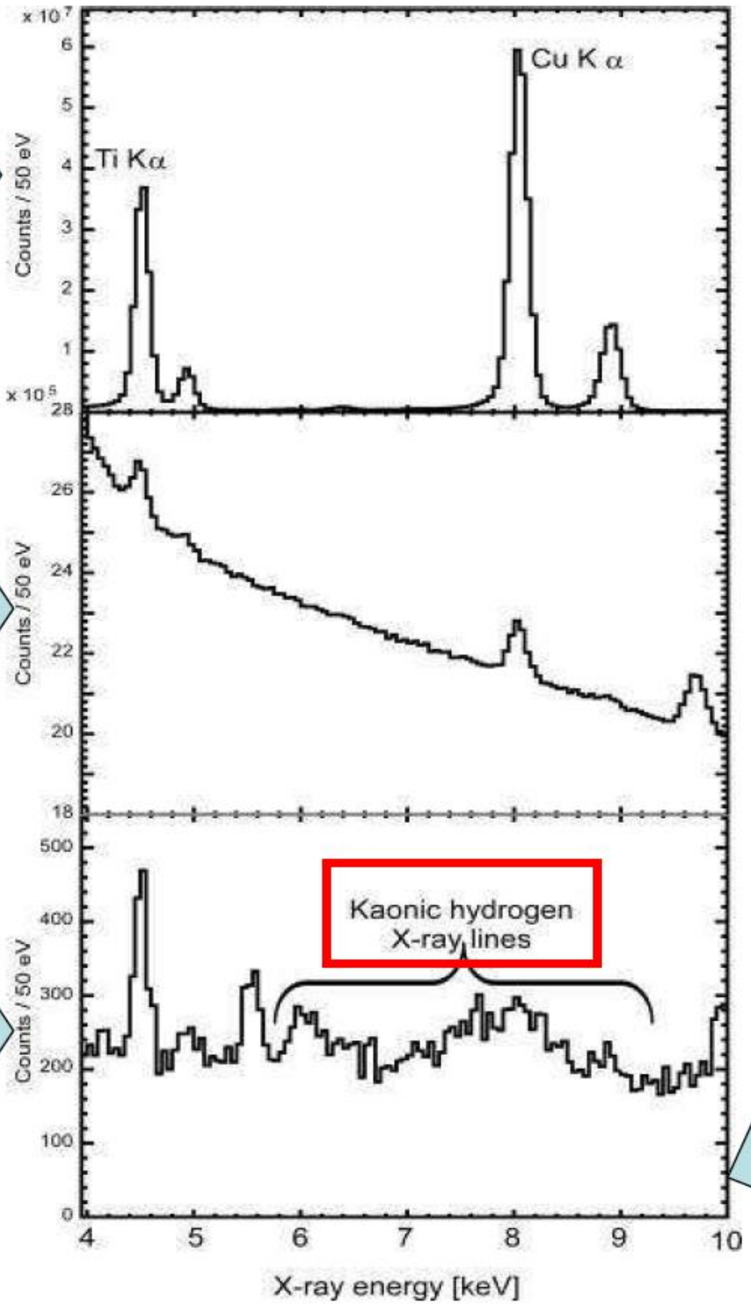

Kaon detector

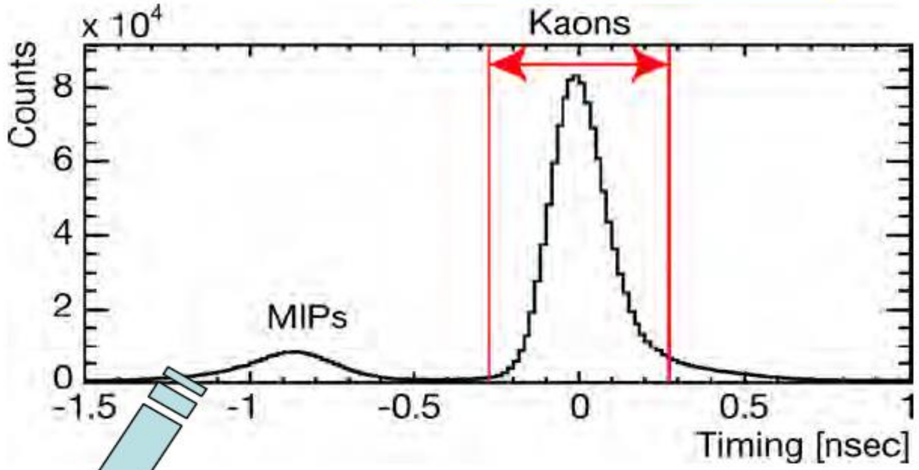

Time difference between SDD & Kaon detector

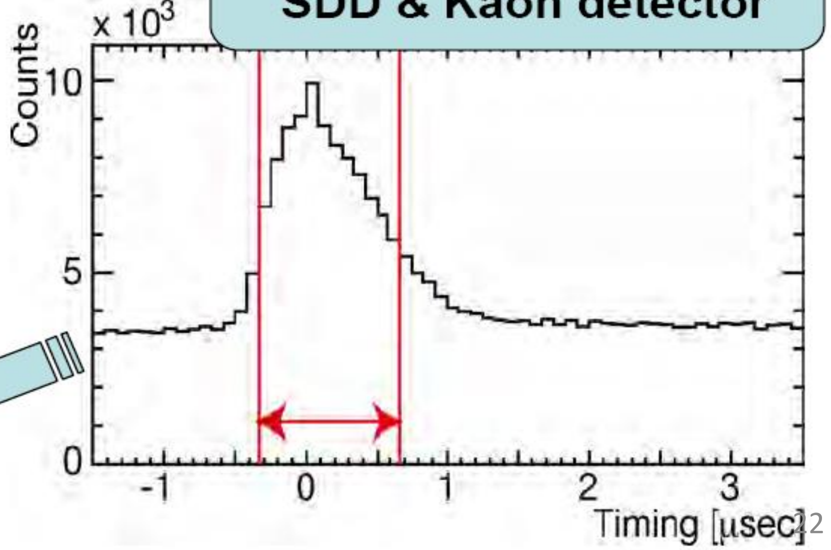

K^-p spectrum after BG subtraction

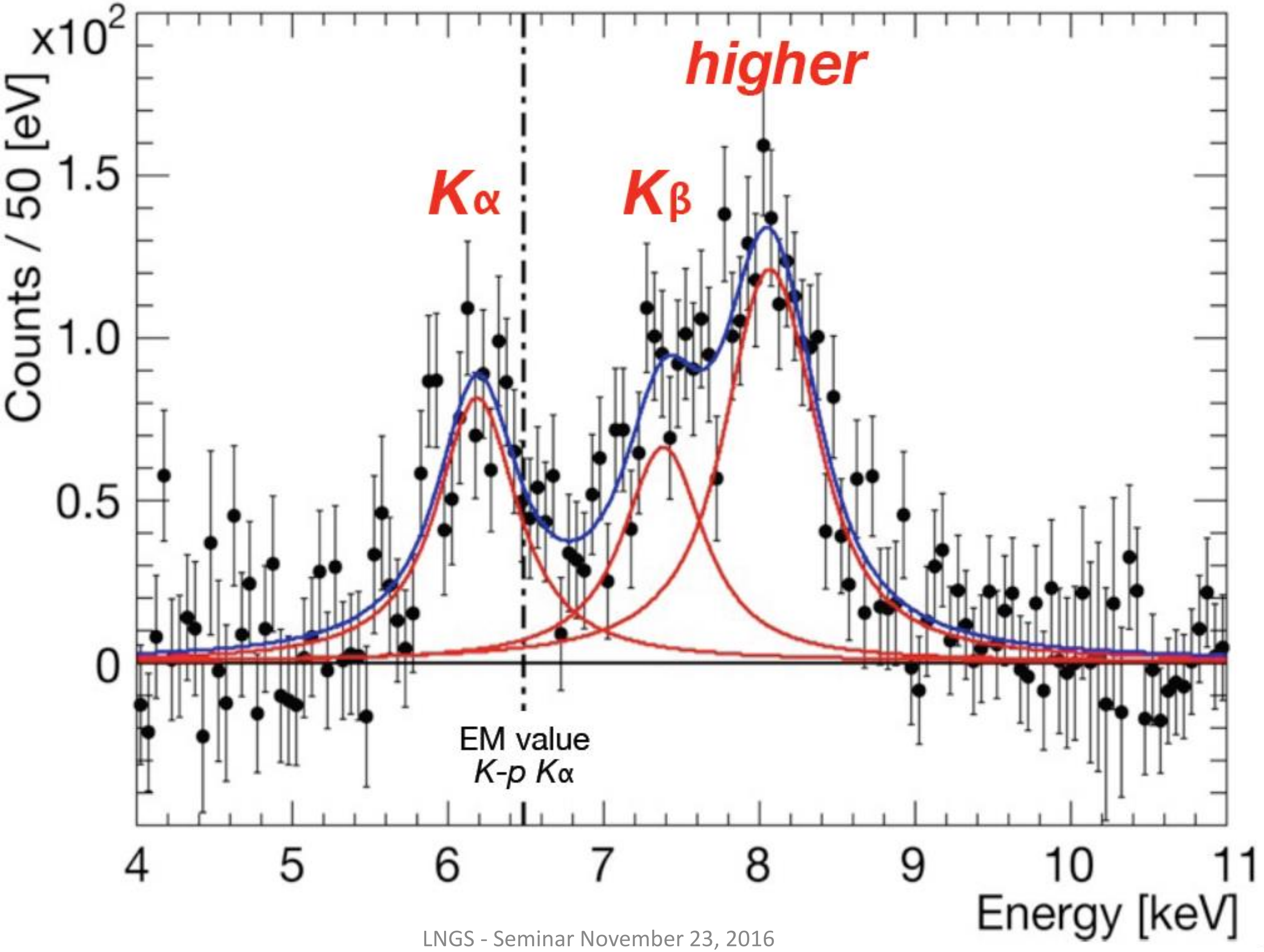

State of the art: Kaonic hydrogen

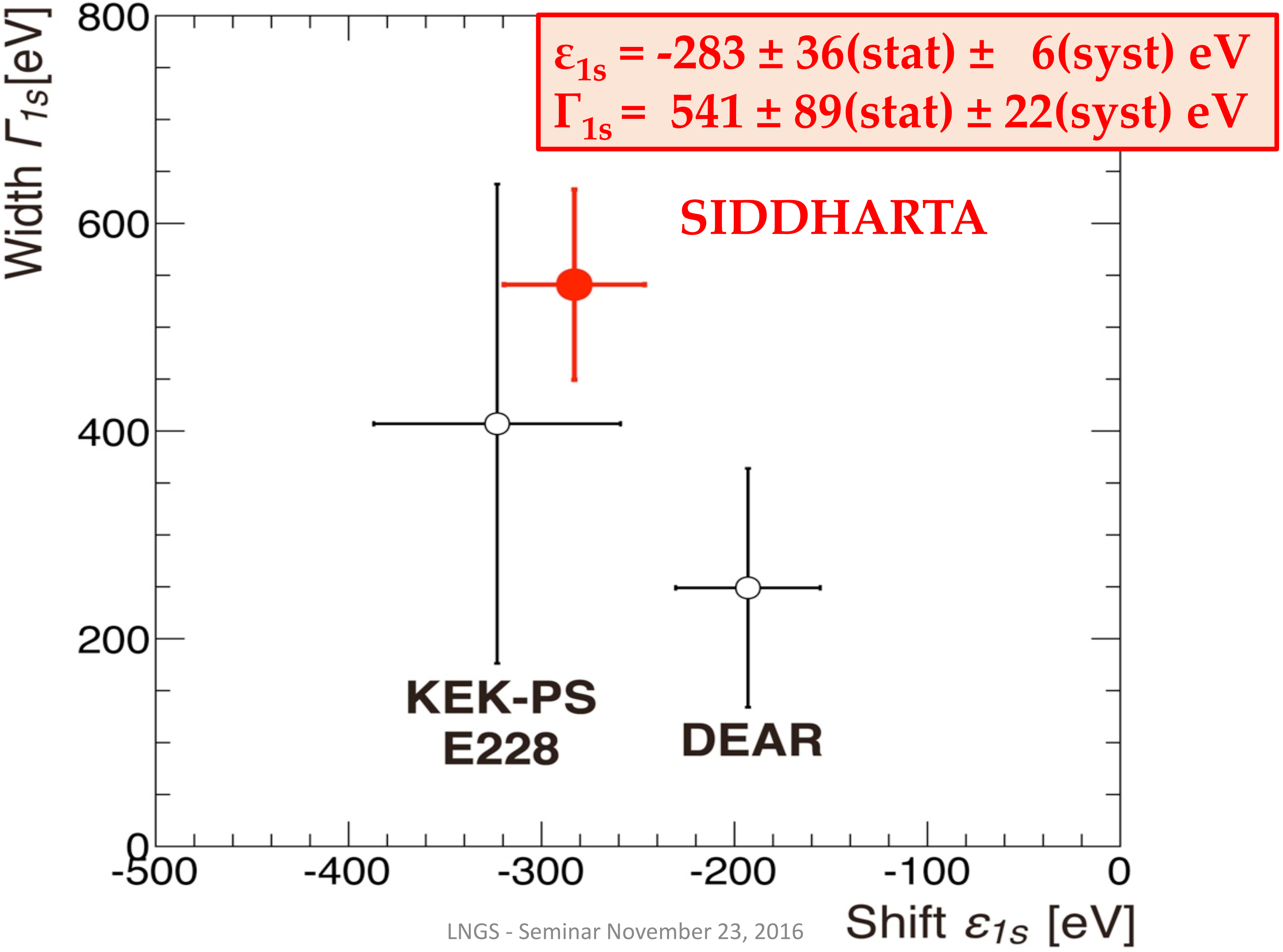

Improved constraints on chiral SU(3) dynamics from kaonic hydrogen

Y. Ikeda, T. Hyodo and W. Weise, PLB 706 (2011) 63

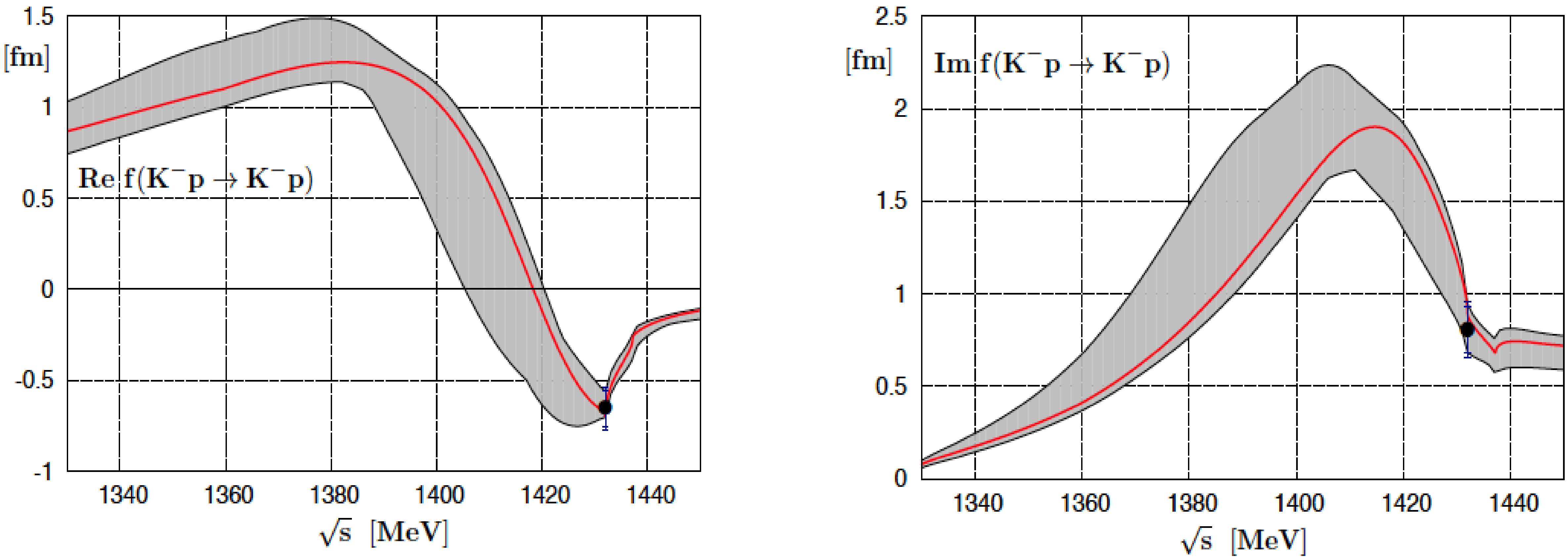

Fig. 3. Real part (left) and imaginary part (right) of the $K^-p \to K^-p$ forward scattering amplitude extrapolated to the subthreshold region. The empirical real and imaginary parts of the K^-p scattering length deduced from the recent kaonic hydrogen measurement (SIDDHARTA [7]) are indicated by the dots including statistical and systematic errors. The shaded uncertainty bands are explained in the text.

SDD - front-end readout strategy

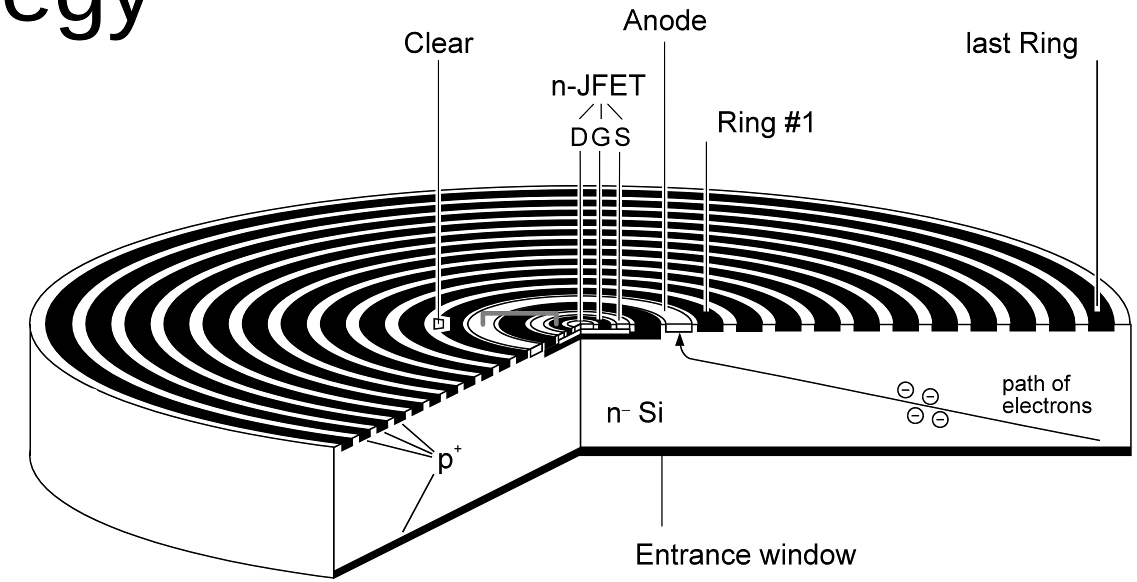

- **SIDDHARTA**
  - JFET integrated on SDD
  - lowest total anode capacitance
  - limited JFET performance
  - sophisticated SDD+JFET technology

- **SIDDHARTA-2**
- **$K^{-}d$ @ J-PARC**
  - external CUBE preamplifier (MOSFET input transistor)
  - larger total anode capacitance
  - better FET performances
  - standard SDD technology

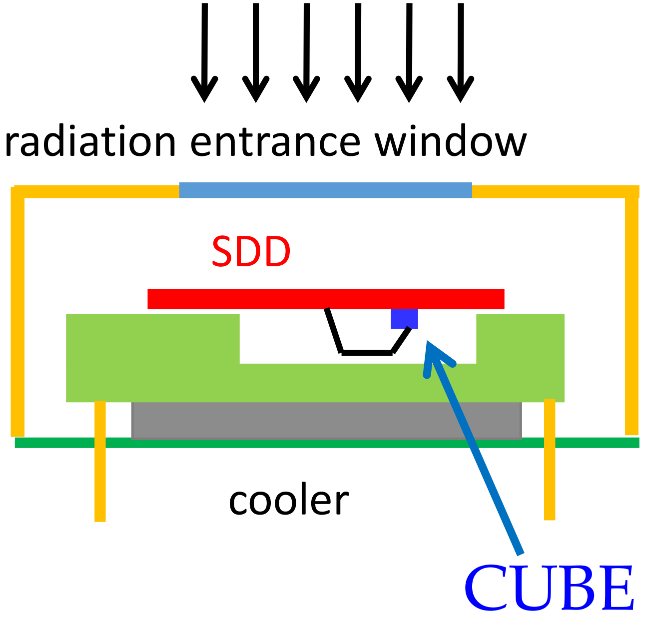

The CUBE preamplifier

- A full CMOS preamplifier is mounted on ceramic board - connected via bonding
- The CUBE replaces the JFET, which was direct implanted on the anode side on the SIDDHARTA type SDDs
- Short bonding lines from CUBE to SDD, no difference in the detector performance
- Advantage, the preamplifier is connected close to the SDD and not only the FET → ASIC of analogue processing can be placed relatively up to ~100 cm away

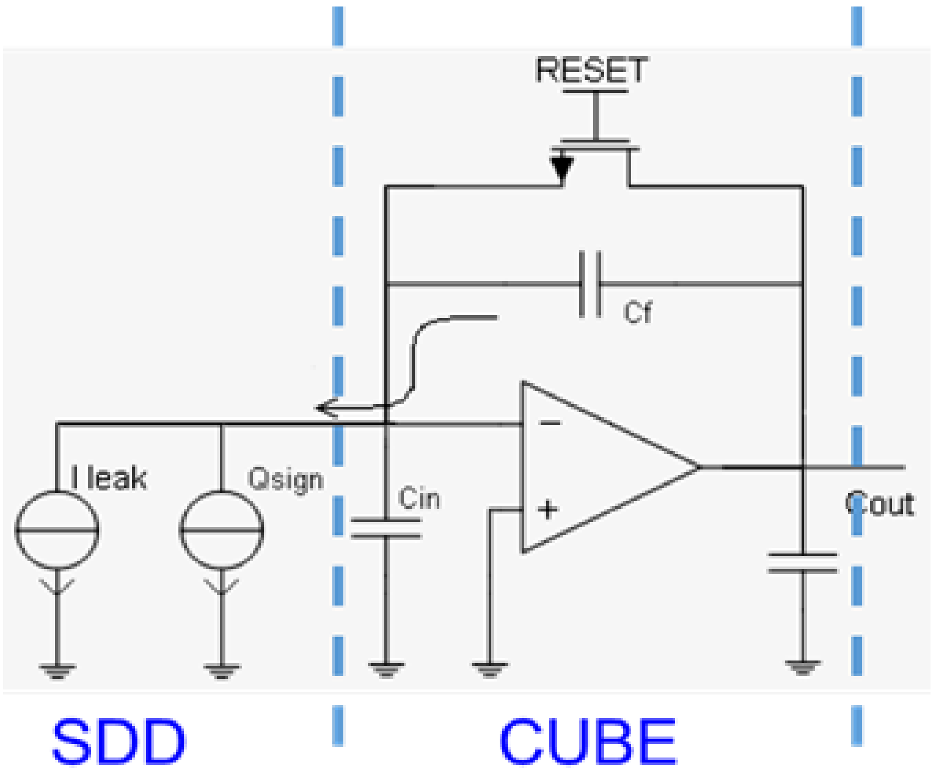

Large area Silicon Drift Detector

developed by Politech Milano and FBK-Trento, Italy

Array: 9 SDDs (8 x 8 mm^2 each)

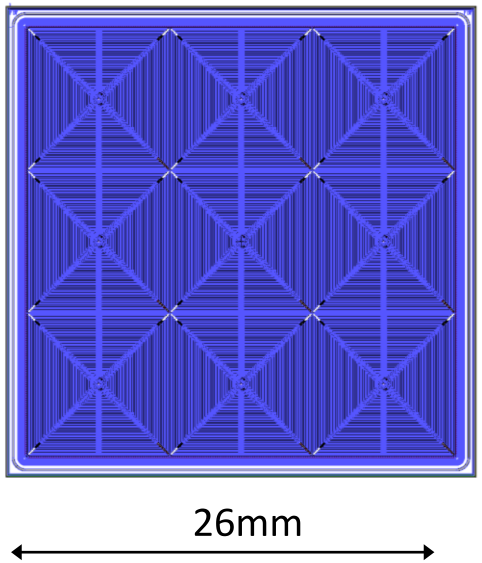

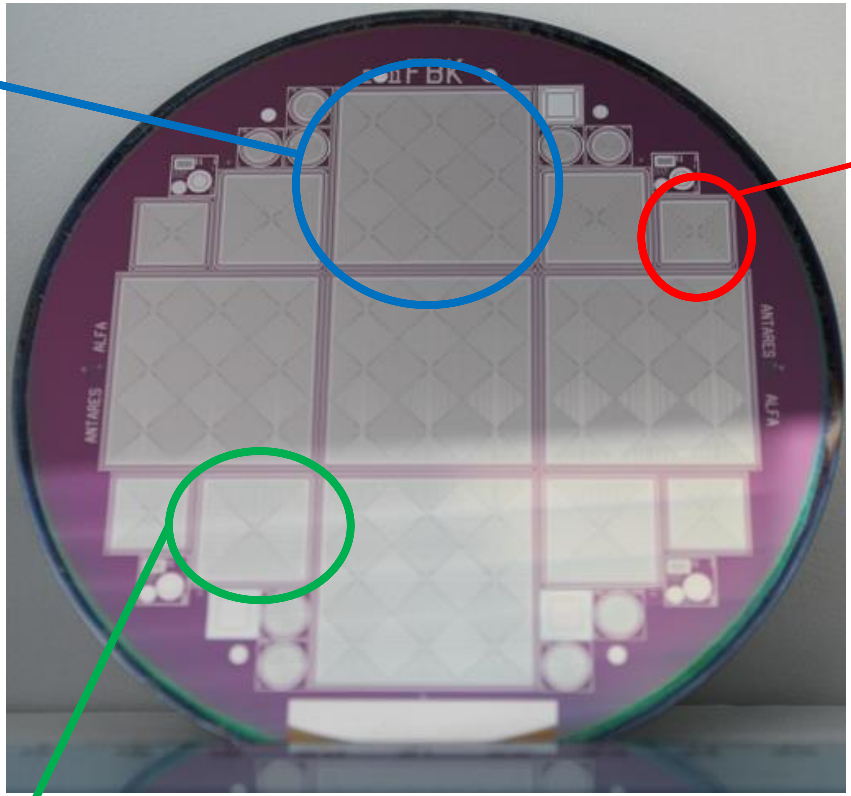

8 x 8 mm^2 single SDD

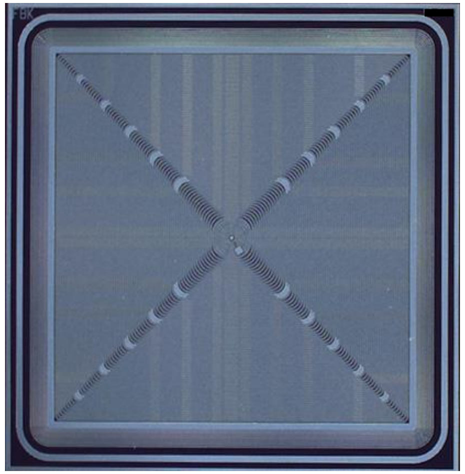

12 x 12 mm single SDD

FBK production:
- 4” wafer
- 6” wafer upgrade just finished

Prototype of a 3x3 matrix SDD chips

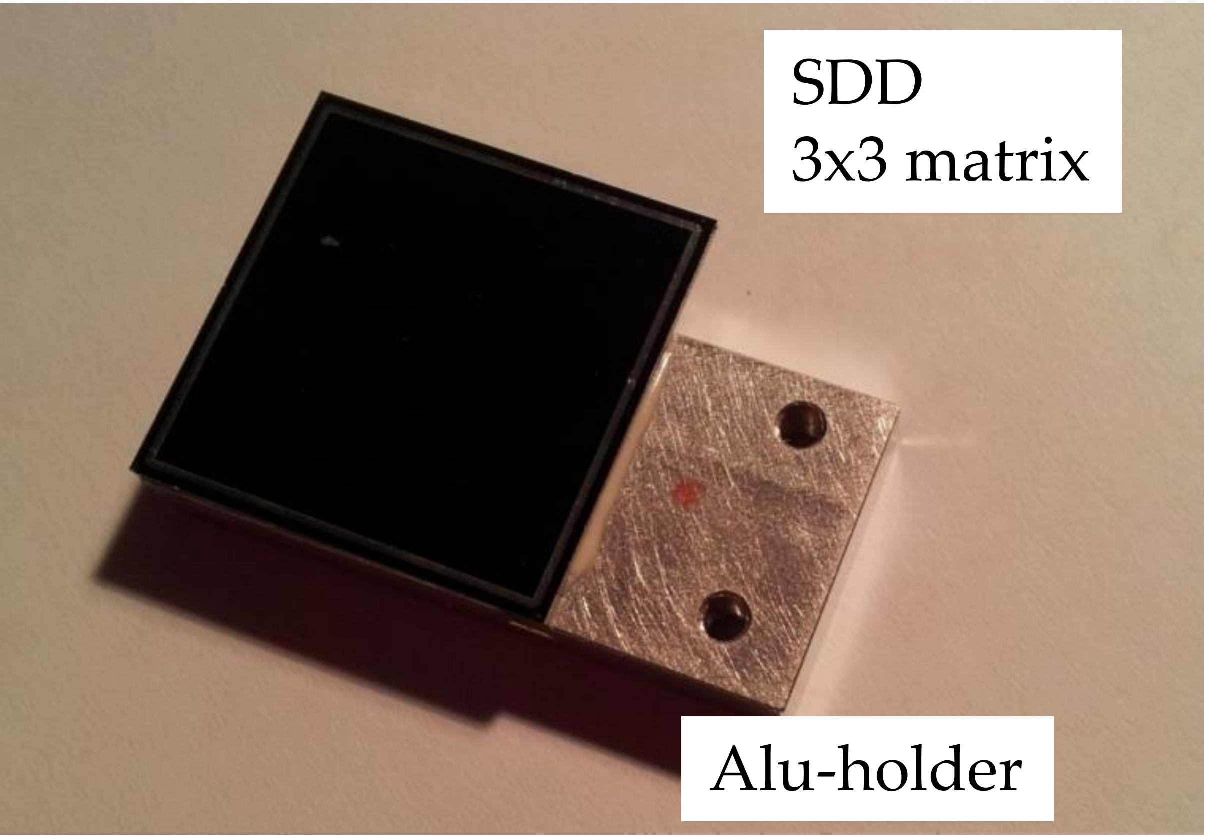

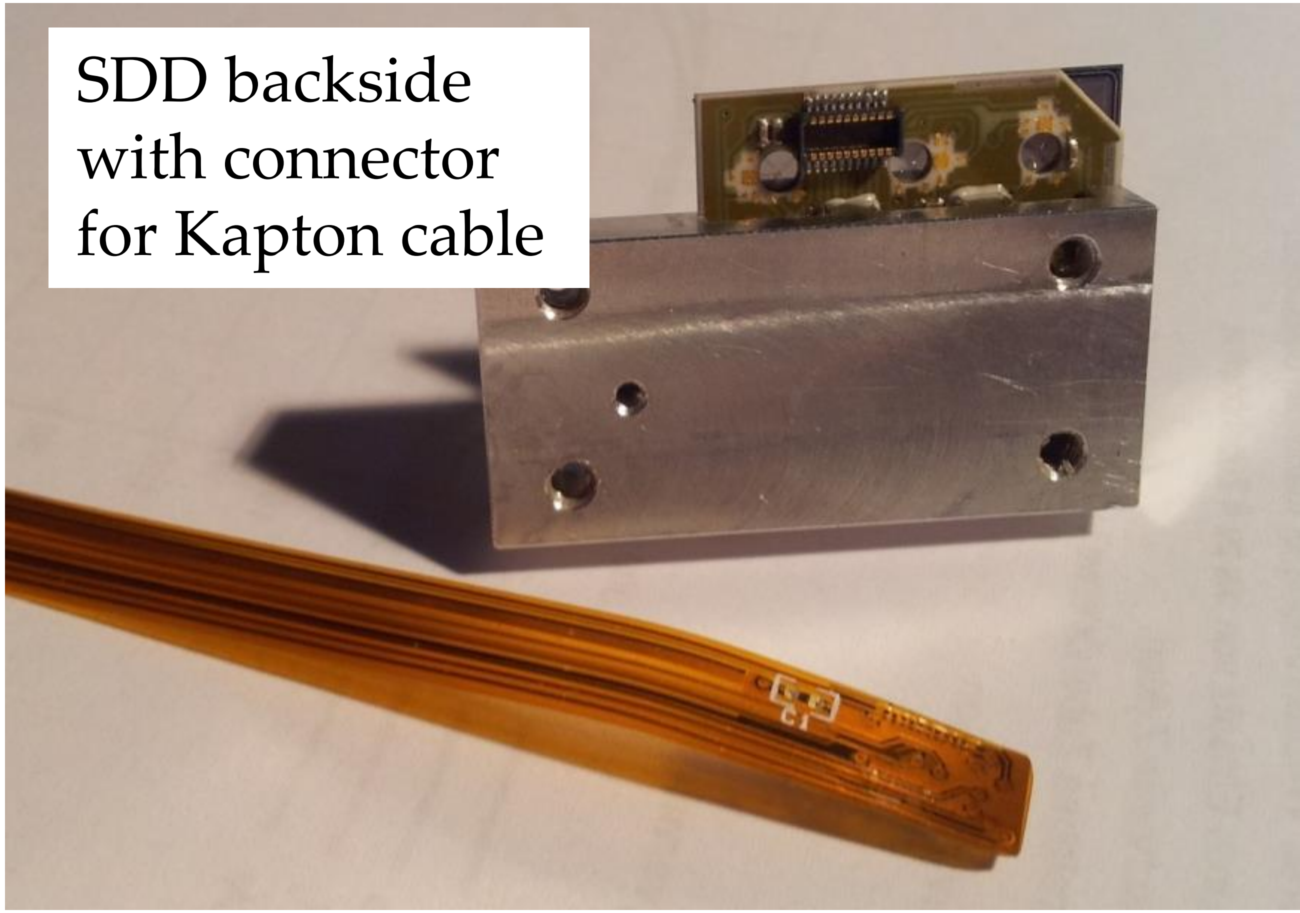

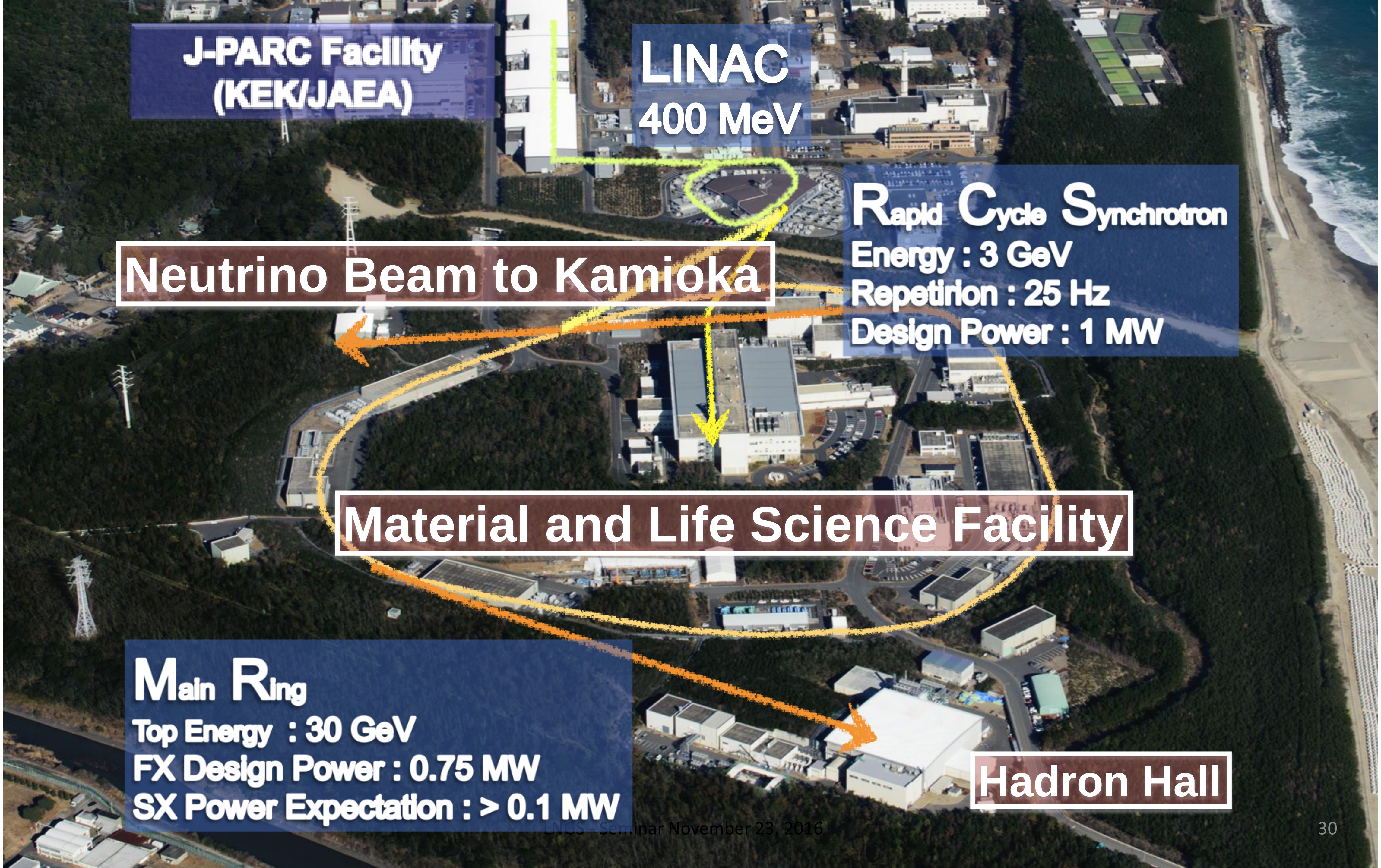
J-PARC Facility
(KEK/JAEA)
LINAC
400 MeV
Rapid Cycle Synchrotron
Energy : 3 GeV
Repetirion : 25 Hz
Design Power : 1 MW
Neutrino Beam to Kamioka
Material and Life Science Facility
Main Ring
Top Energy : 30 GeV
FX Design Power : 0.75 MW
SX Power Expectation : > 0.1 MW
Hadron Hall

First SDD tested at J-PARC K1.8BR

beam time June 2016

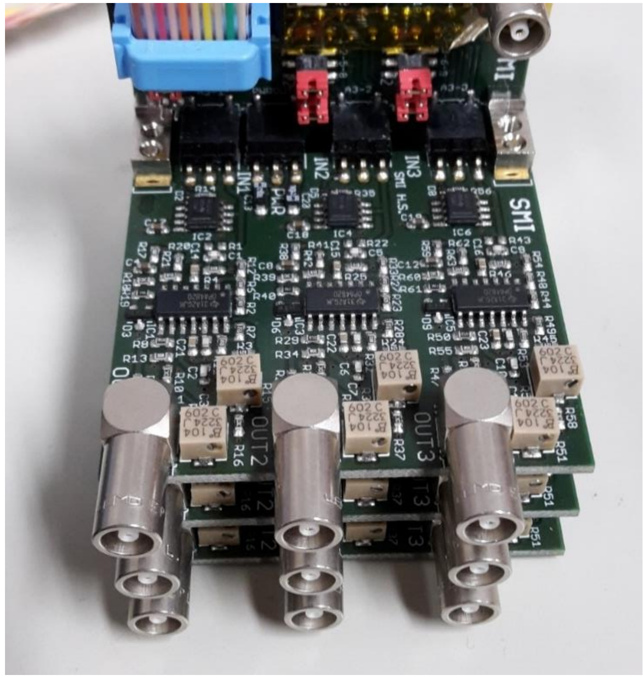

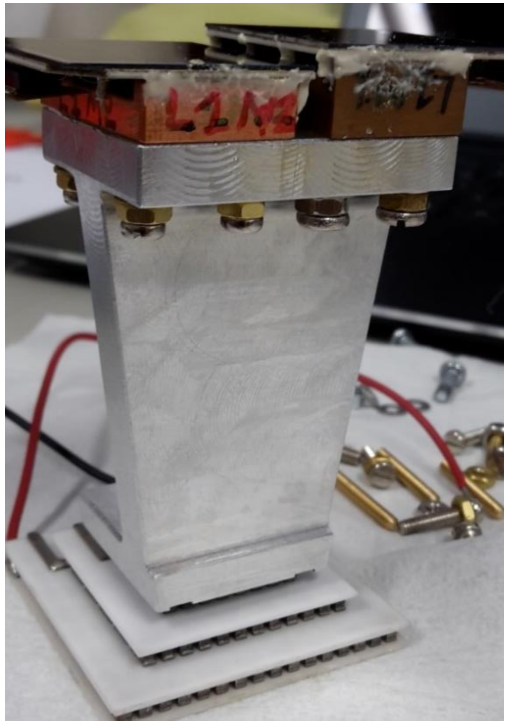

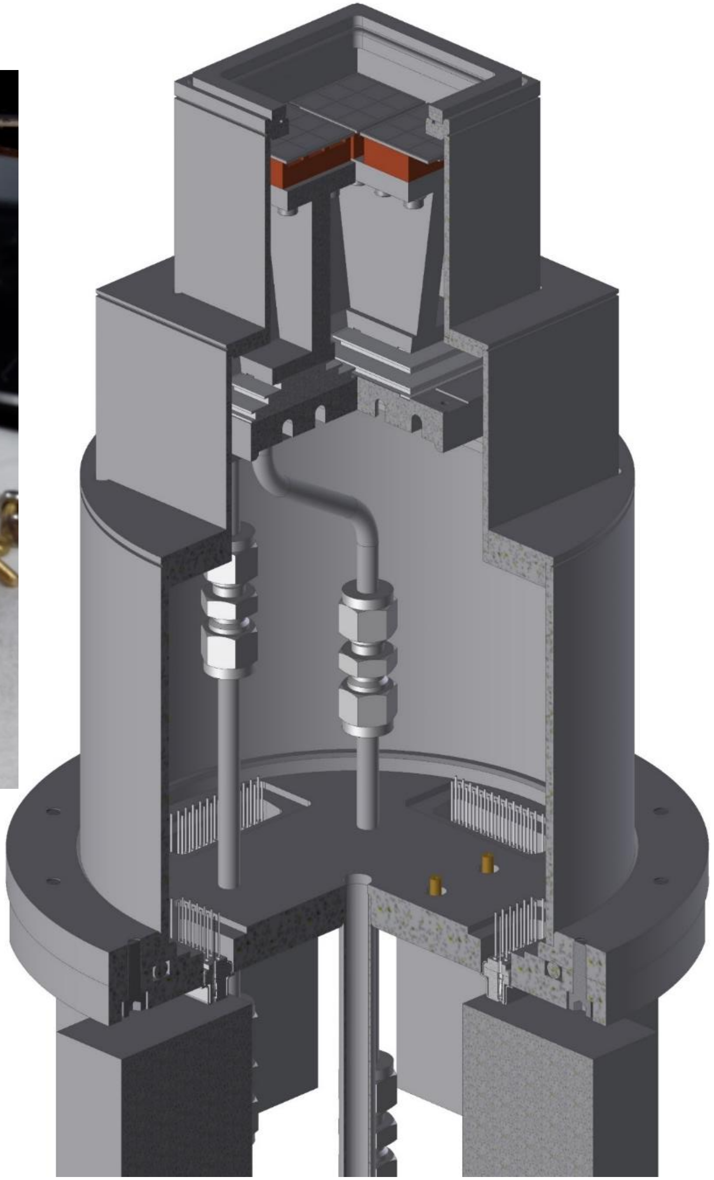

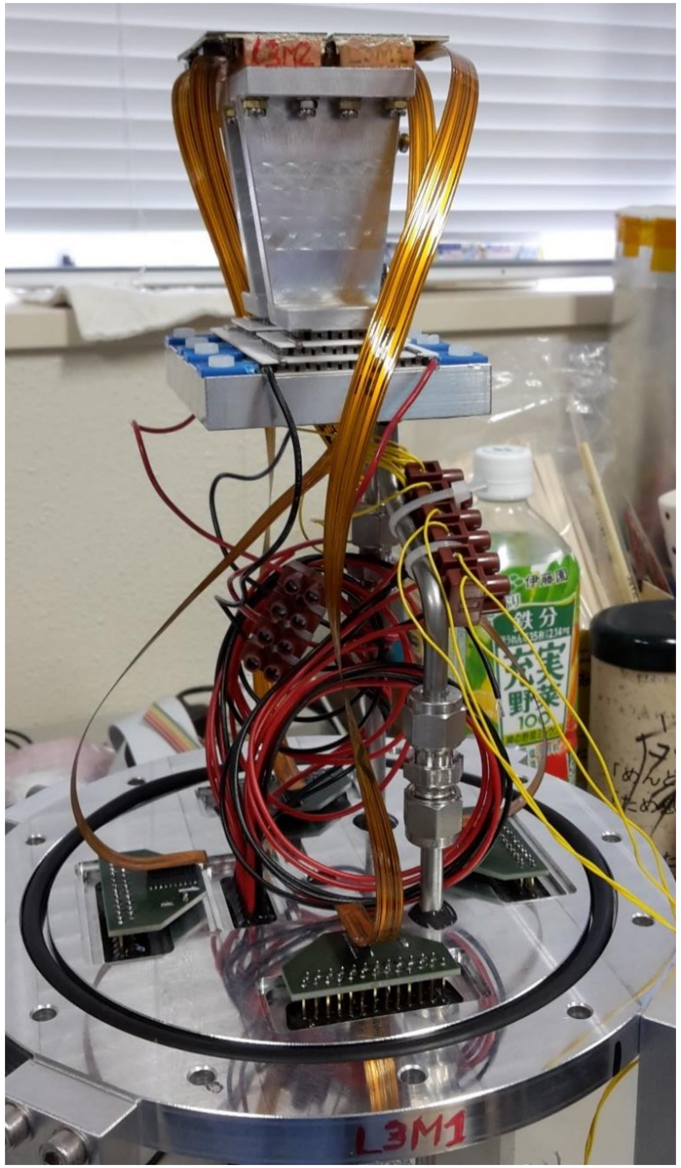

First SDD tests at J-PARC

- SDD calibration Fe-55

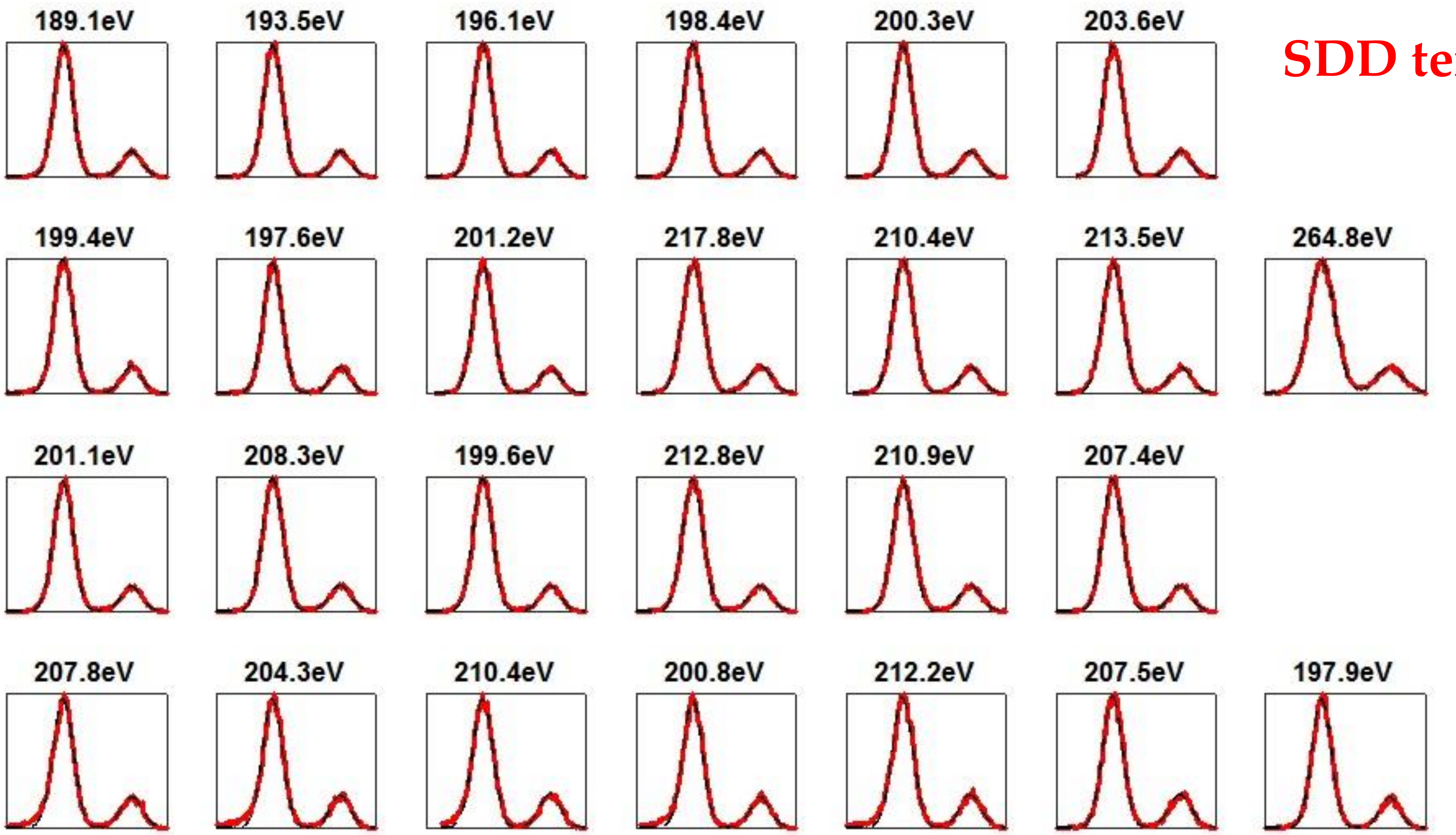

SDD temp. - 40°C

Kaonic Lithium 3→2

- ✓ Sum of all K^{-} runs (0.7 and 0.9 GeV/c)
- ✓ 15.323 ± 0.008 keV ~ 1200 counts
- ✓ resolution 160 eV (sigma)

$K^{-}Li_{L\alpha}$ transition:
15.330 keV (QED)

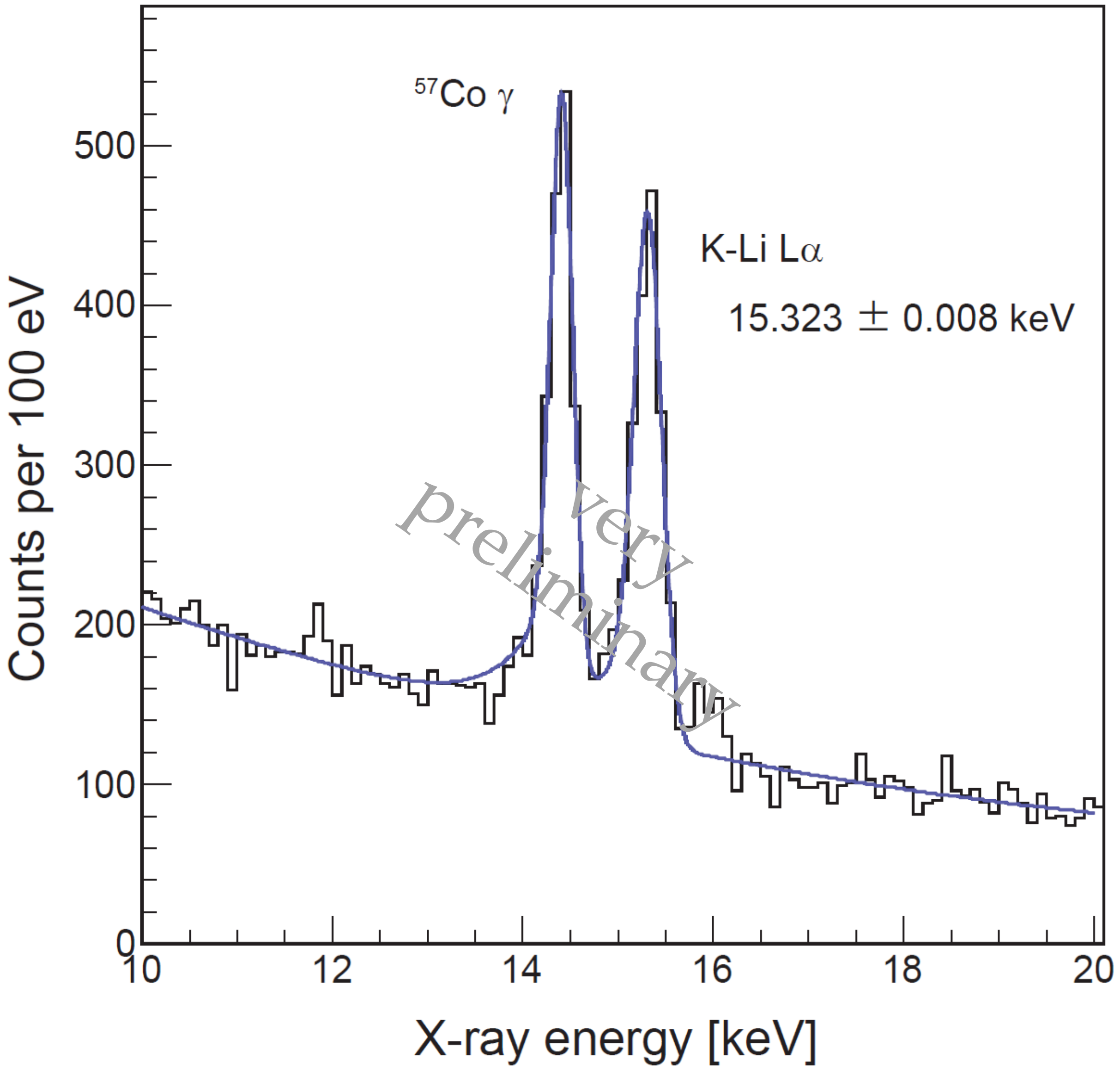

4x2 Silicon Drift Detector array

single cell 8x8 mm^2

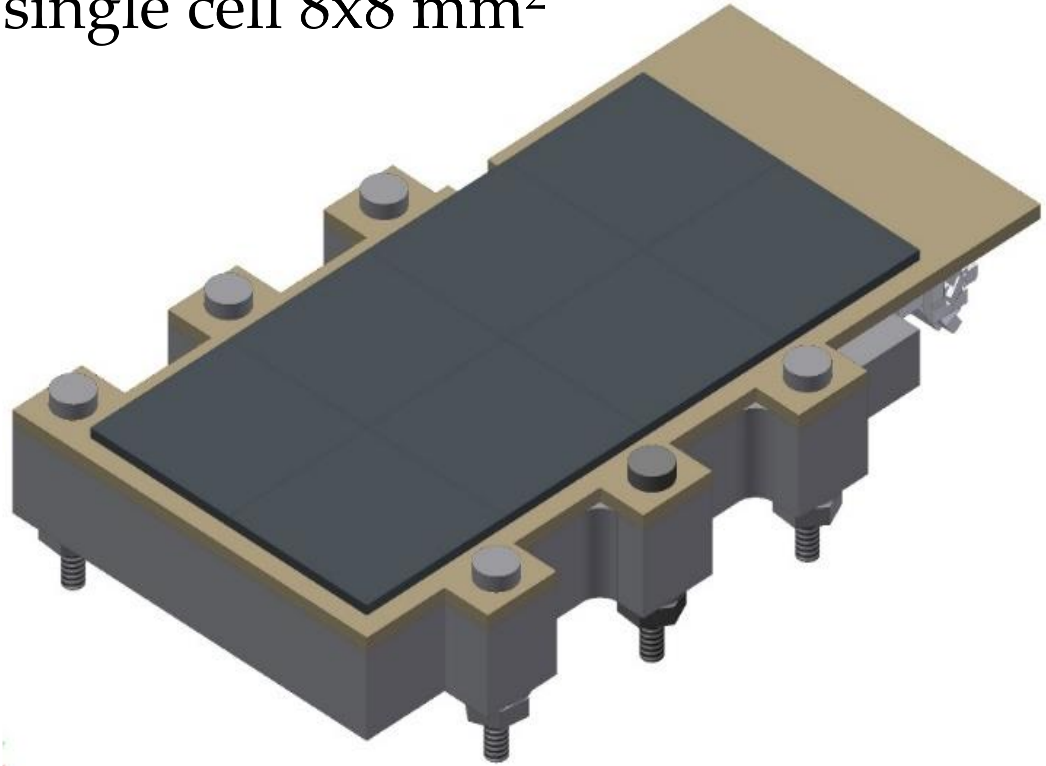

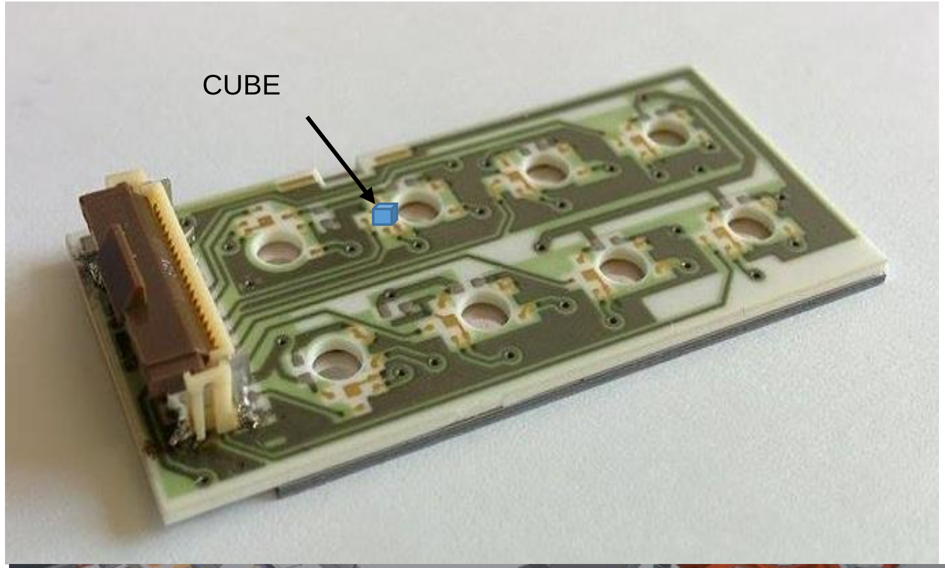

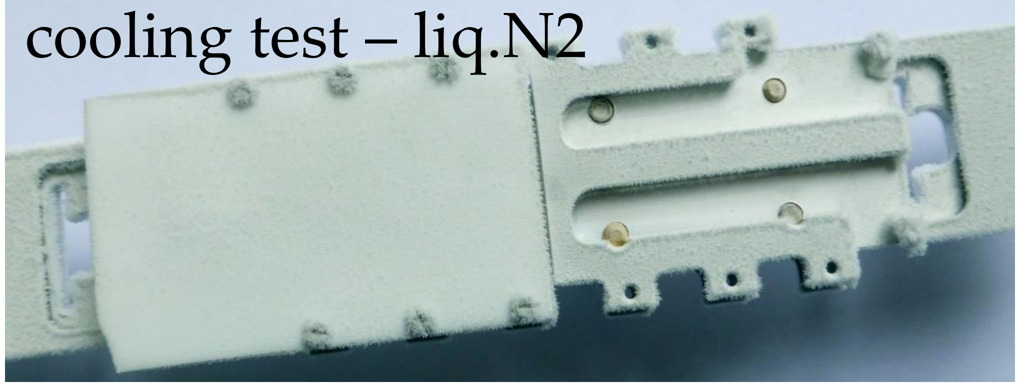

cooling test – liq.N2

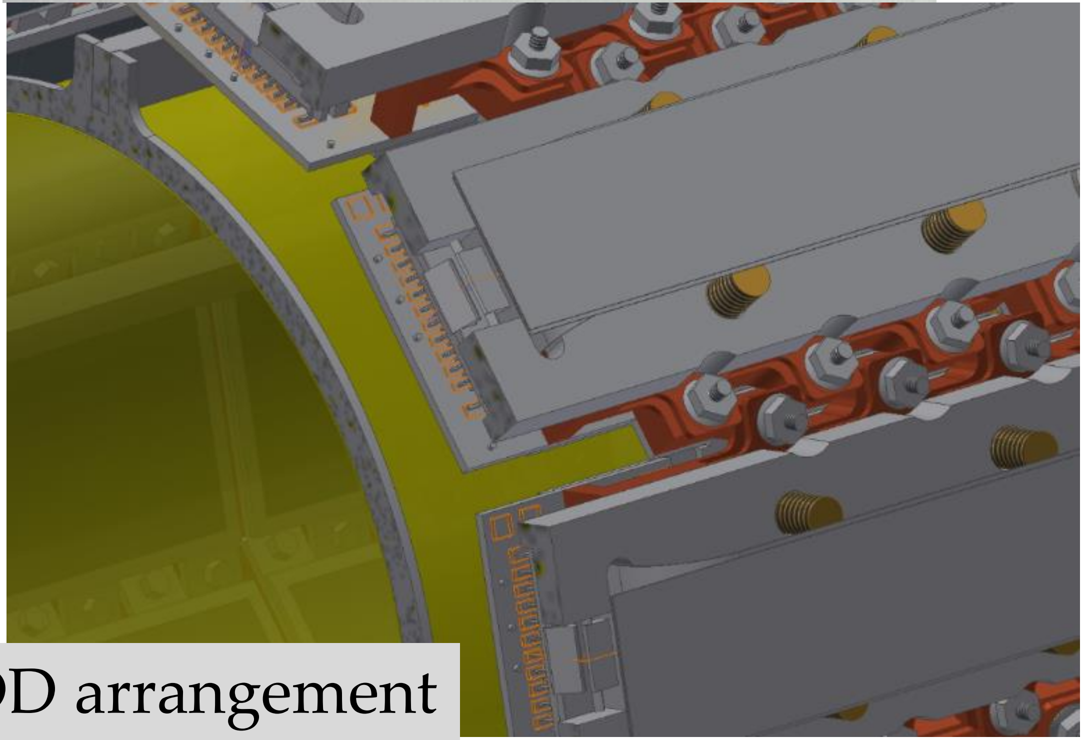

SDD arrangement

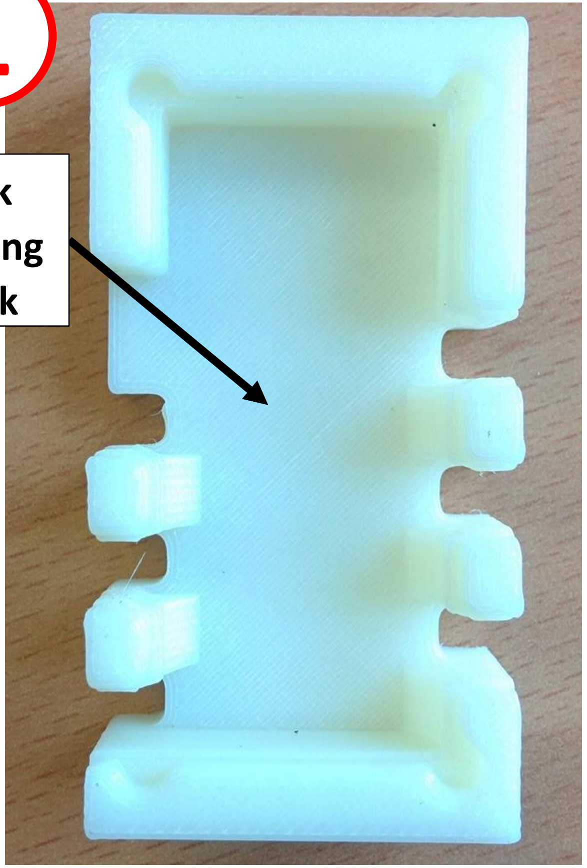

Take the Back bonding block.

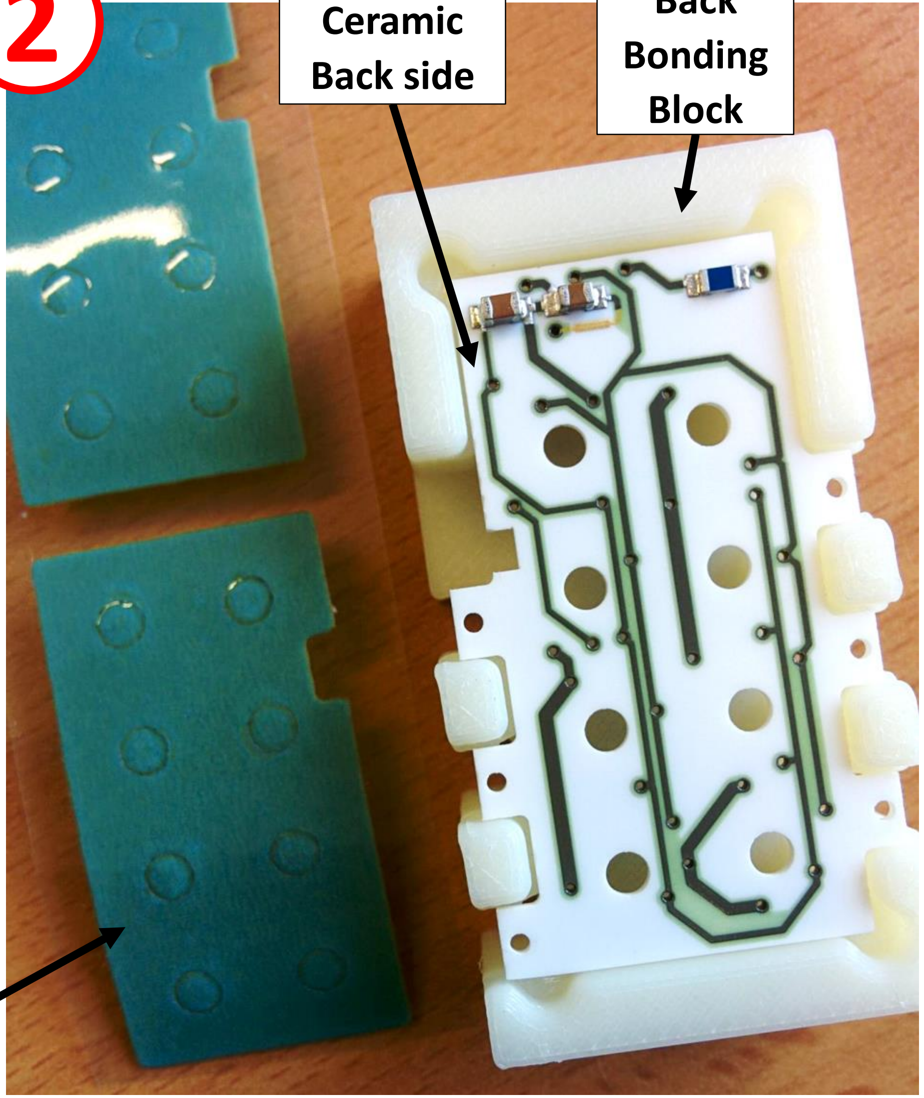

Place the Ceramic board in the back bonding block.

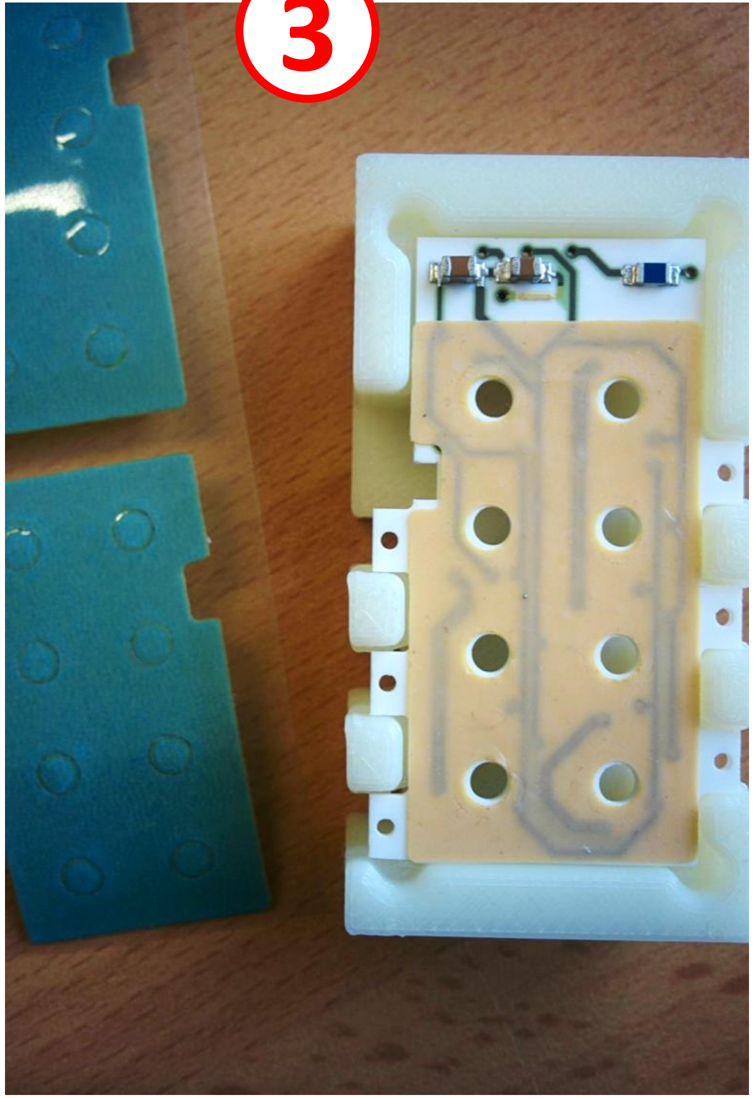

Place the Kapton Biadhesive correctly on the ceramic back side.

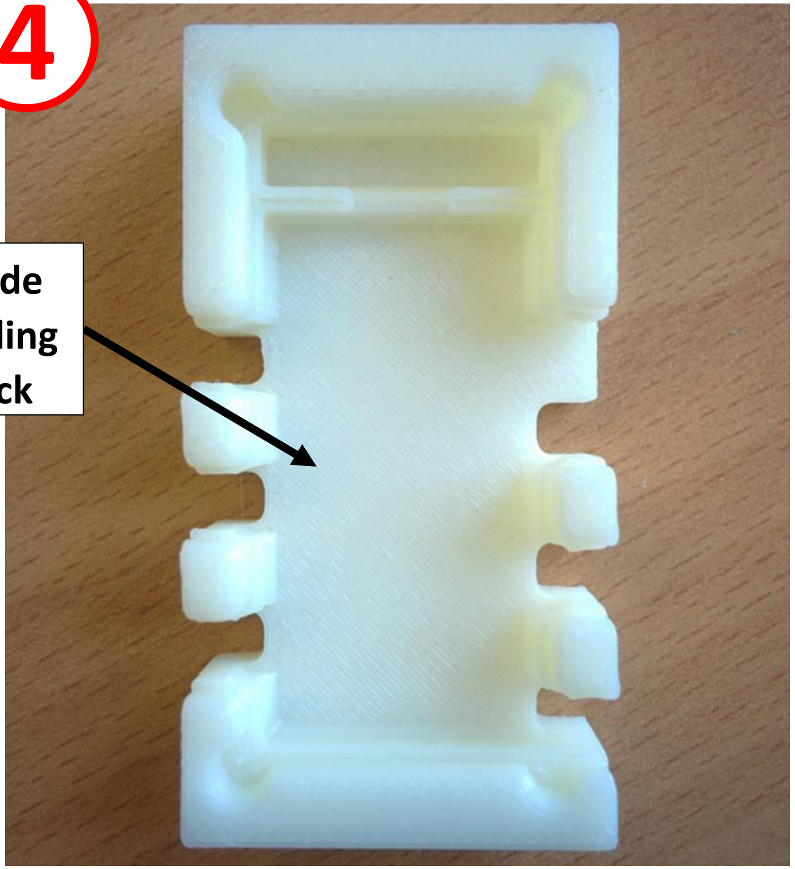

Take the Anode bonding block.

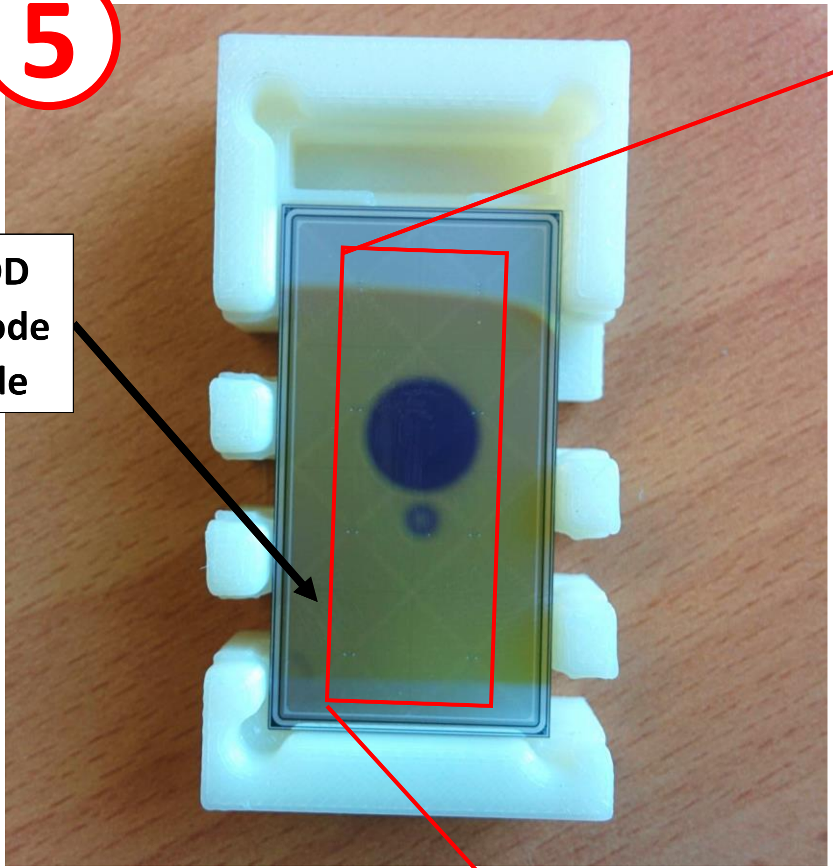

Place the SDD array (anode side up) on the Anode Bonding block with the vacuum pick up tool.

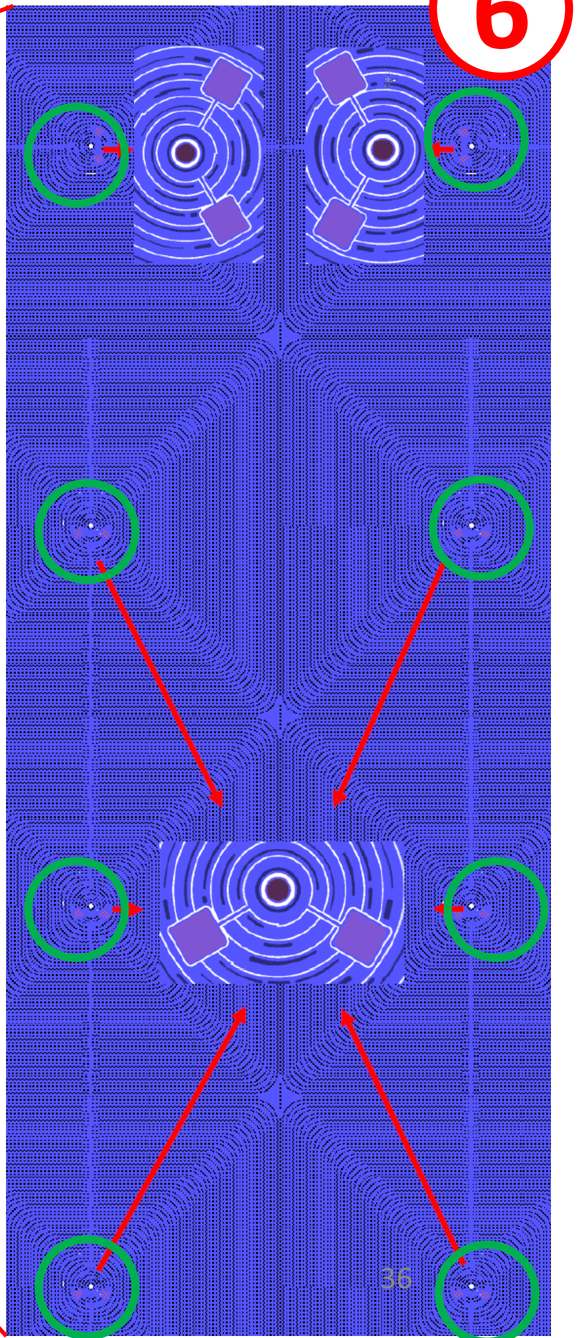

Ensure that the SDD array is facing the correct direction by looking at the Ring 1 bonding pads through the microscope.

7

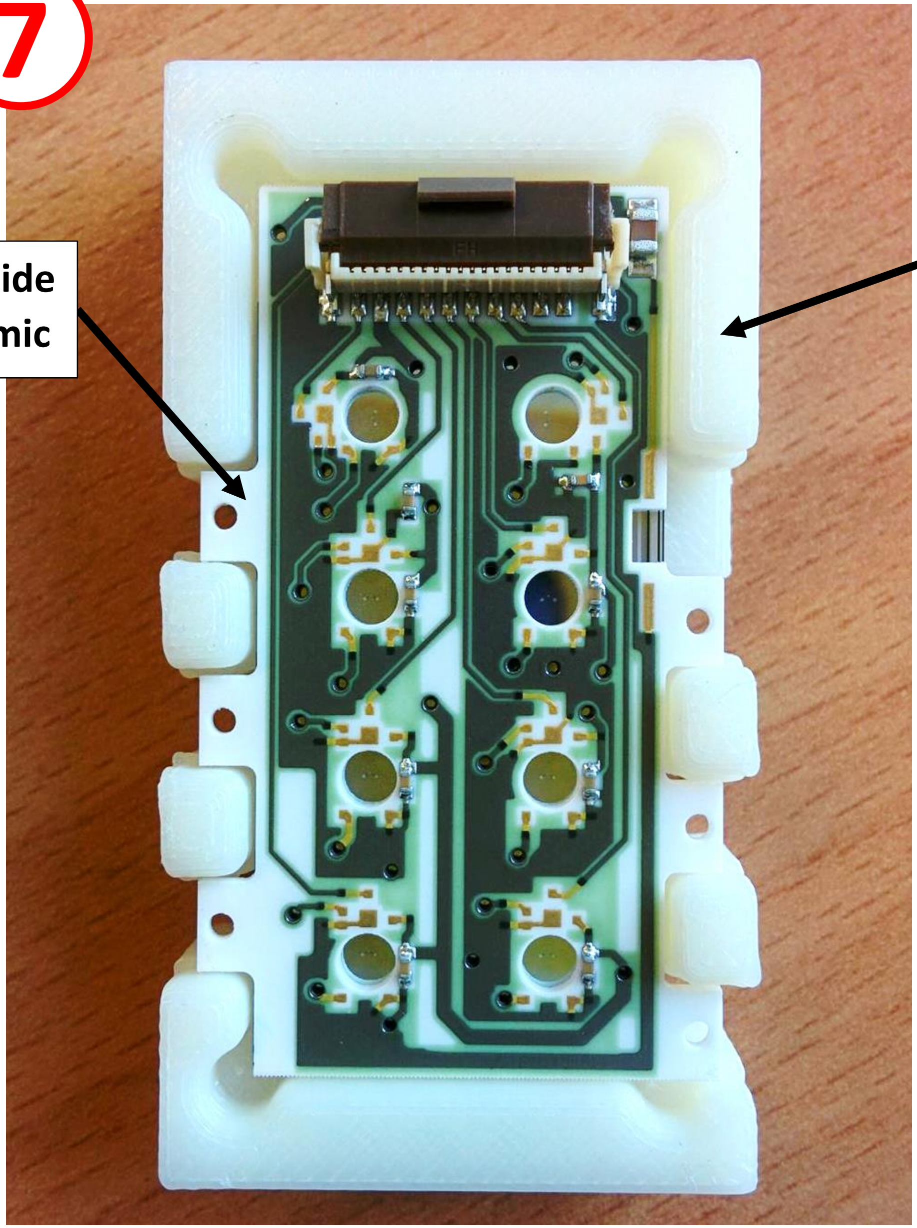

Place the ceramic of step 3 onto the SDD array present in the anode bonding block after step 5 and 6.

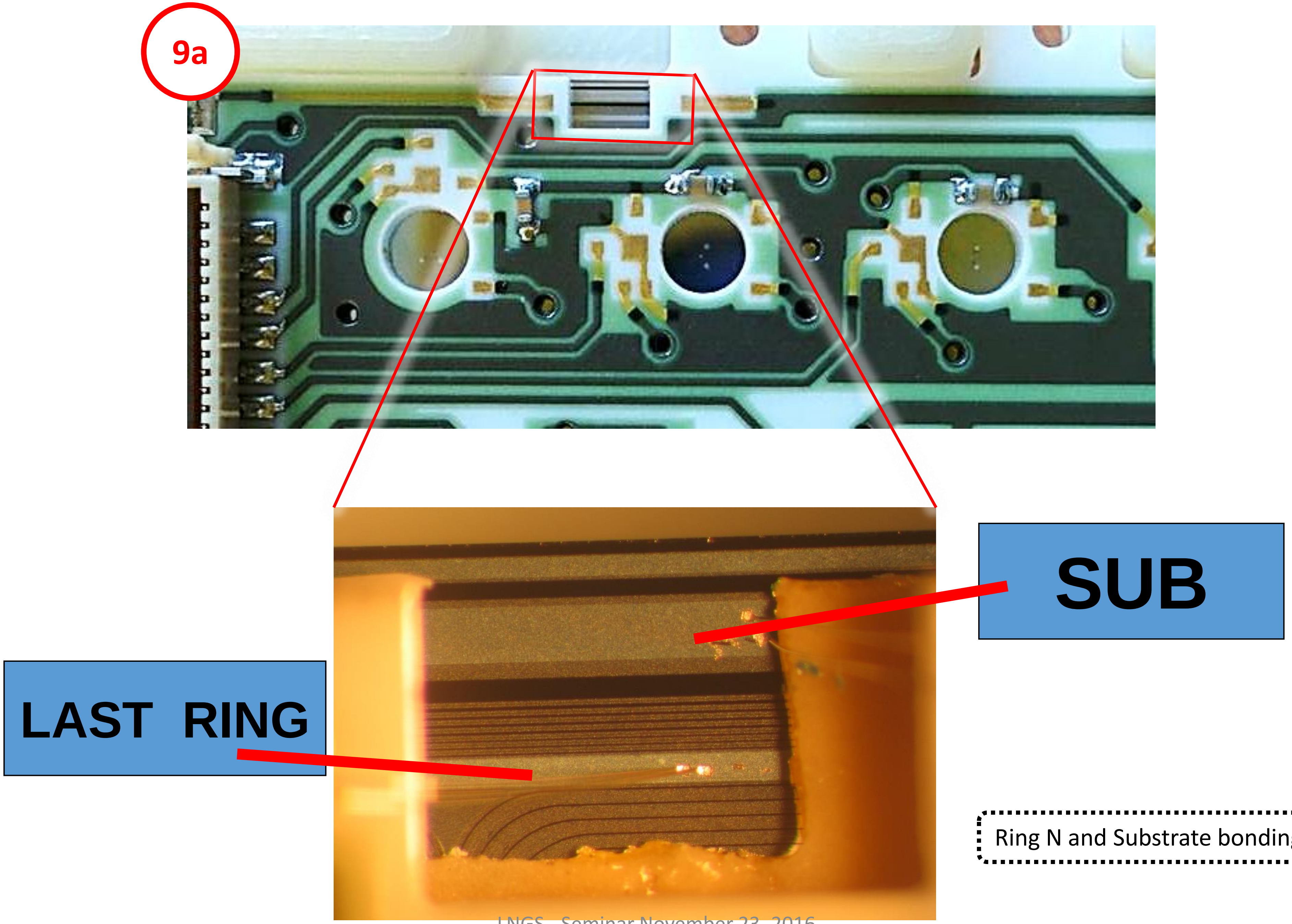

Ring N and Substrate bonding

8

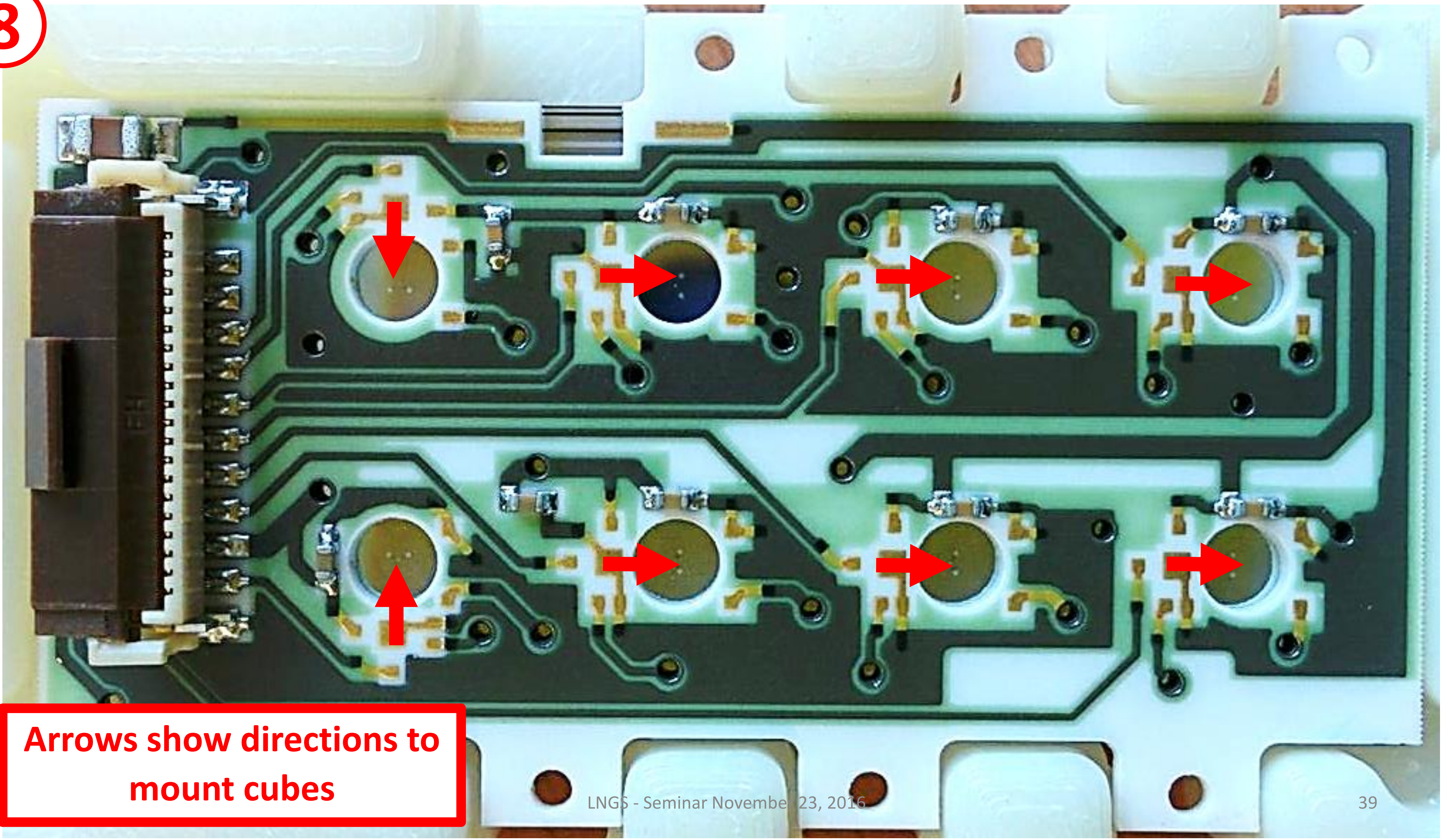

Arrows show directions to mount cubes

9

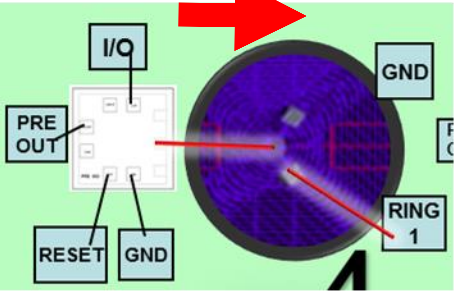

Complete working channel bonding

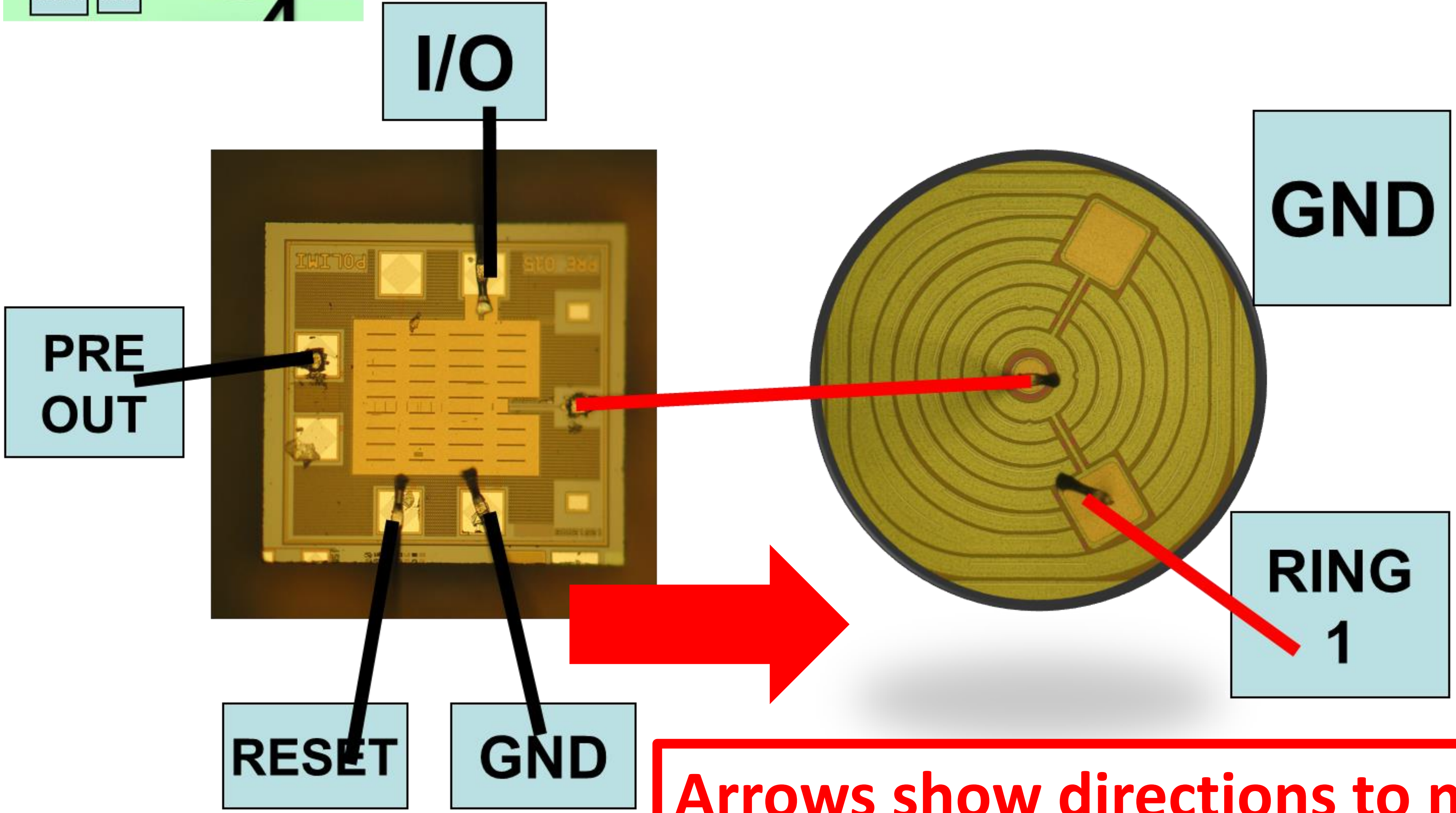

Arrows show directions to mount cubes

10

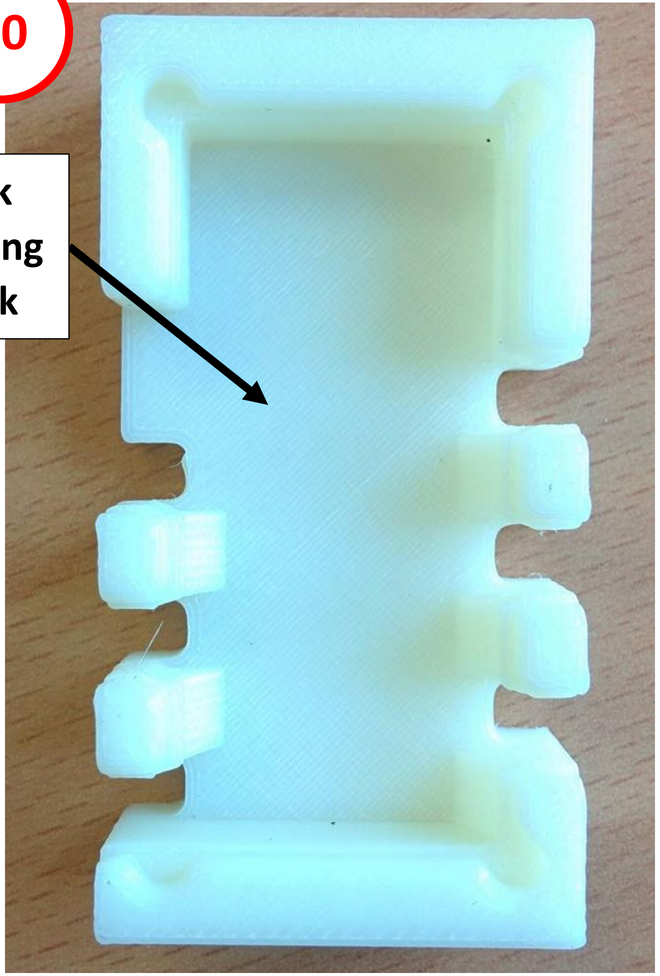

Take the Back bonding block.

11

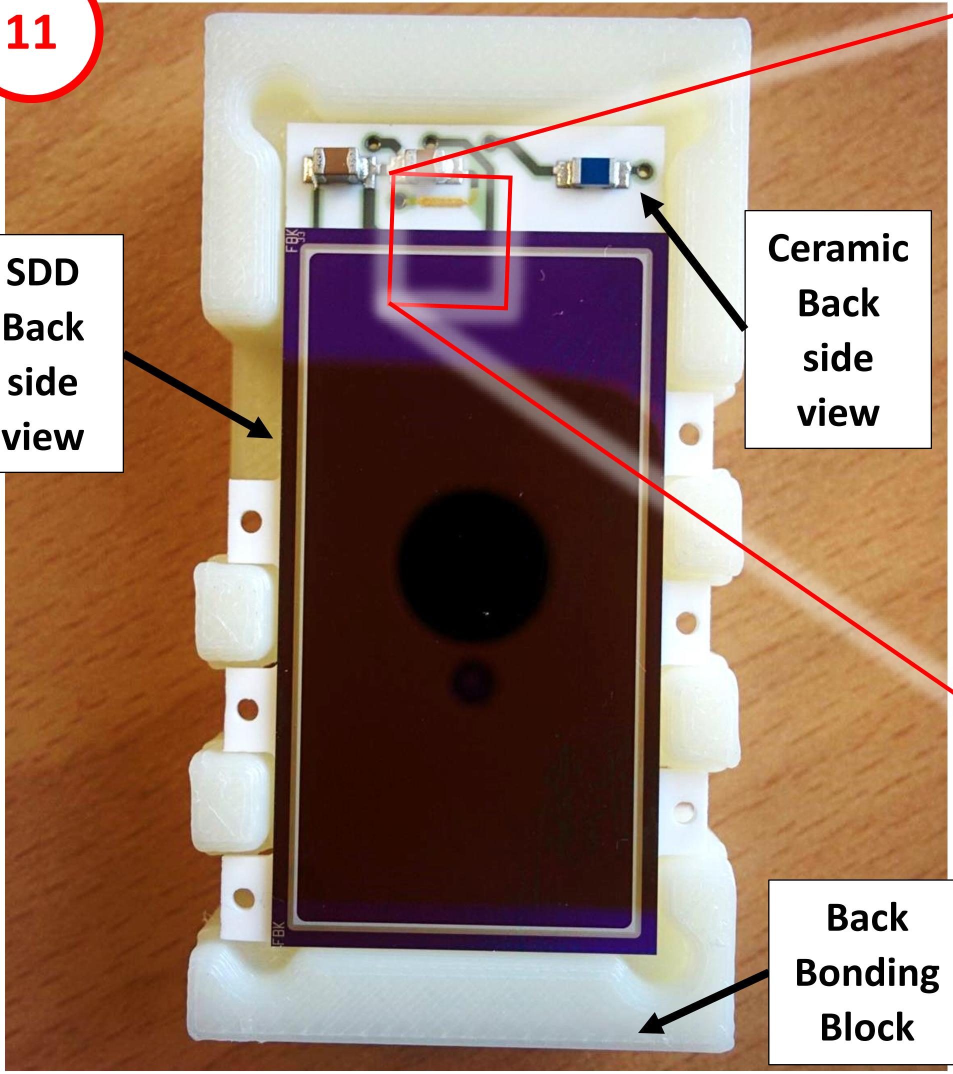

Place the ceramic board with SDD Back side up on the Back bonding block.

12

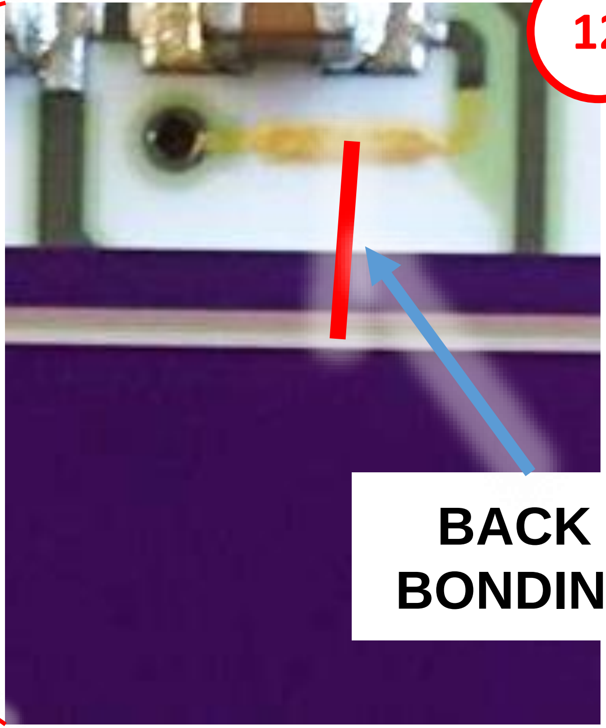

Perform back bonding.

4x2 SDD array cooling test

- 3 cooling cycles
- Cryostat set to 65 K
- Ceramic temperature 73 K
- No visual damage of SDD/ceramic

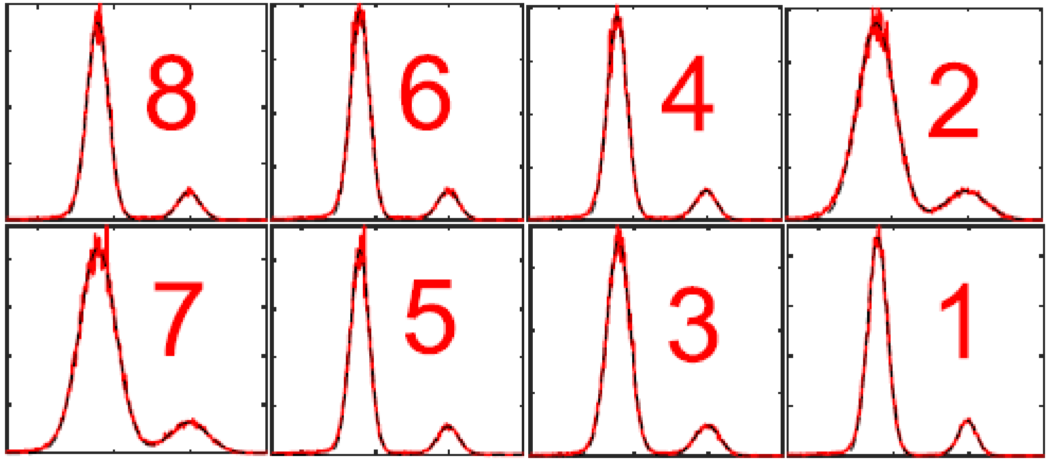

Fig. 5. Eight X-ray spectra acquired by irradiating a 2×4 SDD array with an un-collimated ^{55}Fe X-ray source at a temperature of -30 °C with 3 μs shaping time using.

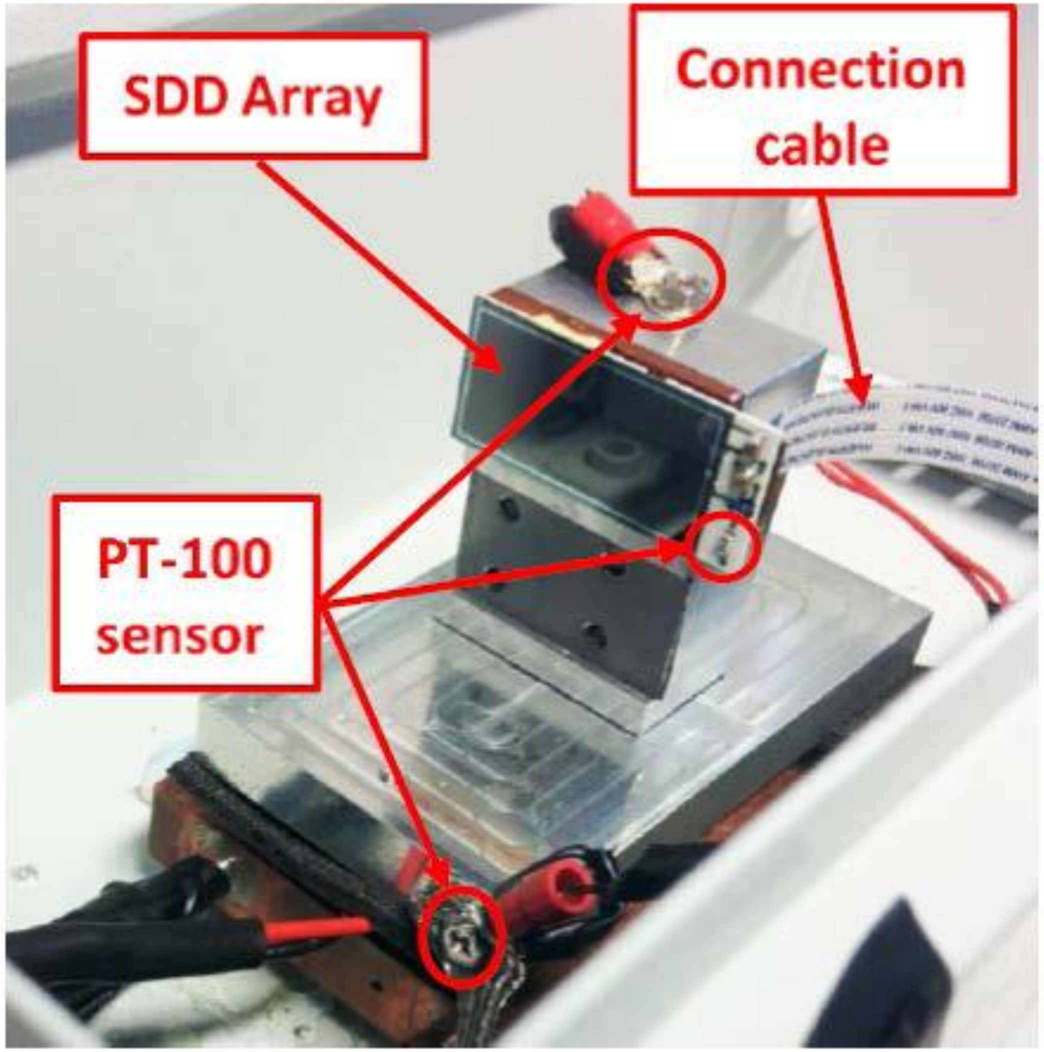

Fig. 4. Experimental setup employing thermoelectric (Peltier) cooling stage to characterize Siddharta-II arrays at a temperature of -30 °C.

New SDD technology: CUBE preamplifier

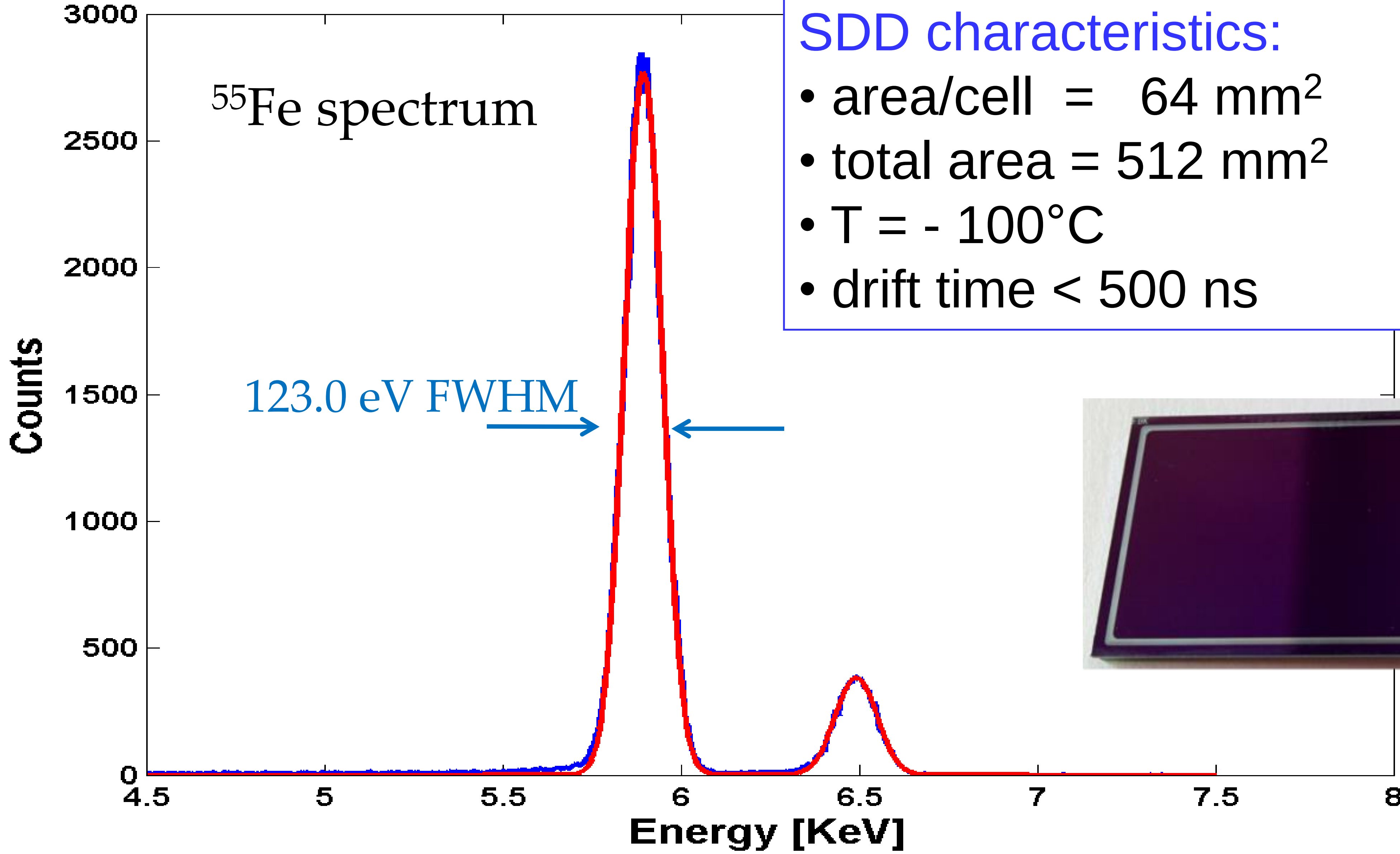

SDD characteristics:

- area/cell = 64 mm^2
- total area = 512 mm^2
- T = - 100°C
- drift time < 500 ns

Kaonic deuterium setup E57 @ J-PARC

cryogenic deuterium gas target
and detector layout:

module with 4 SDD-chips
→ 32 cells

final setup
→ 12 modules

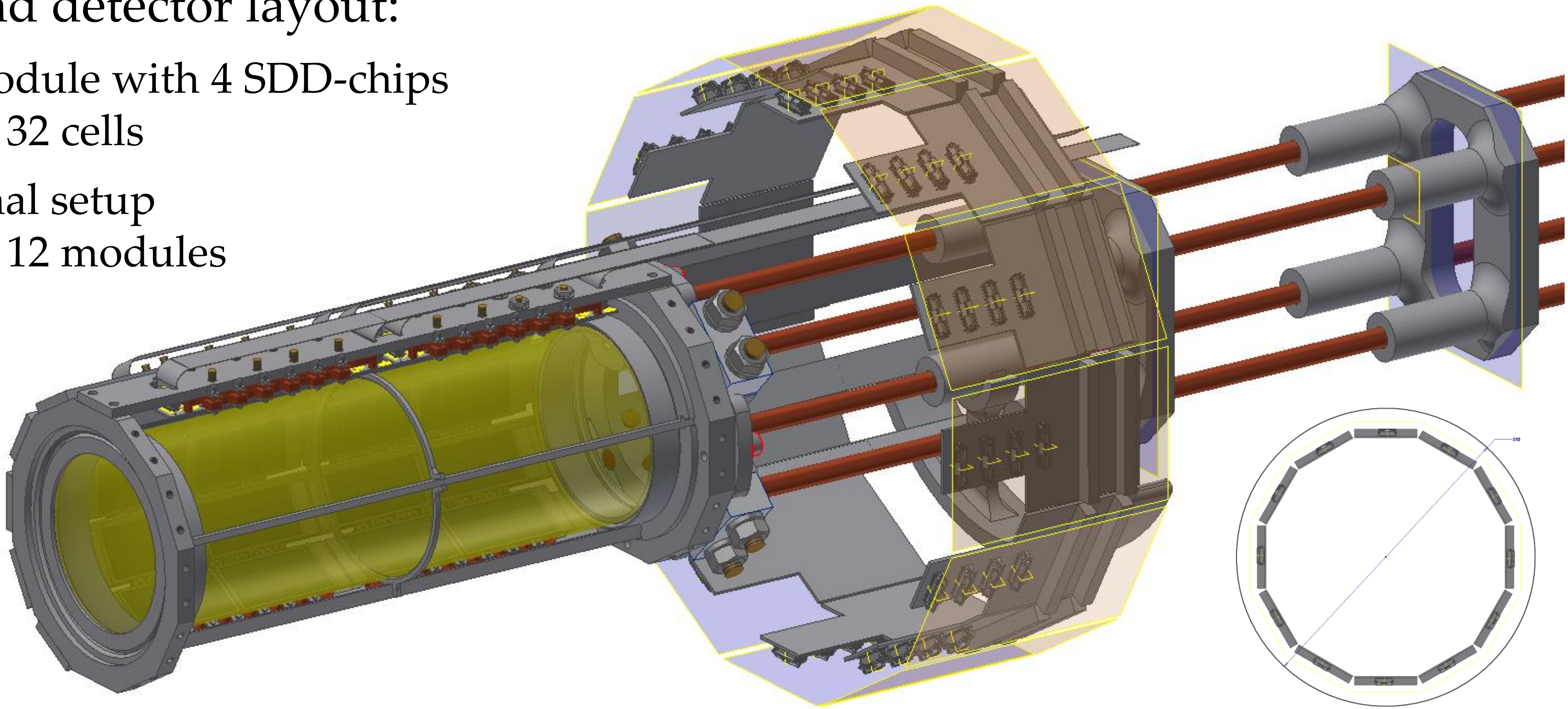

SIDDHARTA-2 setup at DAΦNE

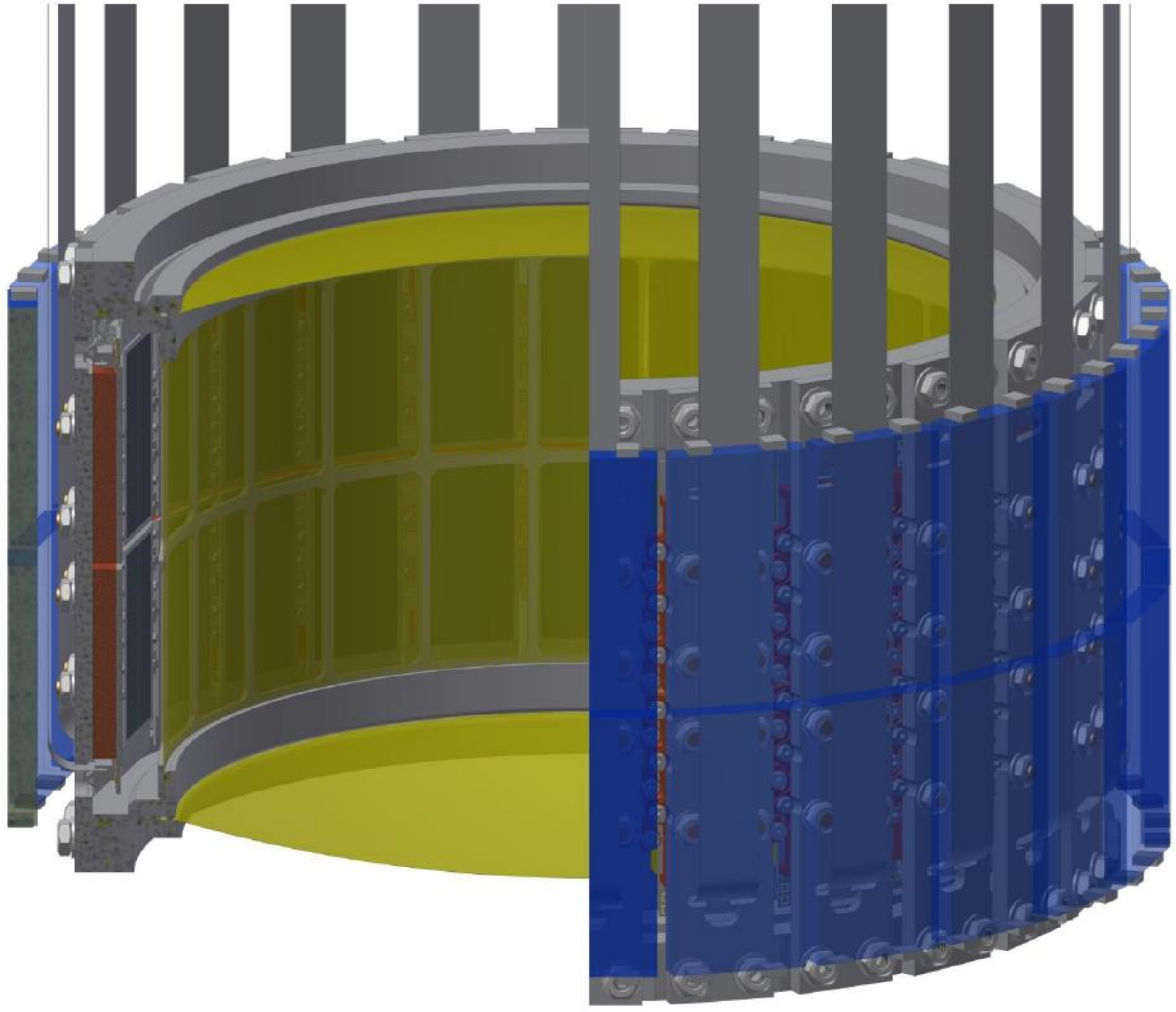

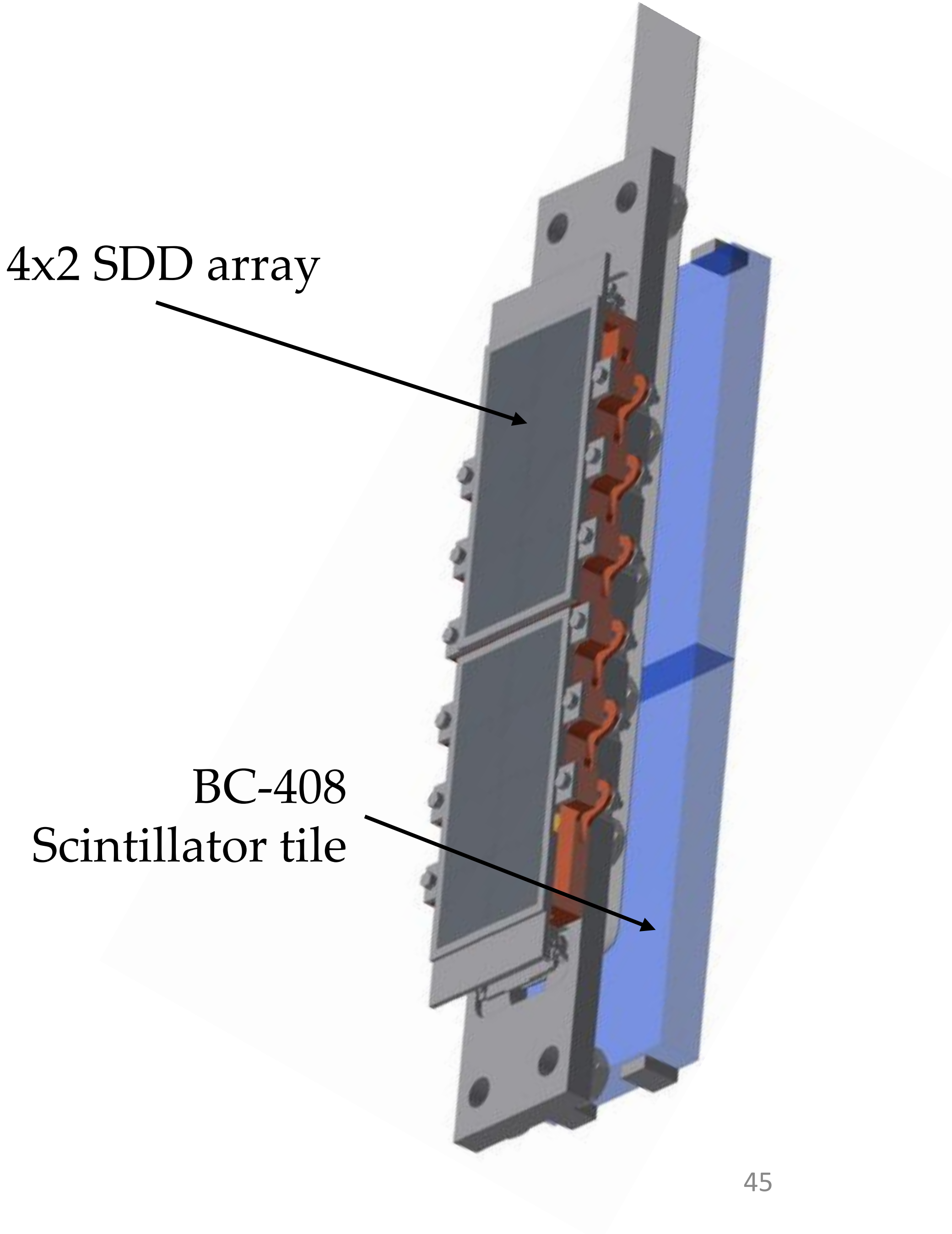

Geant4 simulated $K^{-}d$ X-ray spectrum for 800 pb^{-1}

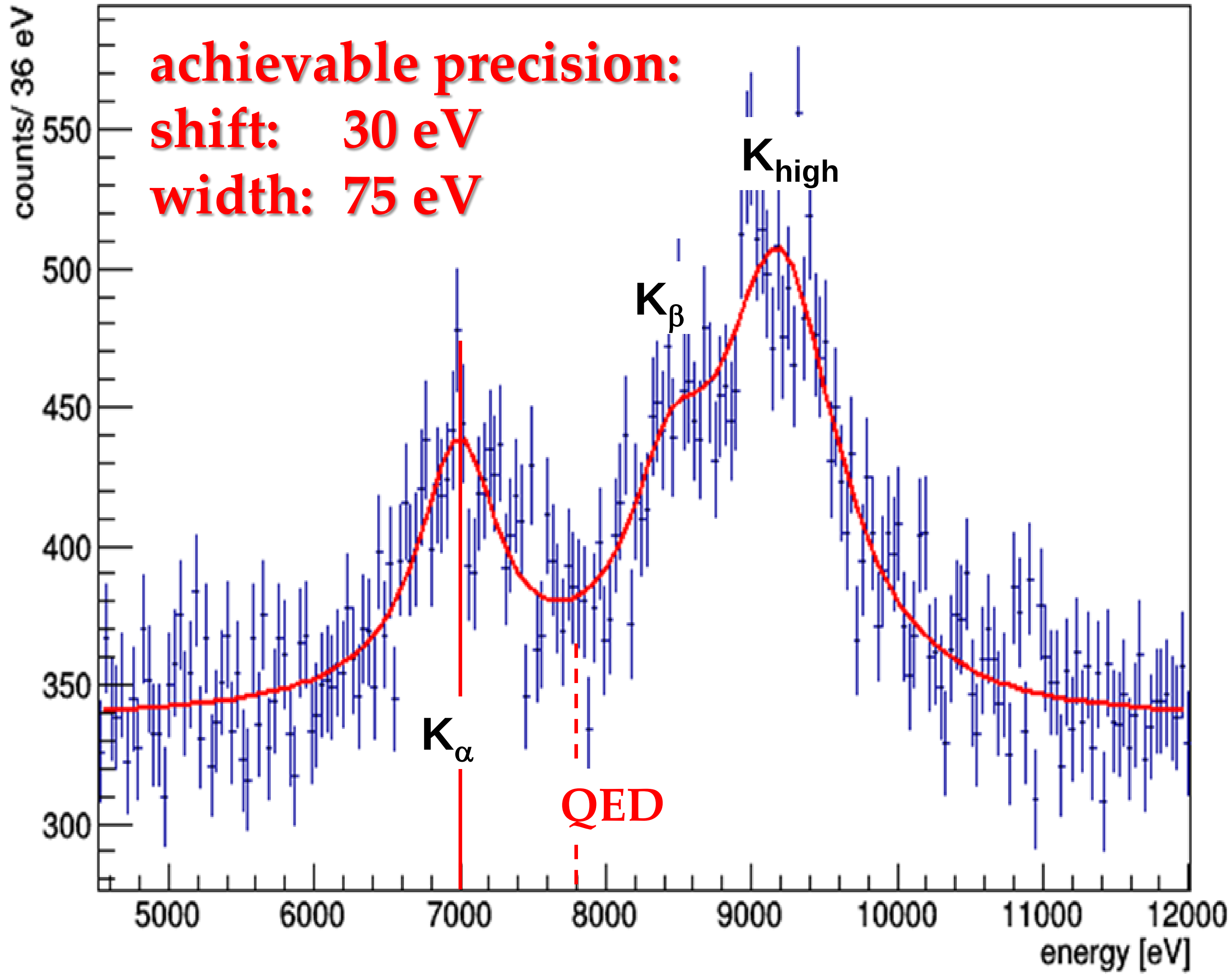

signal: shift - 800 eV
width 800 eV
density: 3% (LHD)
detector area: 246 cm^2

Kα yield: 0.1 %
yield ratio as in $K^{-}p$
S/B ~ 1 : 3

- charged particle veto
- asynchronous BG

Application of SDDs in gamma-ray spectroscopy and imaging

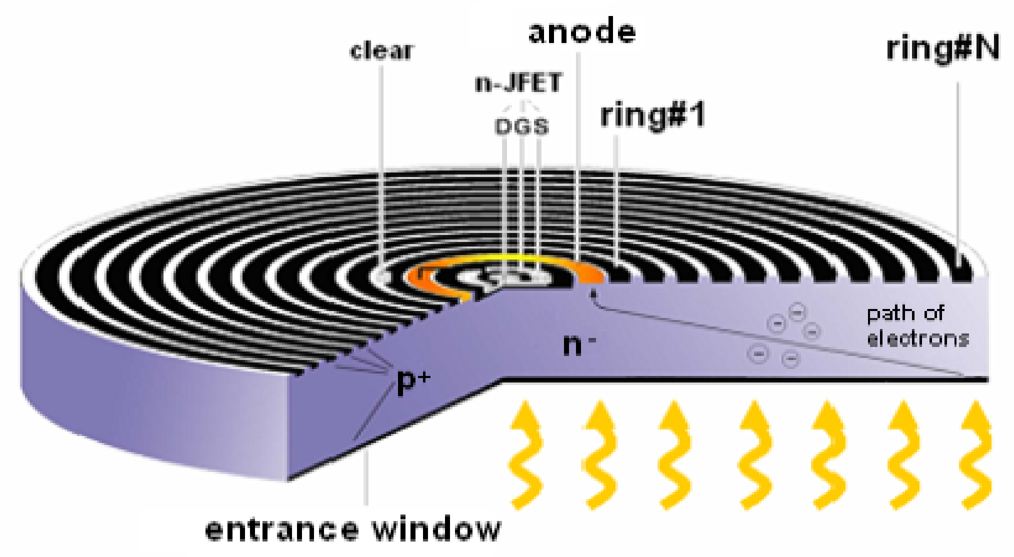

Advantages of SDDs with respect to other photodetectors:

- high quantum efficiency (~ 90 %) @ 565nm of CsI(Tl)
- compact, mechanical robust
- no statistical spread due to multiplication
- low operating voltages
- smaller sensitivity to bias and temperature variations
- insensitivity to magnetic fields

Applications:

- medical imaging
- gamma-ray astronomy
- homeland security
- nuclear physics experiments

Gamma-ray spectroscopy with an SDD coupled to $LaBr_3$

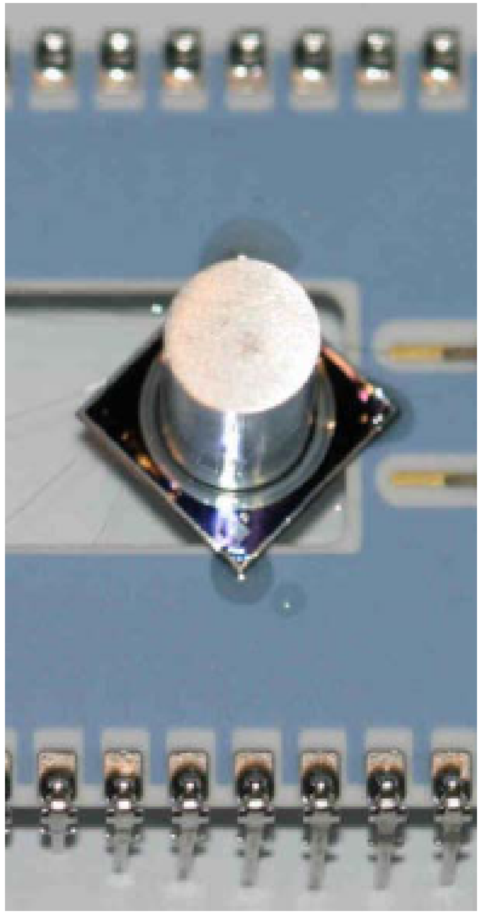

- 30mm² SDD
- Brillance 380
  5mm Ø,
  5mm thick

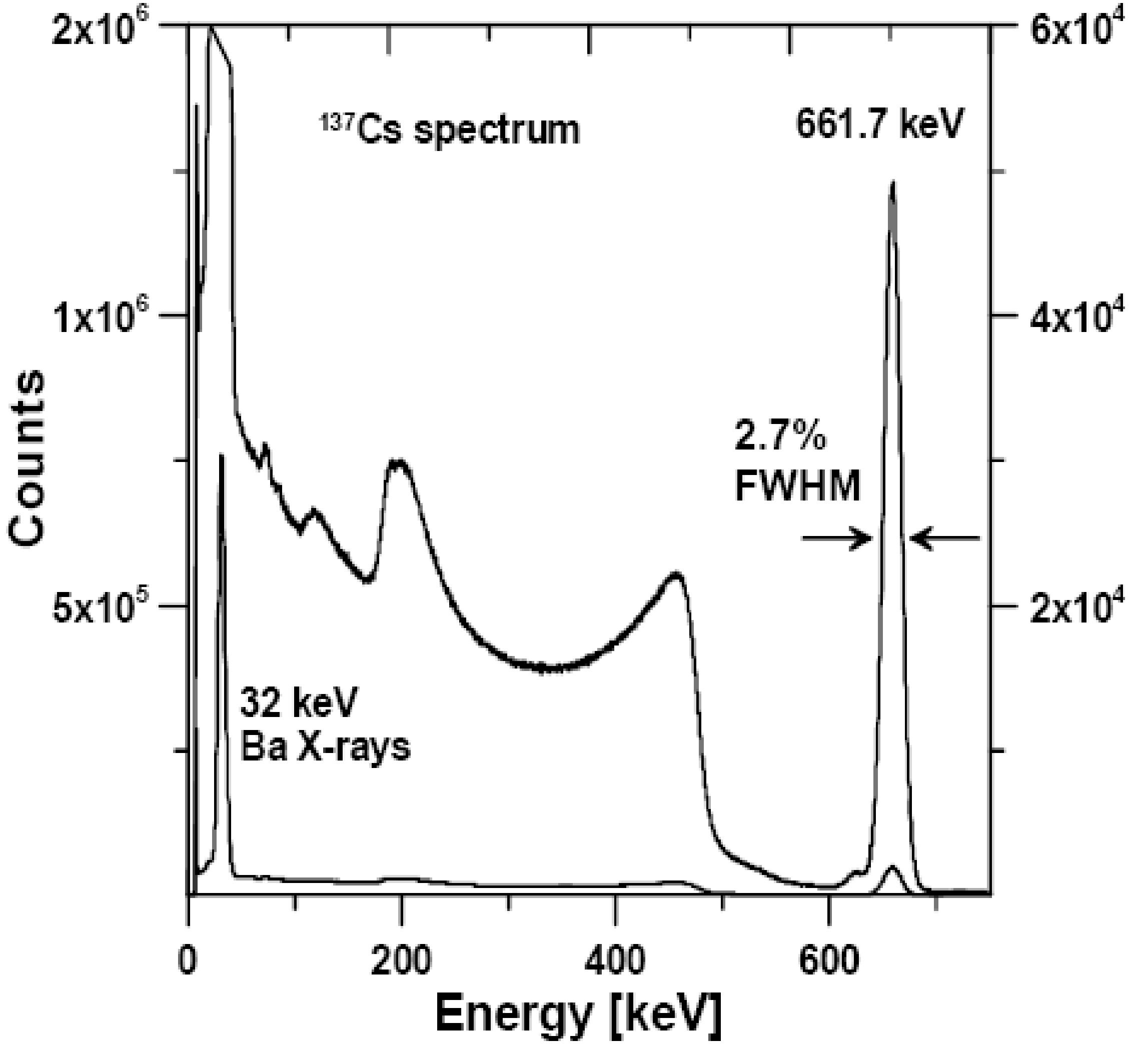

Drastic improvement in resolution

FWHM ~ 150 eV

Effective area :
1 SDD : 100 mm^2
8 SDDs = 800 mm^2 in total

FWHM ~ 5 eV

Effective area :
1 pixel : 300 x 320 μm^2
240 array ~ 23 mm^2 in total

Comparison: Silicon Drift Detector – Transition Edge Sensor

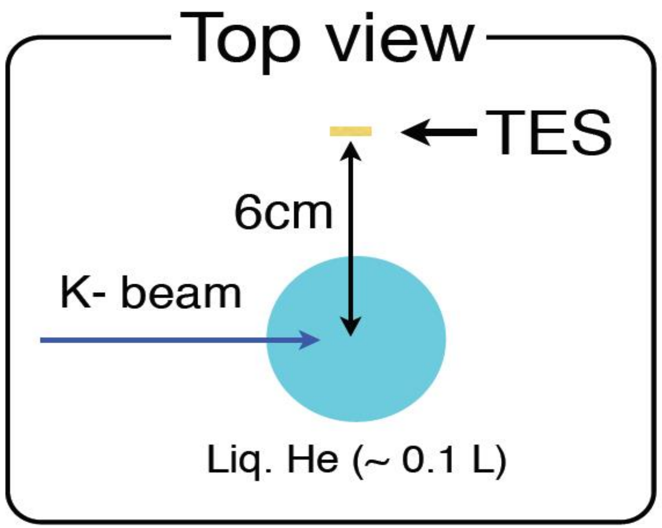

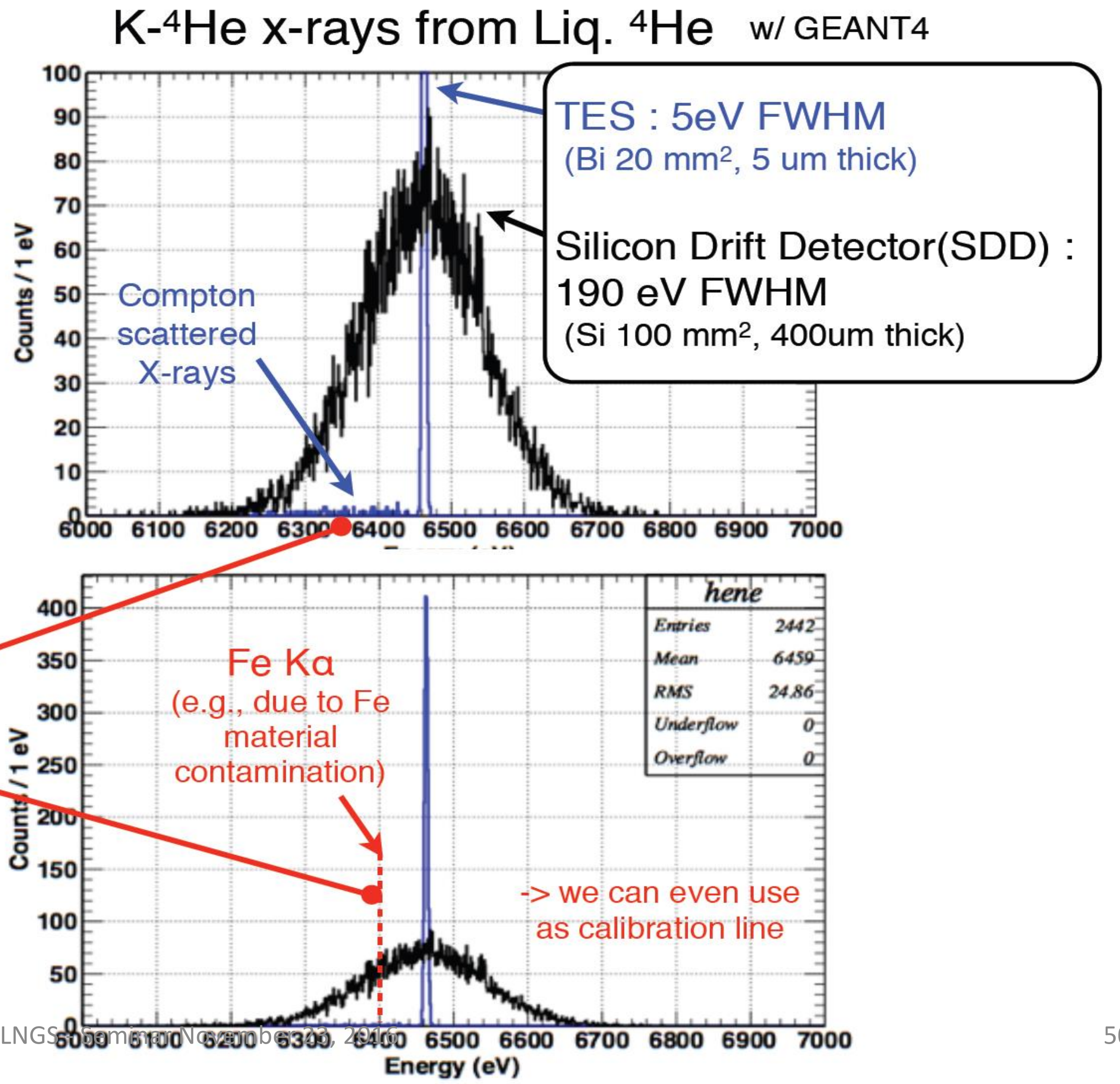

well separated from
"Compton scattered X-rays"
and "Fe Ka energy".

Both have been serious problems
in the prev. experiments.

Transition-Edge-Sensor microcalorimeters

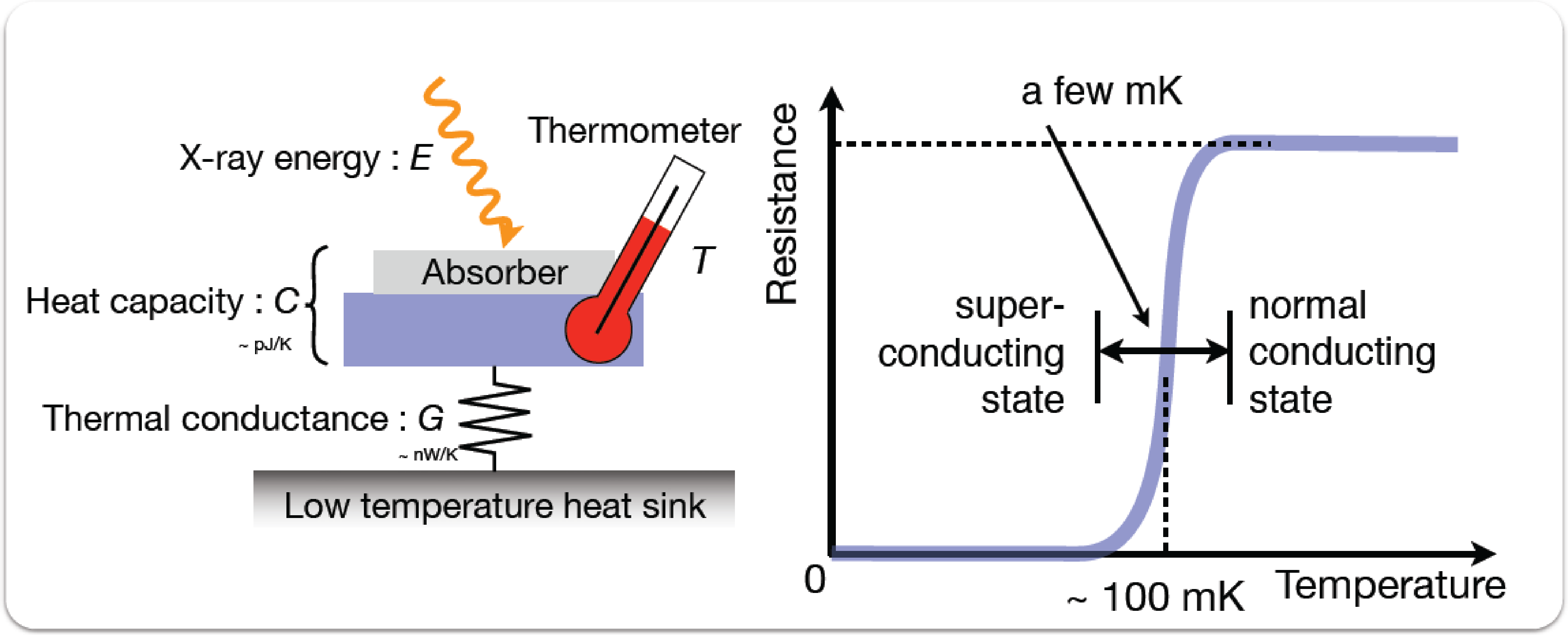

✓ Excellent energy resolution ~2 eV FWHM@ 6 keV

✓ Wide dynamic range possible

Breakthrough in energy resolution!

c.f. Silicon detectors: 150 eV FWHM @ 6 keV

TES micro-calorimeter

a thermal detector measures the energy of an incident X-ray photon
as a temperature rise (= E/C ~ 1 mK)

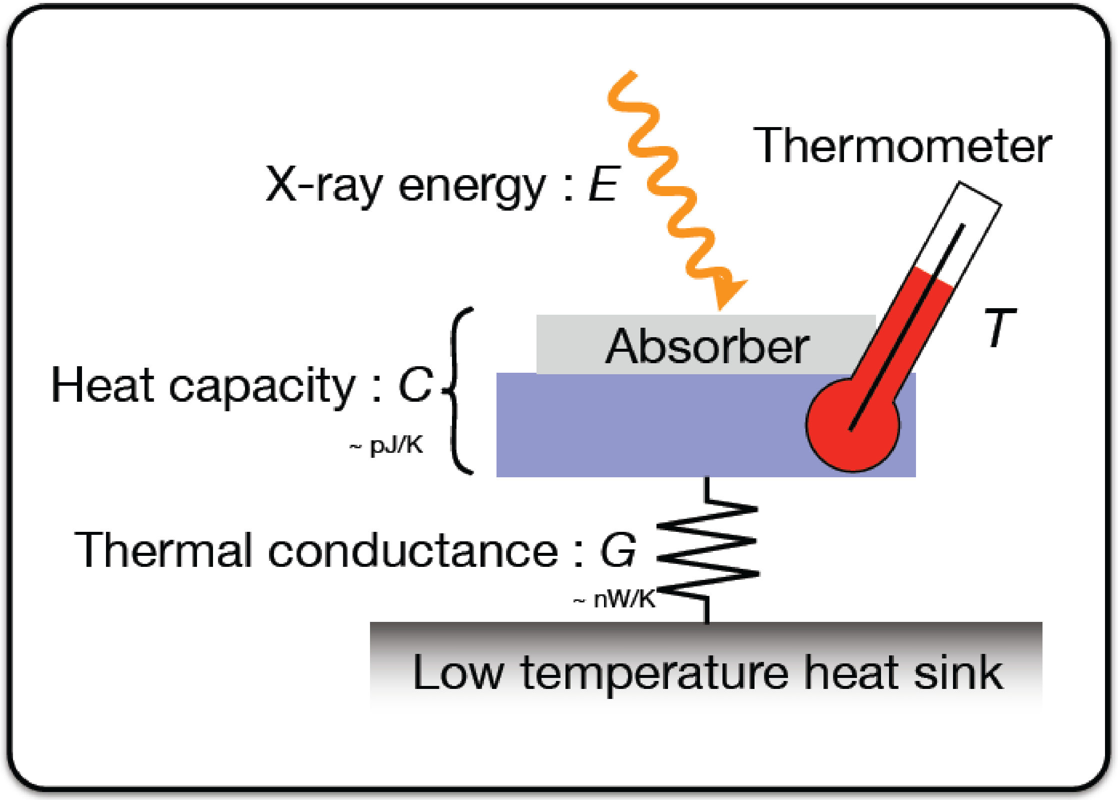

Decay time constant
= C / G (~ 500 µs)

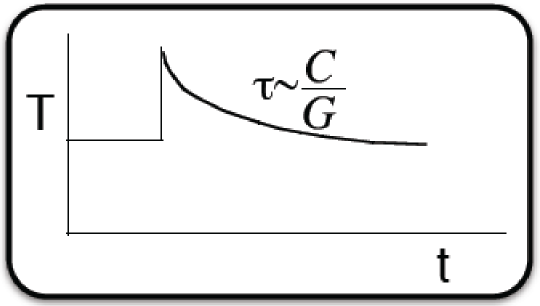

Absorber with larger "Z" (to stop higher energy X-rays),
e.g. Bi (320 µm × 300 µm, 4 µm thick)
Thermometer : thin bi-layer film of Mo (~65nm) and Cu (~175nm)

TES = Transition Edge Sensor

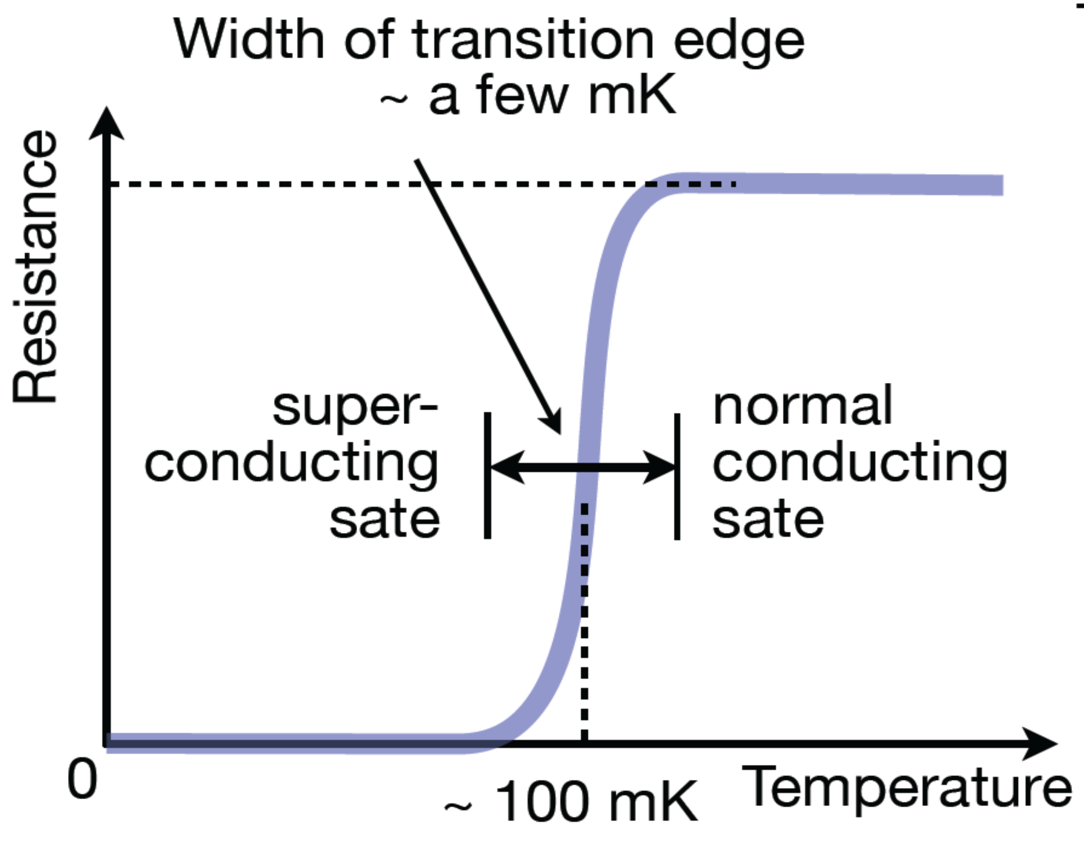

--> developed by Stanford / NIST at the beginning

Thermometer sensitivity

$$\alpha \equiv \frac{d\ \ln R}{d\ \ln T} \sim 10^{2\sim3}$$

Energy resolution (σ)

$$\Delta E = \sqrt{\frac{k_B T^2 C}{\alpha}}$$

(Johnson noise and phonon noise are the most fundamental)

Dynamic range

$$E_{max} \sim C T_C / \alpha$$

Trade-off between dynamic range and energy resolution : $\Delta E \sim \sqrt{E_{max}}$

applications : astrophysics (space satellite) etc.

- using the sharp transition between normal and superconducting state to sense the temperature

NIST TES system

J.N. Ullom et al., Synchrotron Radiation News, Vol. 27, 24 (2014)

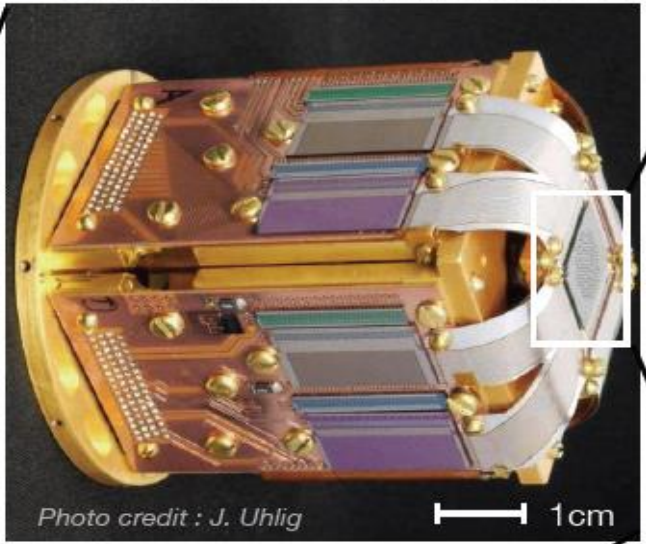

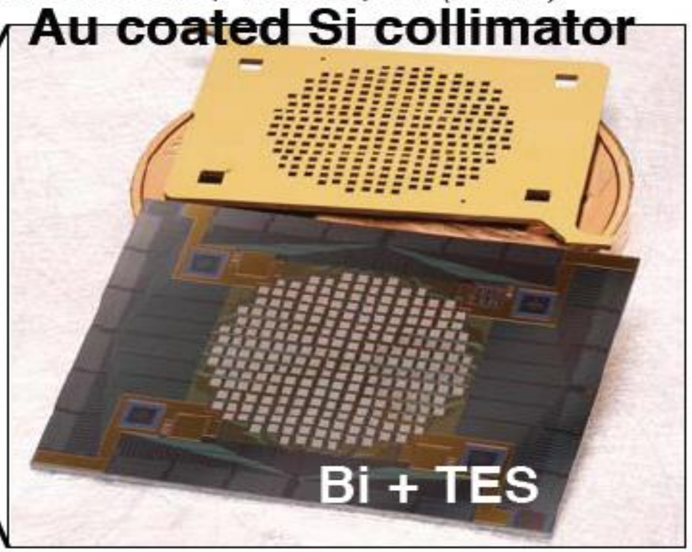

- **50mK cryostat**
  - Pulse tube (60K, 3K) + ADR (1K, 50mK)
  - ADR hold time: > 1 day
  - Manufactured by High Precision Devices, Inc.
- **Detector snout**
  - 240 pixel Mo-Cu bilayer TES
    30 ch TDM(time division multiplexing) readout
  - 1 pixel : 300 x 320 um^2 → total ~ 23 mm^2
  - 4 um Bi absorber → efficiency ~0.85@6 keV

Mn Kα spectrum

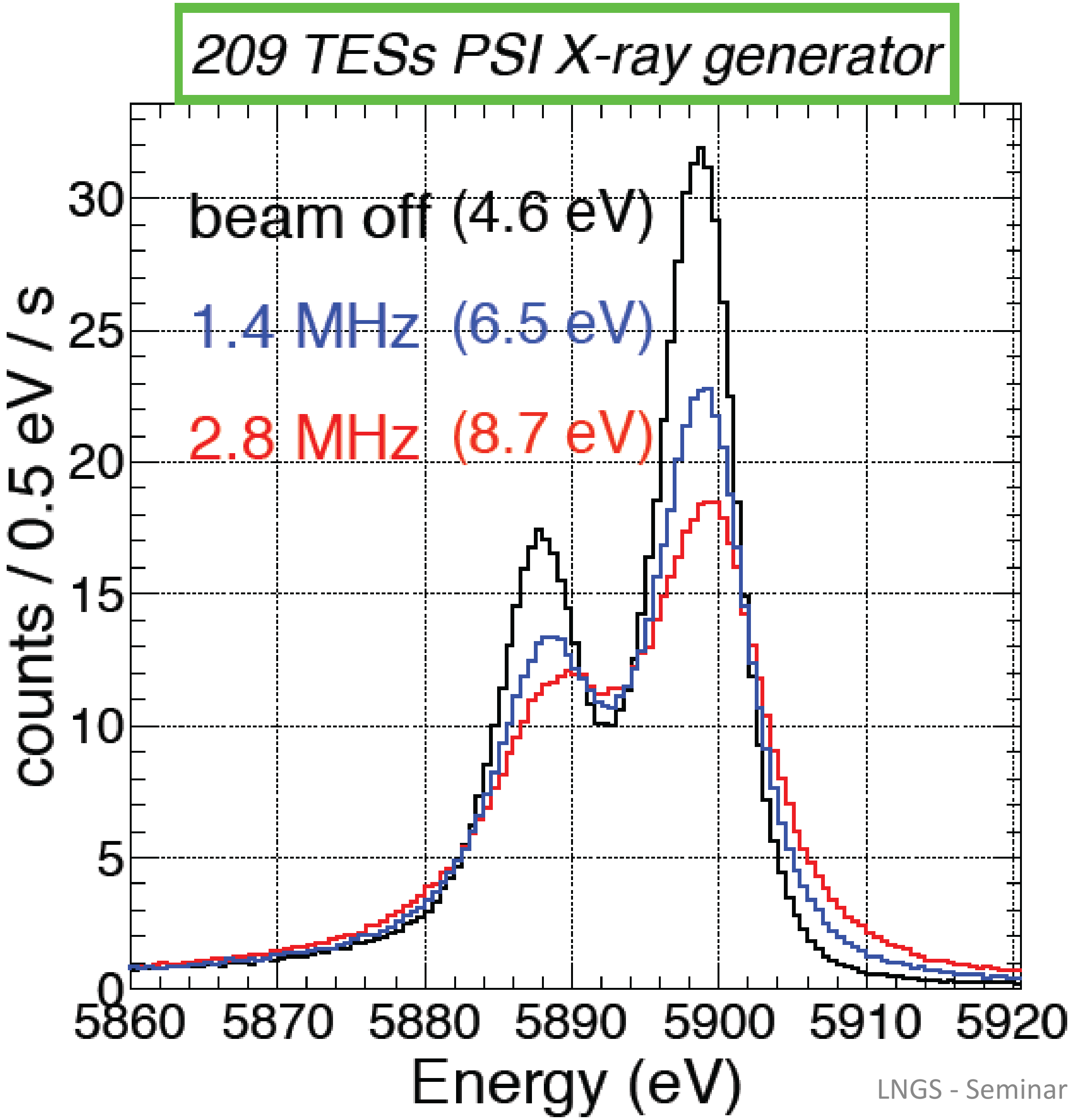

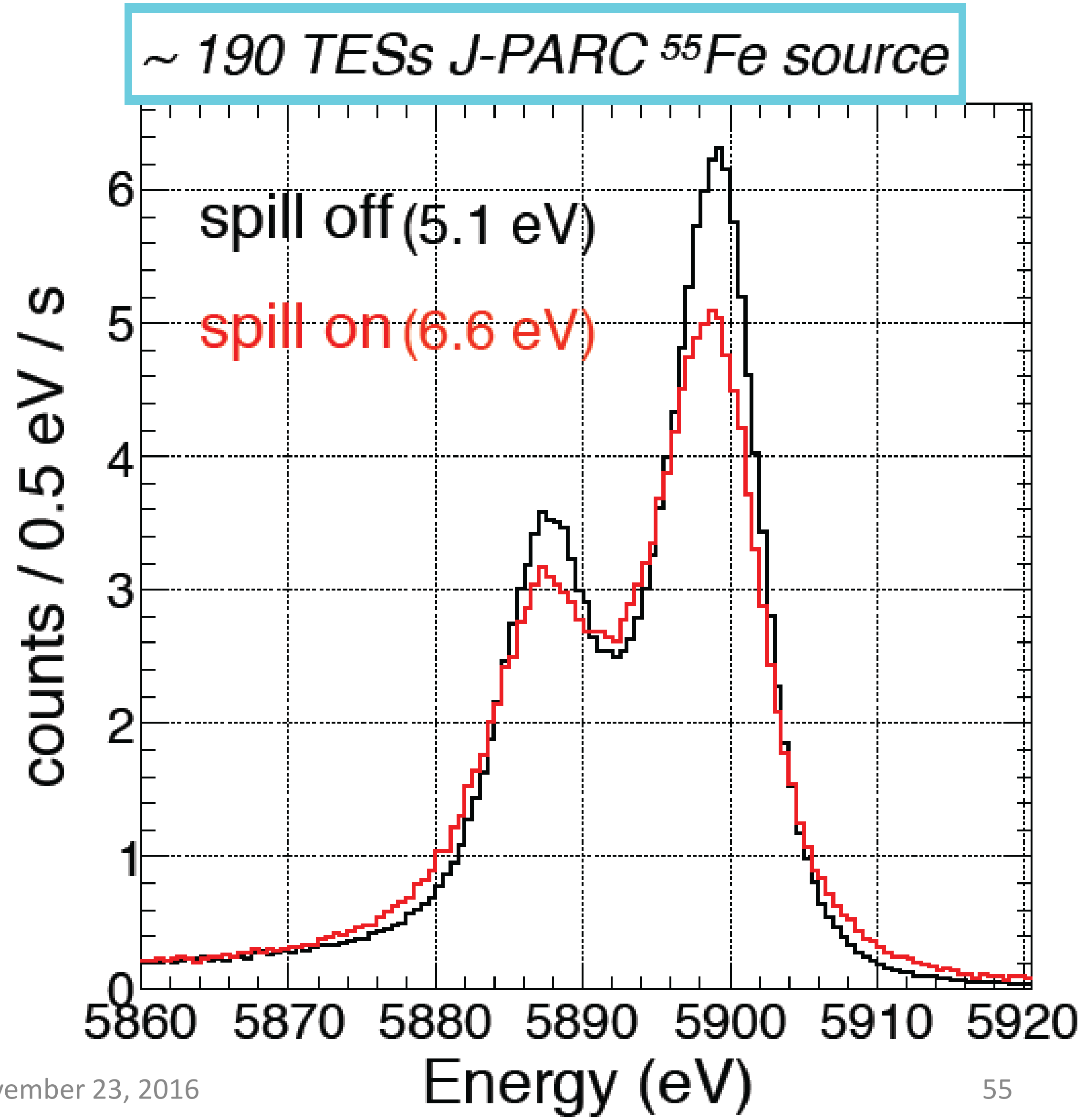

PSI – TES tested with pions

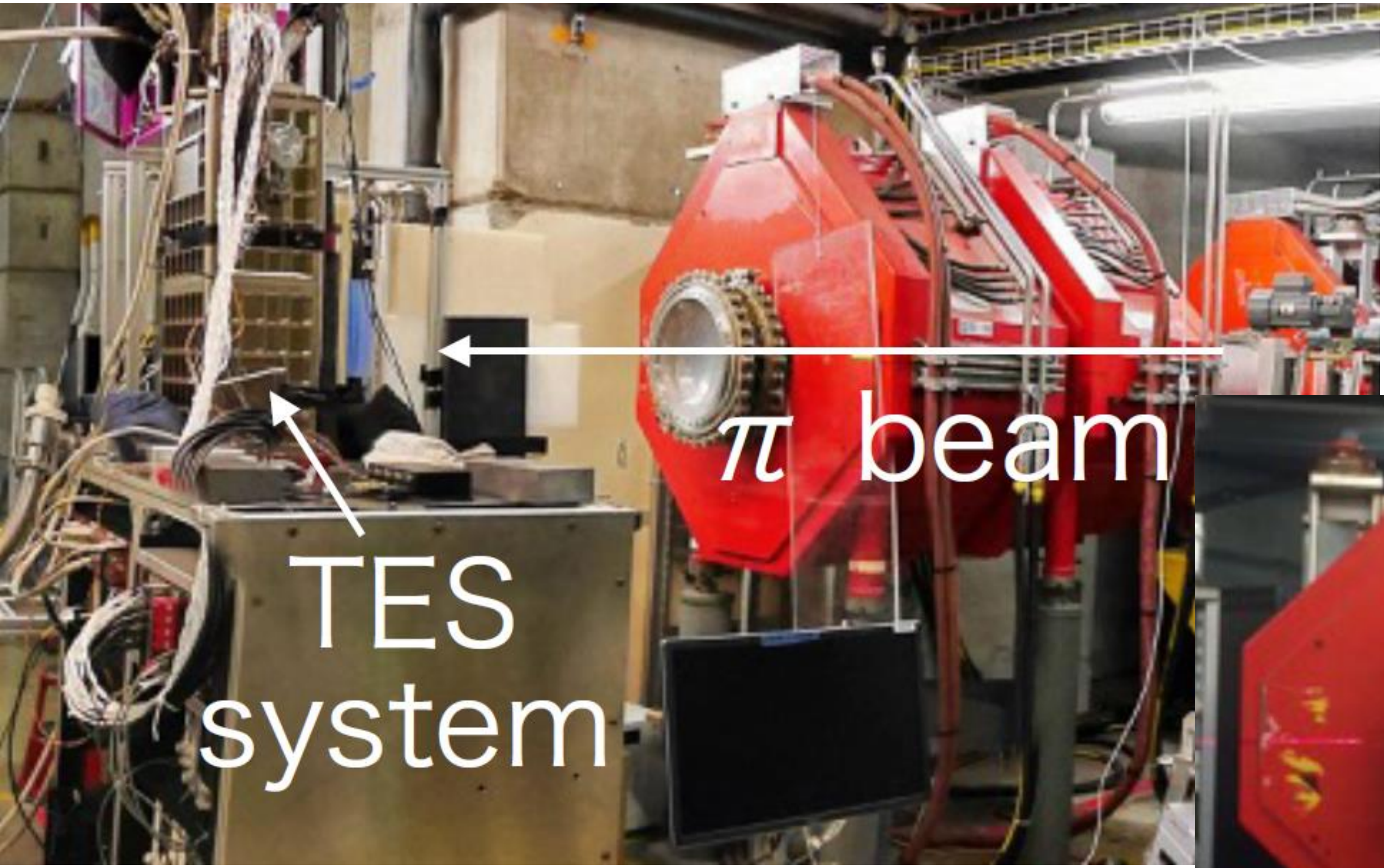

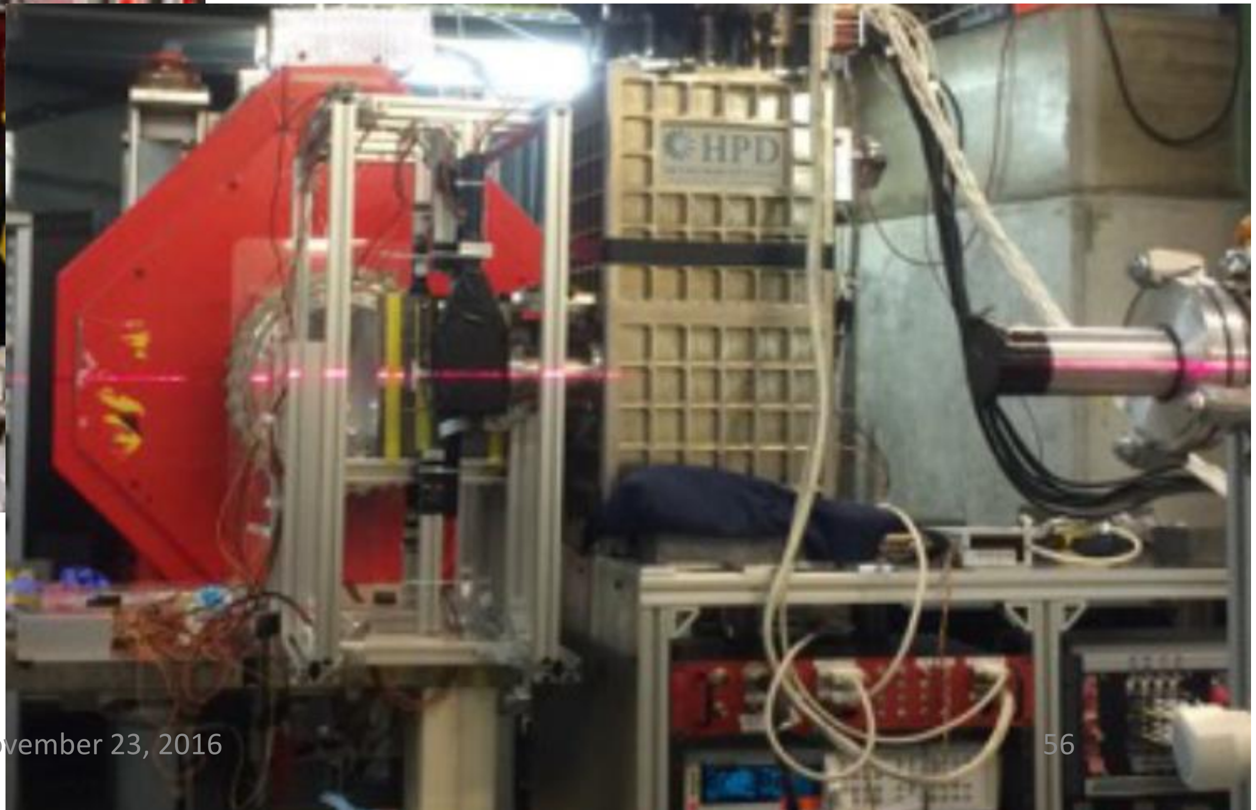

PSI: pionic carbon X-rays

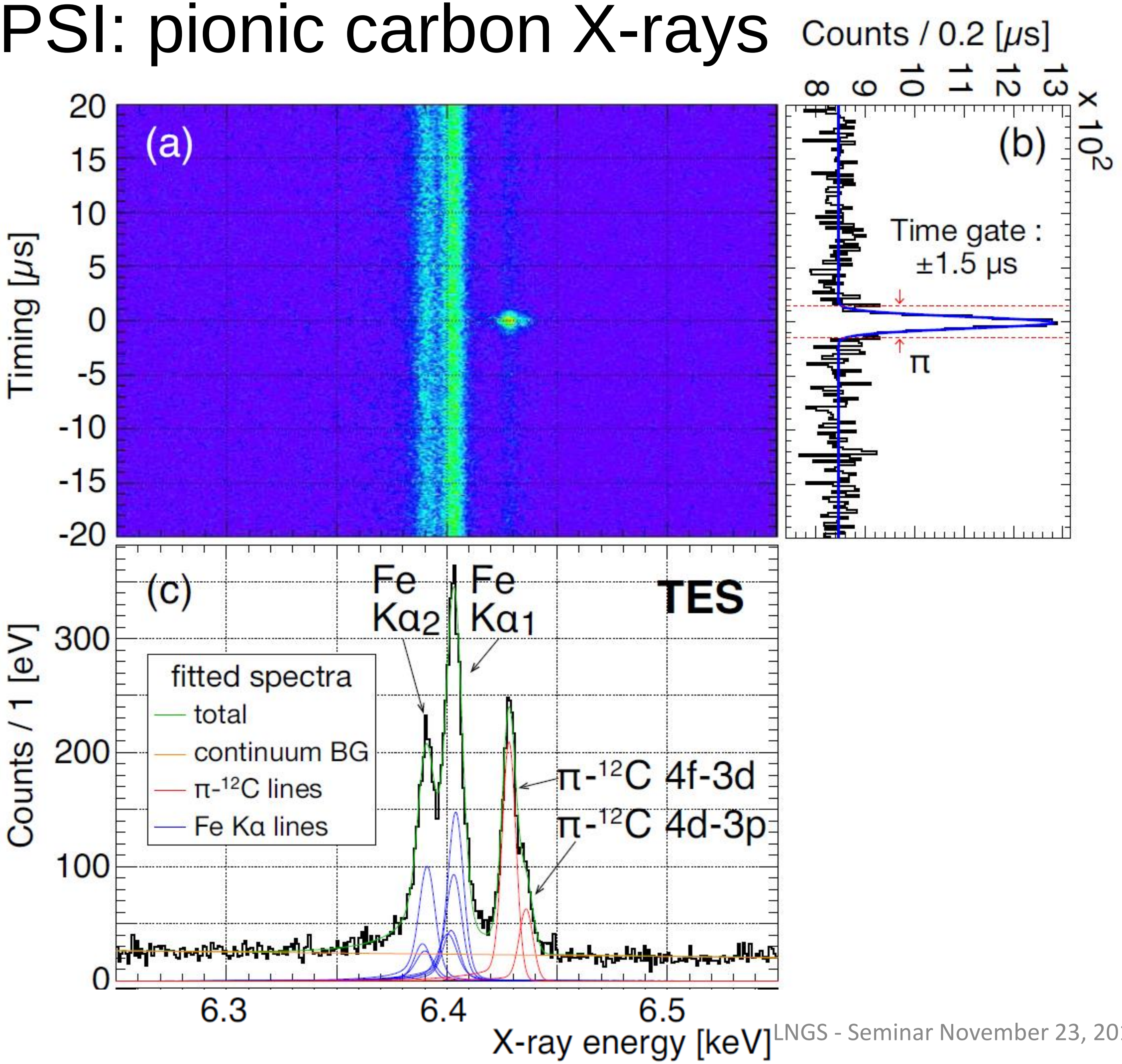

a) A correlation plot of the time difference between pion arrival and x-ray detection vs the x-ray energy measured by the TES array.

b) The projection on the time axis showing timing resolution of 1.2 μs (FWHM). A time gate of ± 1.5 μs is used in the analysis.

c) The projection on the energy axis by selecting stopped-π^- time gate.

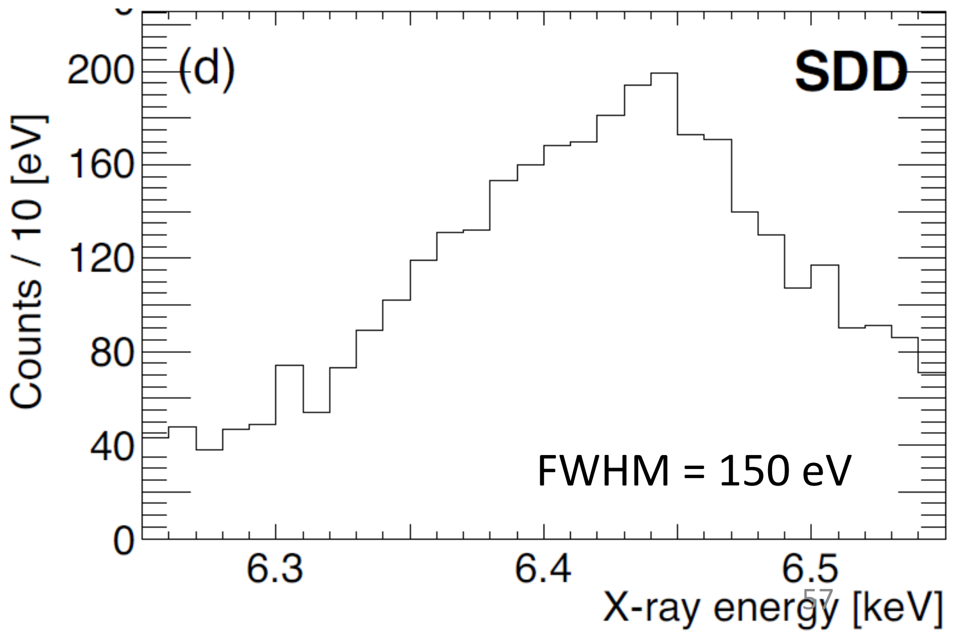

J-PARC – TES tested with kaons

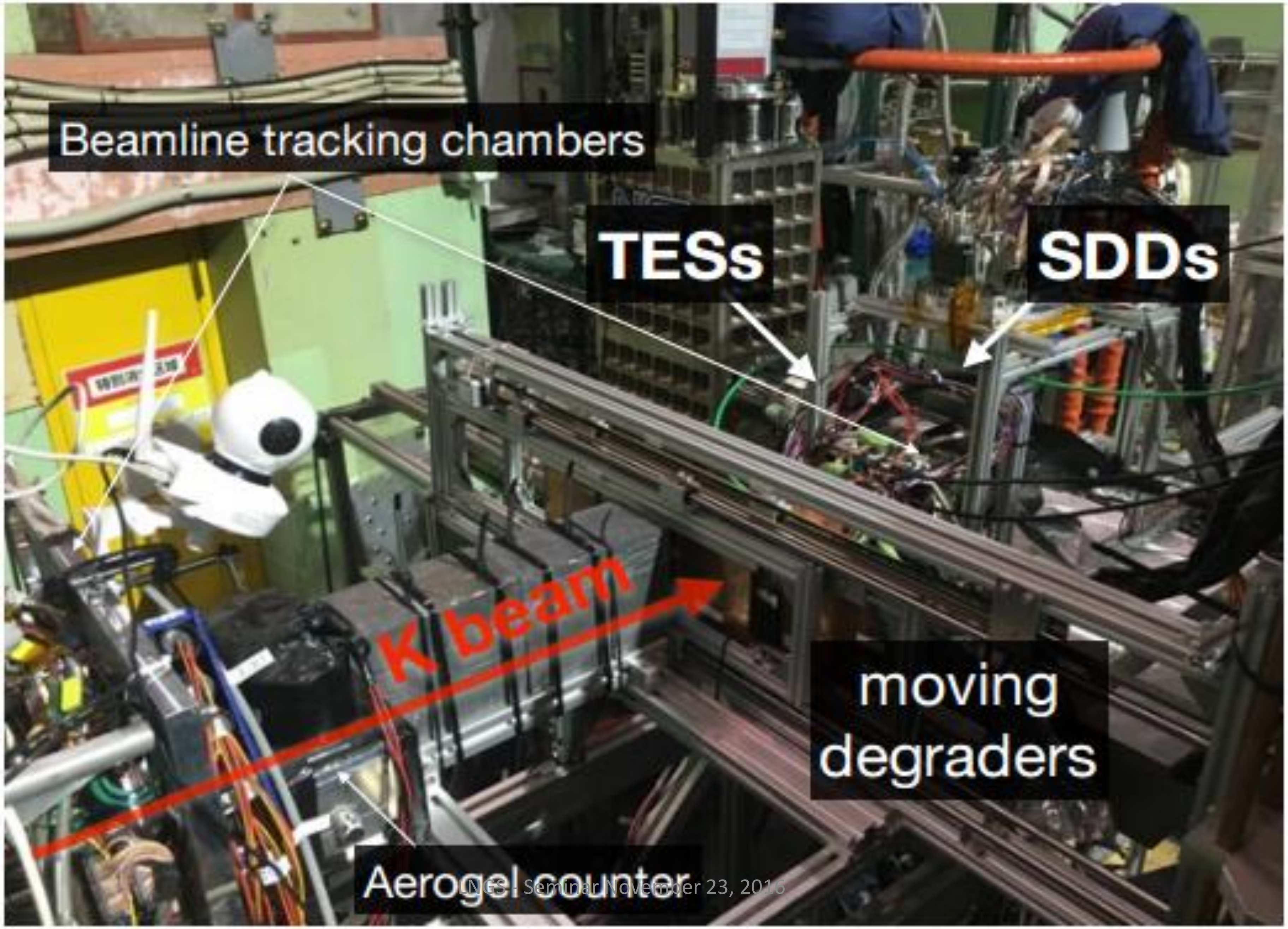

Calibration spectrum

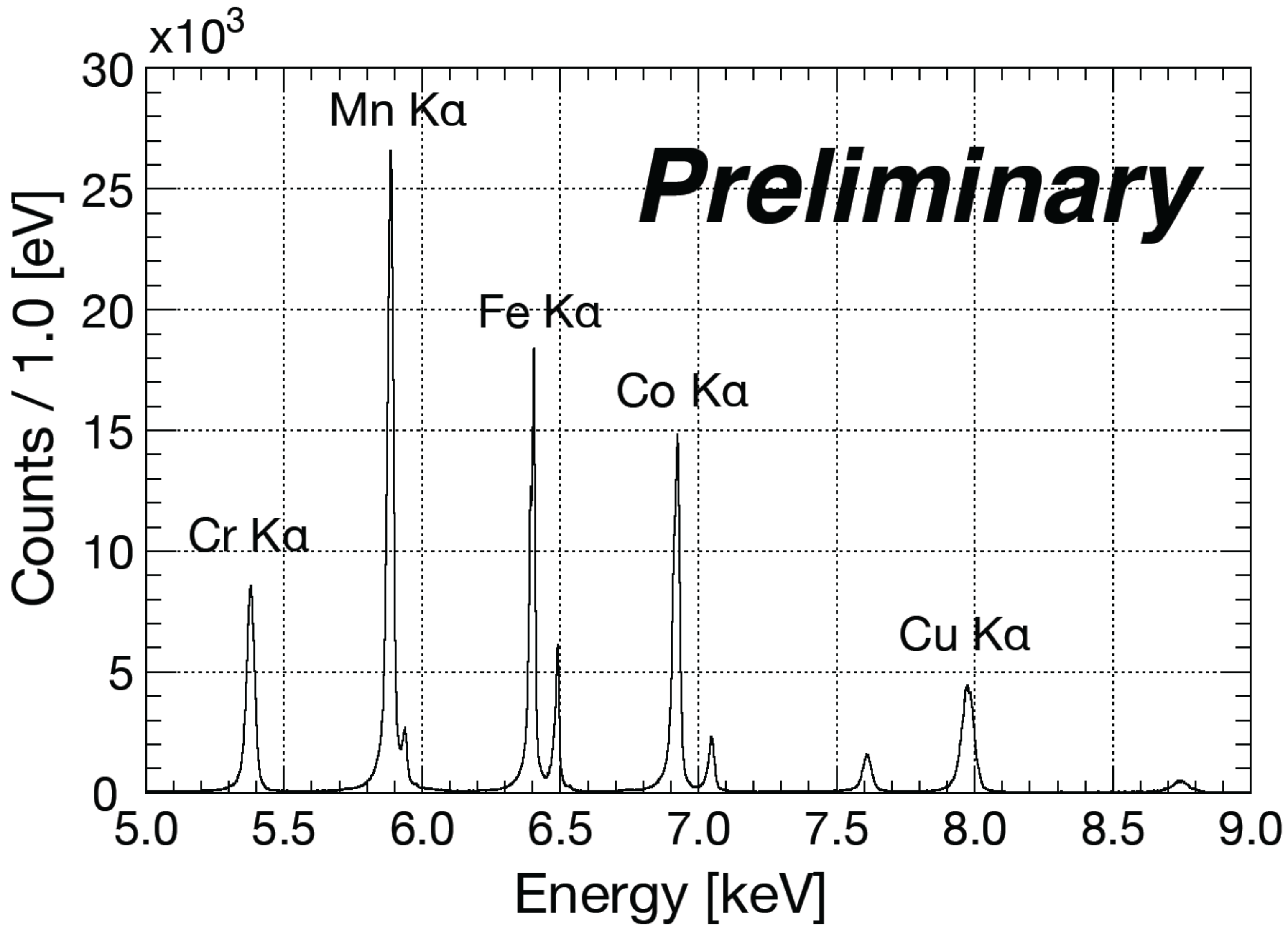

X-ray spectrum with in-beam condition with X-ray tube switched on

Beam intensity vs energy resolution

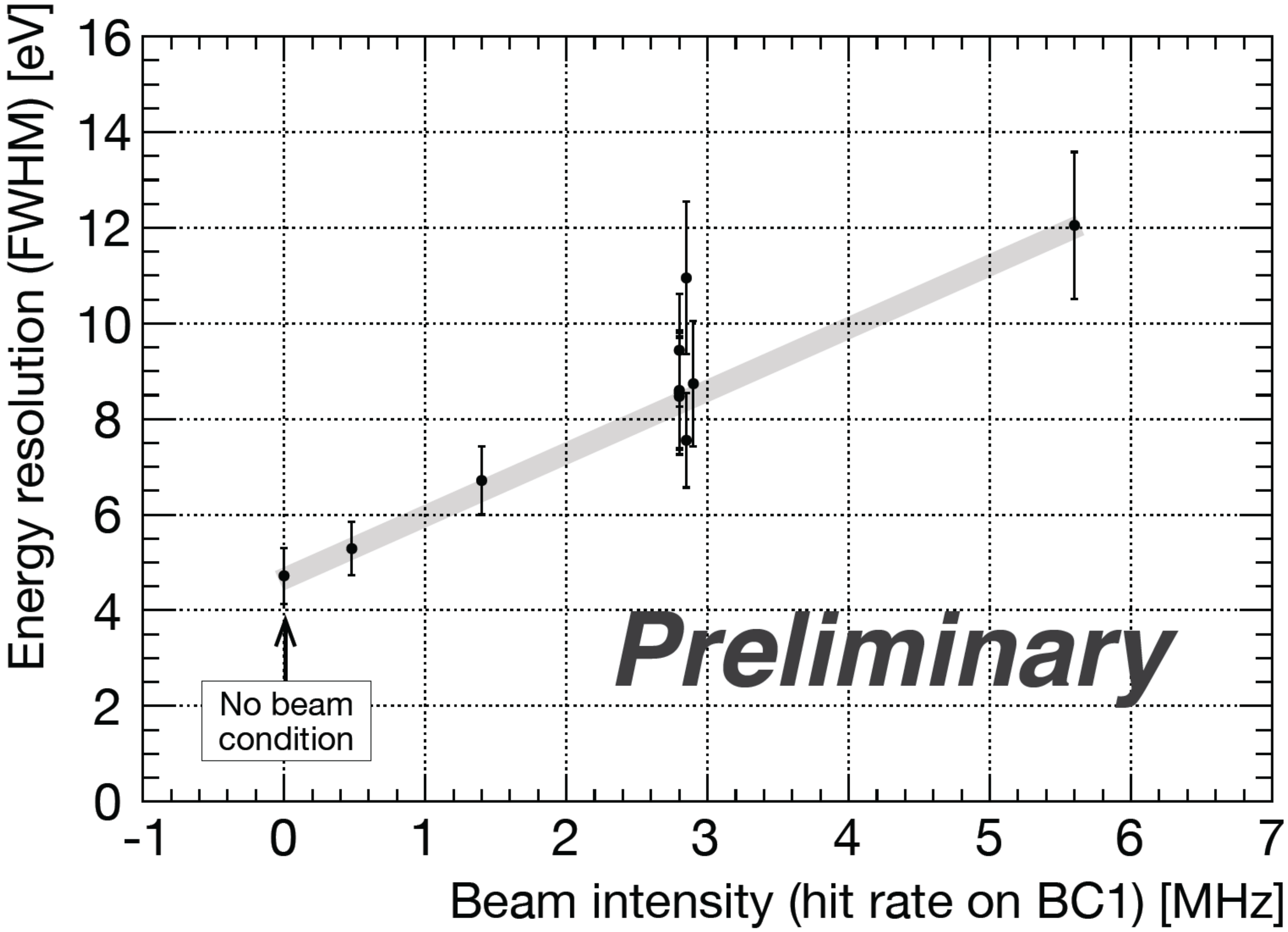

Kaonic helium results

	Shift [eV]	Reference
KEK E570	+2±2±2	PLB653(2007)387
SIDDHARTA (He4 with 55Fe)	+0±6±2	PLB681(2009)310
SIDDHARTA (He4)	+5±3±4	arXiv:1010.4631, PLB697(2011)199
SIDDHARTA (He3)	-2±2±4	

- **calibration under control within few eV**

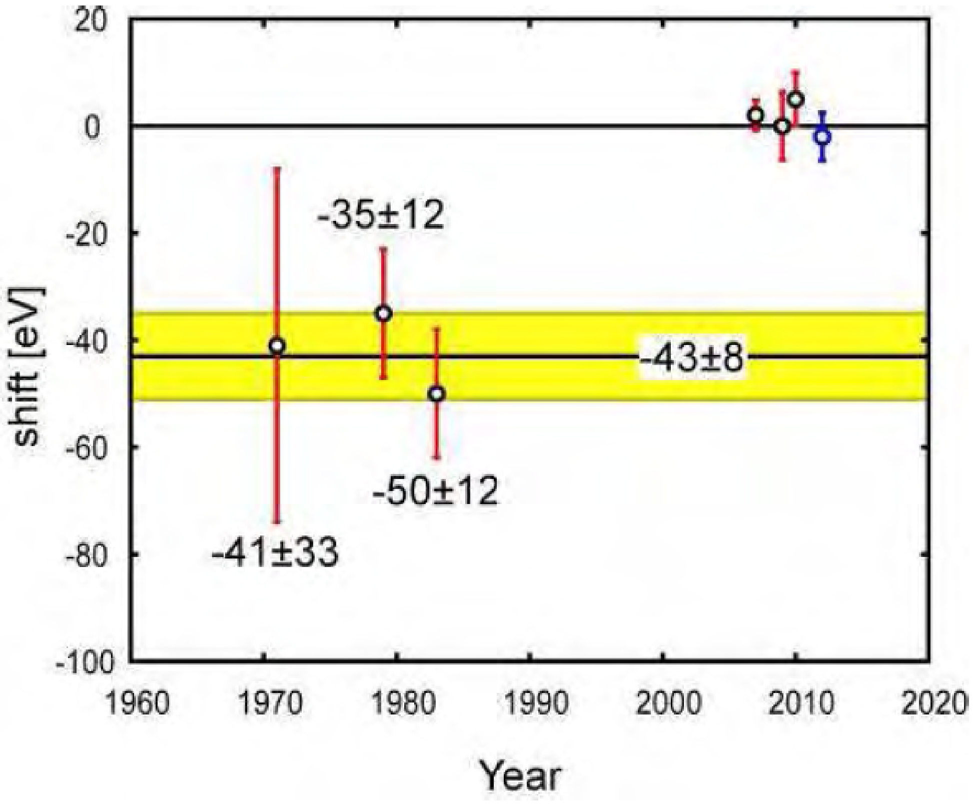

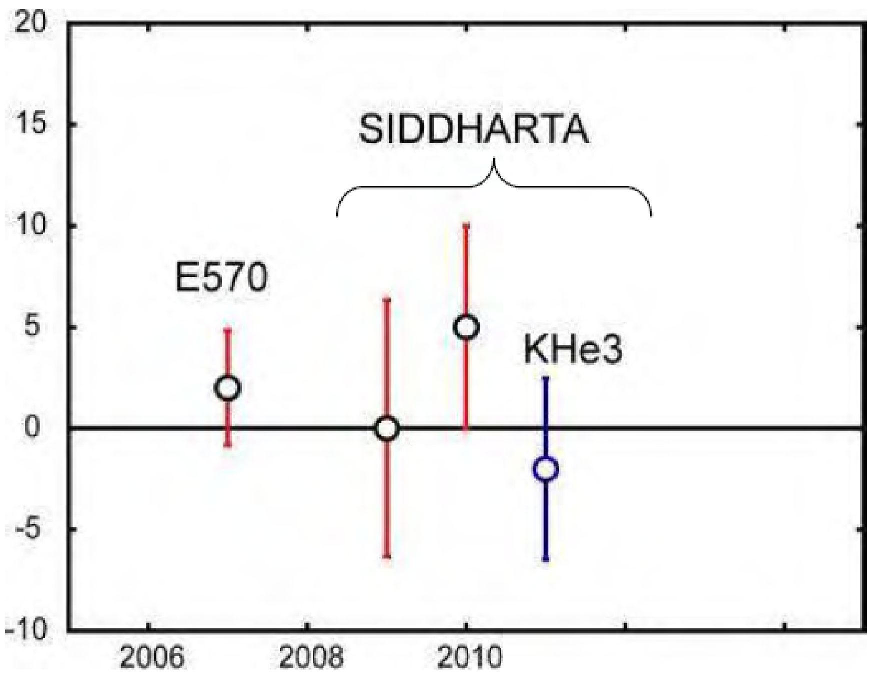

fundamental quantity

Charged Kaon mass measurement with TES

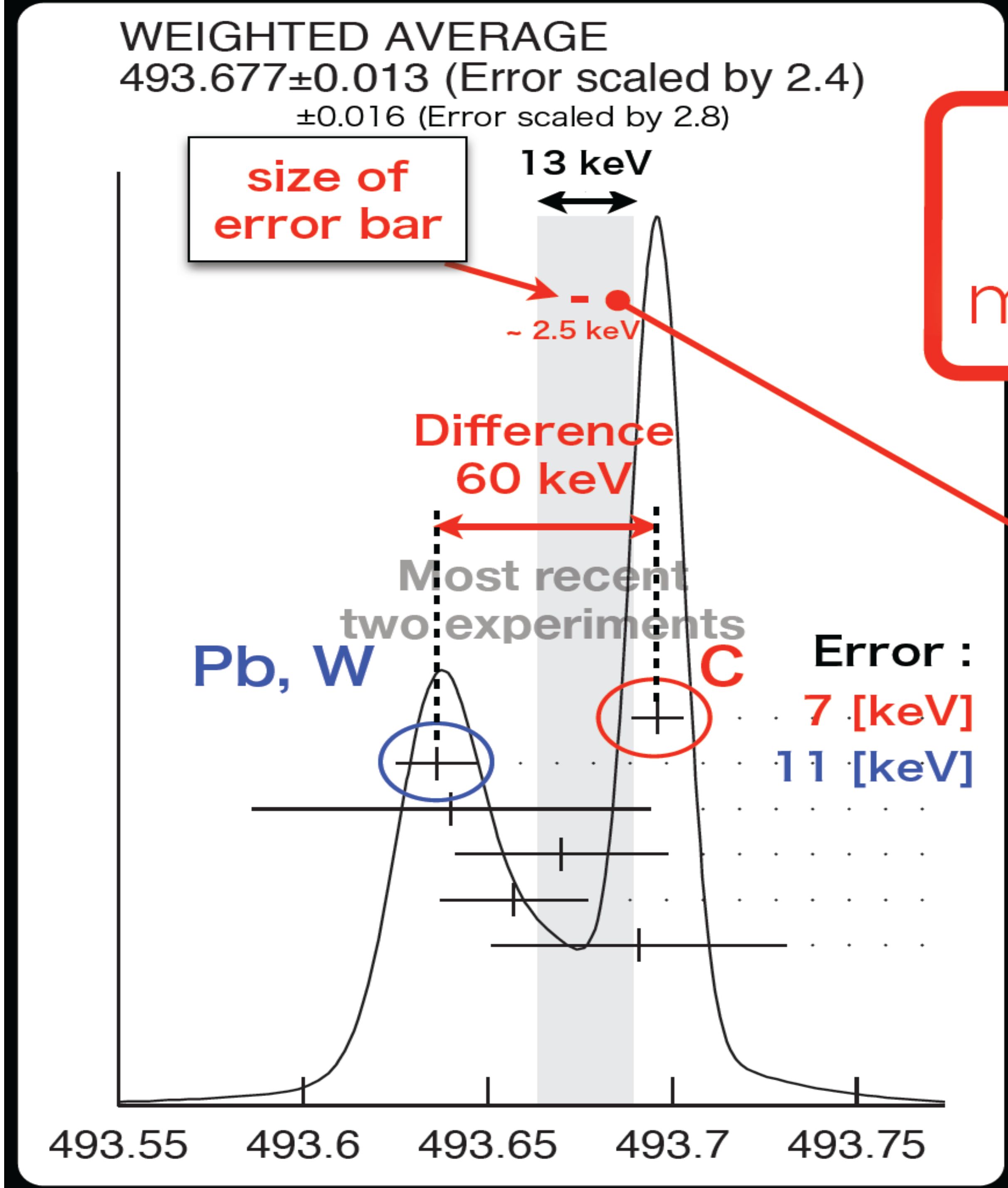

Rough estimation

- K-^{12}C 5→4 x-ray : 10.2 keV
- 2000 events & ΔE=5eV(FWHM)
  - ➡ ΔE (x-ray energy) ~ ± 0.05 eV
  - ➡ Δm (K-mass) ~ **± 2.5 keV**

Kaon mass is essential to determine the strong-interaction shift with 0.1-eV order of magnitude.

(Δm = 16 keV --> EM value for K-He Lα = 0.15eV)

(Δm = 2.5 keV --> EM value for K-He Lα = 0.03eV)

NIST's TES for gamma-rays
100 – 400 keV

e.g., hard-X-ray spectroscopy

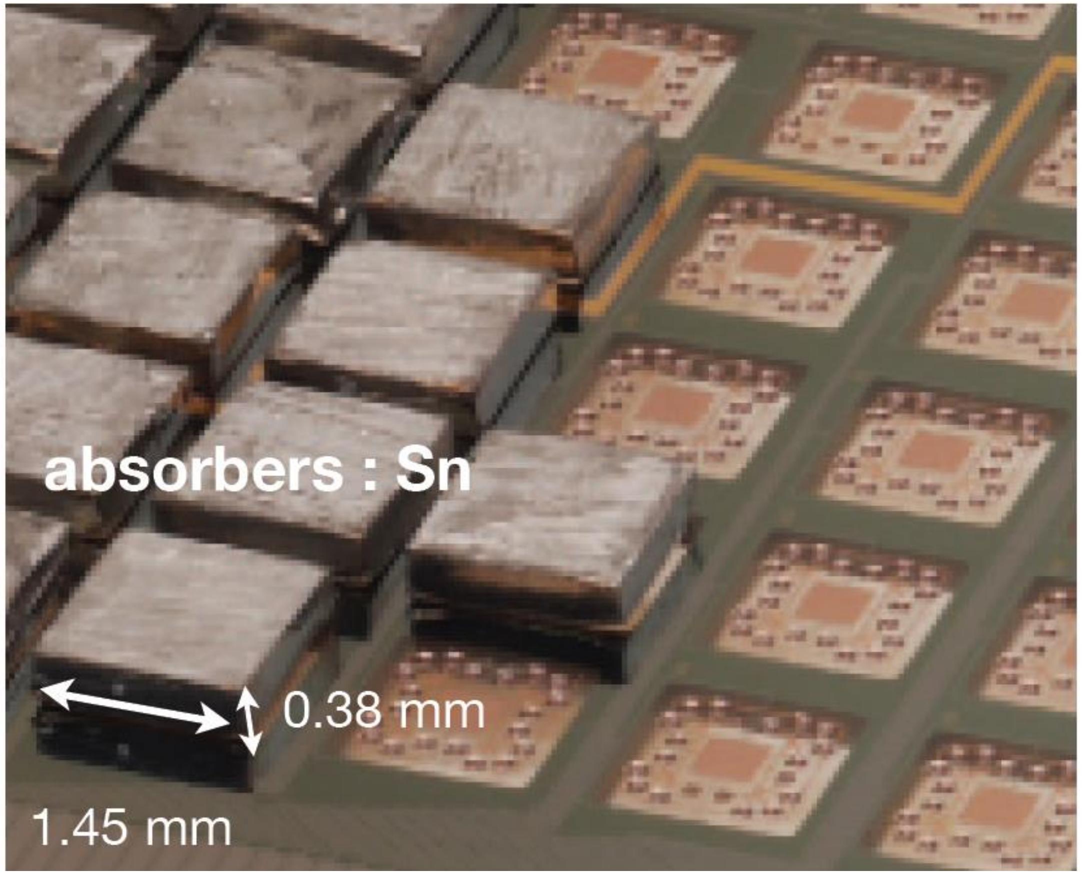

NIST's standard TES

- 1 pixel : 1.45 x 1.45 mm^2
- 256 array : total ~ **5 cm^2**
- **53 eV (FWHM)** @ 97 keV

an order improved resolution

State-of-art high-purity germanium detectors

Can TES's detect γ-rays ? Yes, with bulk absorbers

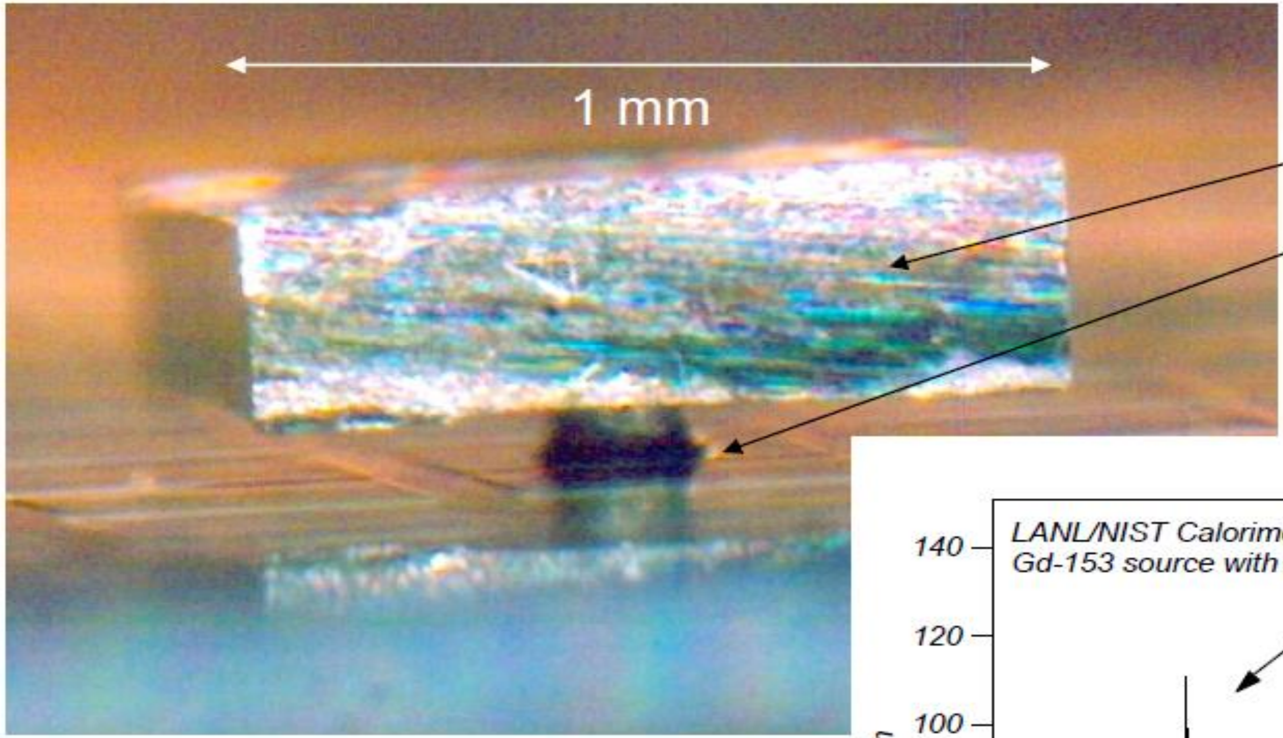

record NIST γ-ray results:
42 eV FWHM at 103 keV

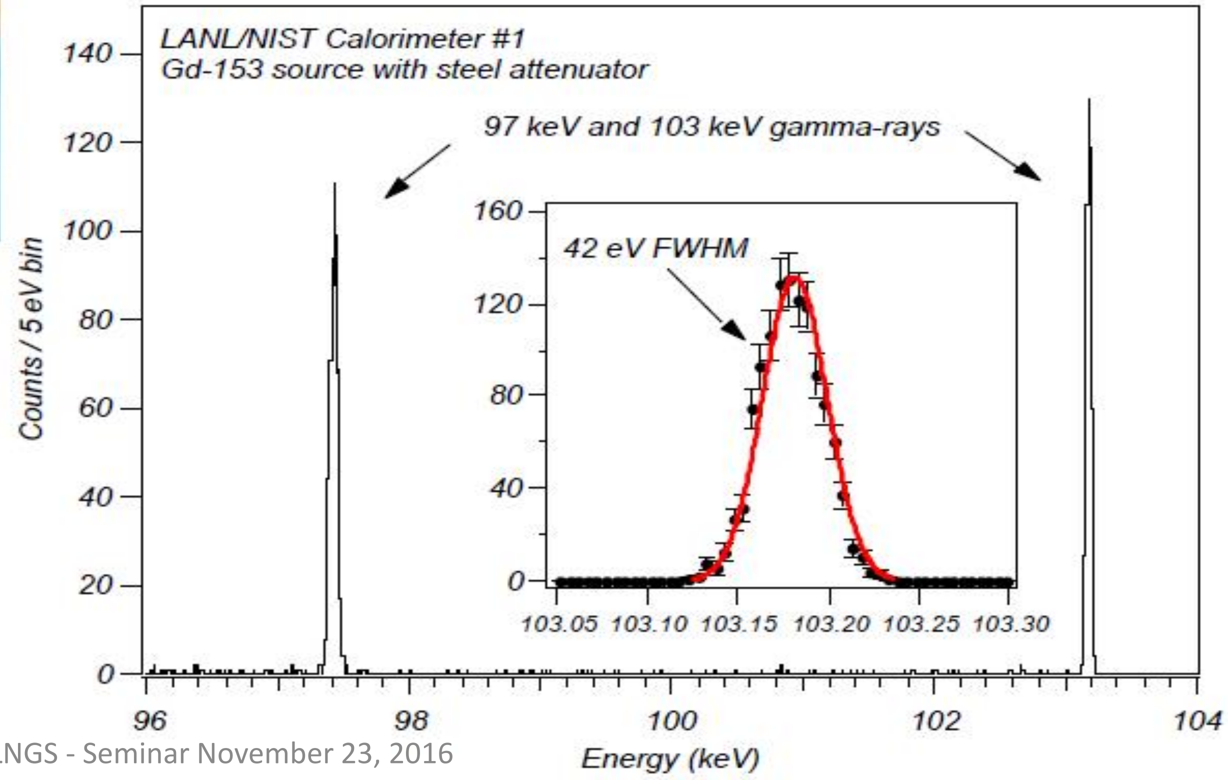

Thank you for your attention!

Future prospects: Kaonic He X-rays at J-PARC

before summer 2017 ??

Expected spectrum based on a background simulation

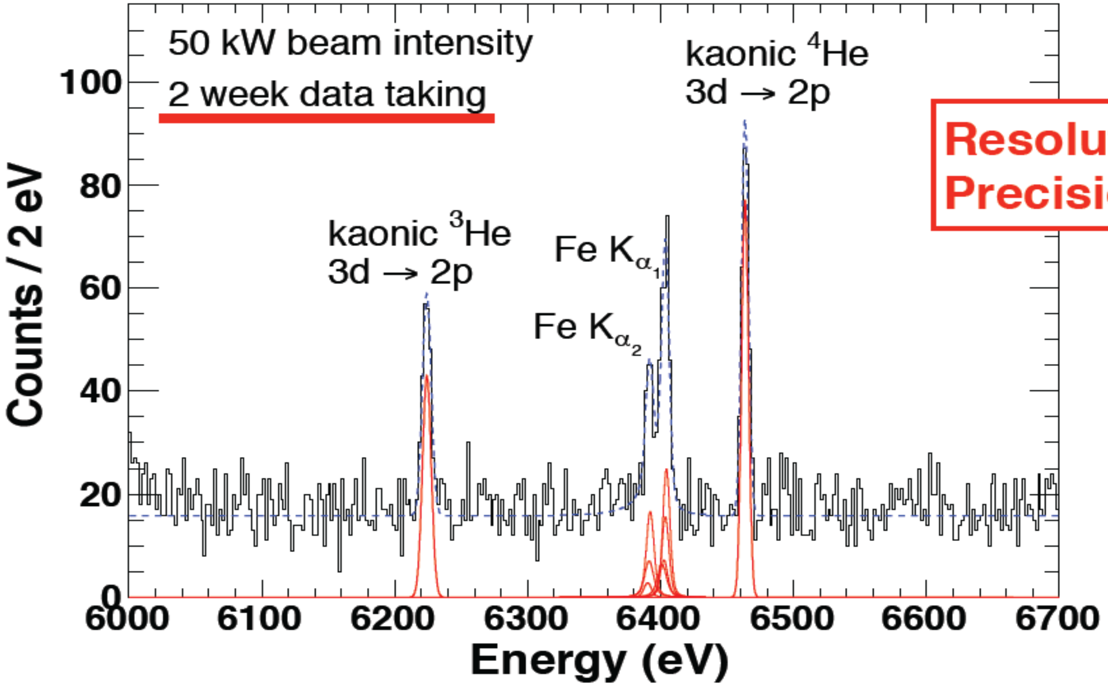

Resolution goal: 6 eV
Precision goal: 0.2 eV

In the actual experiment,
We will measure ^{3}He&^{4}He separately

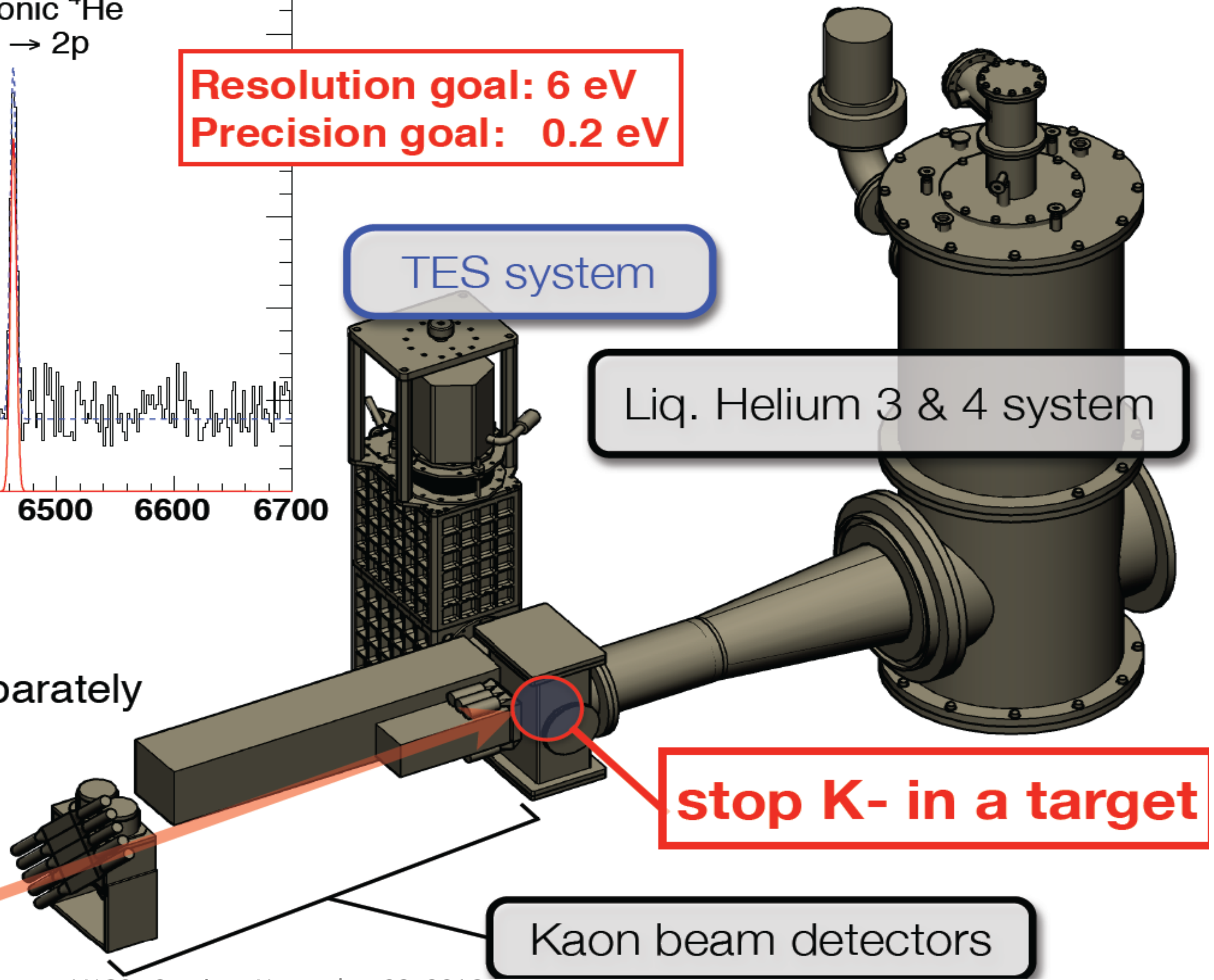

Simple 100 mK cryogenics

Gadolinium gallium garnet

Ferric ammonium alum

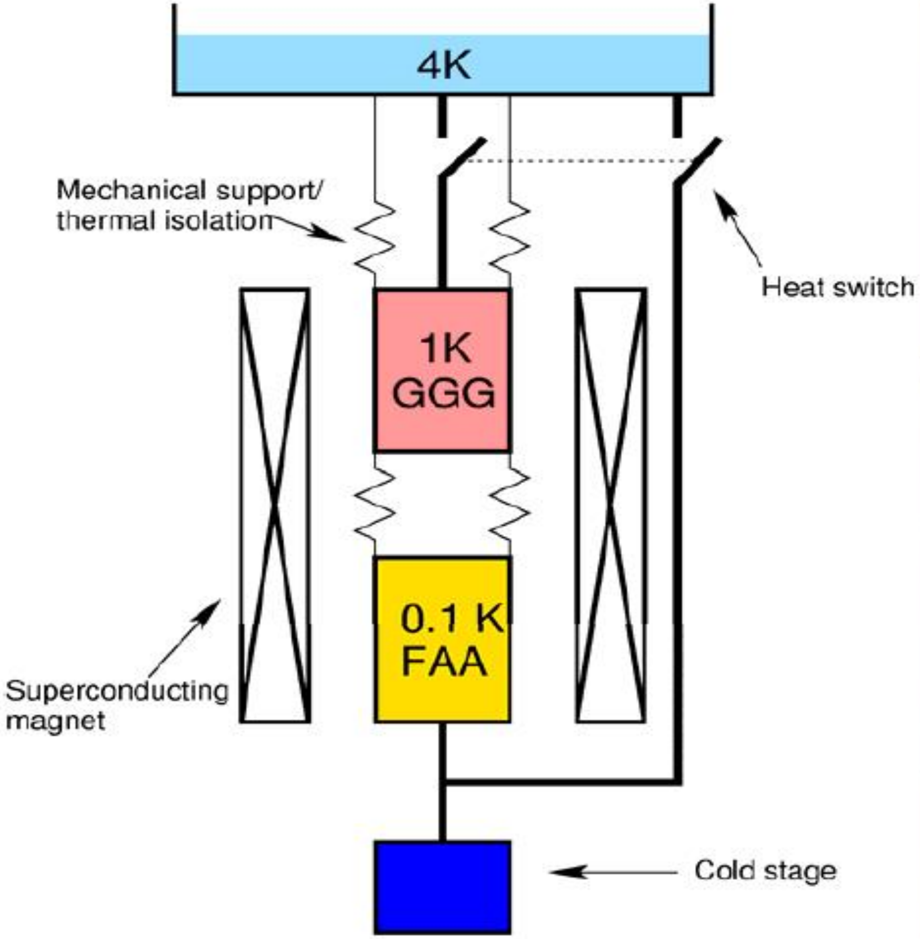

2-stage adiabatic demagnetization refrigerator (ADR)

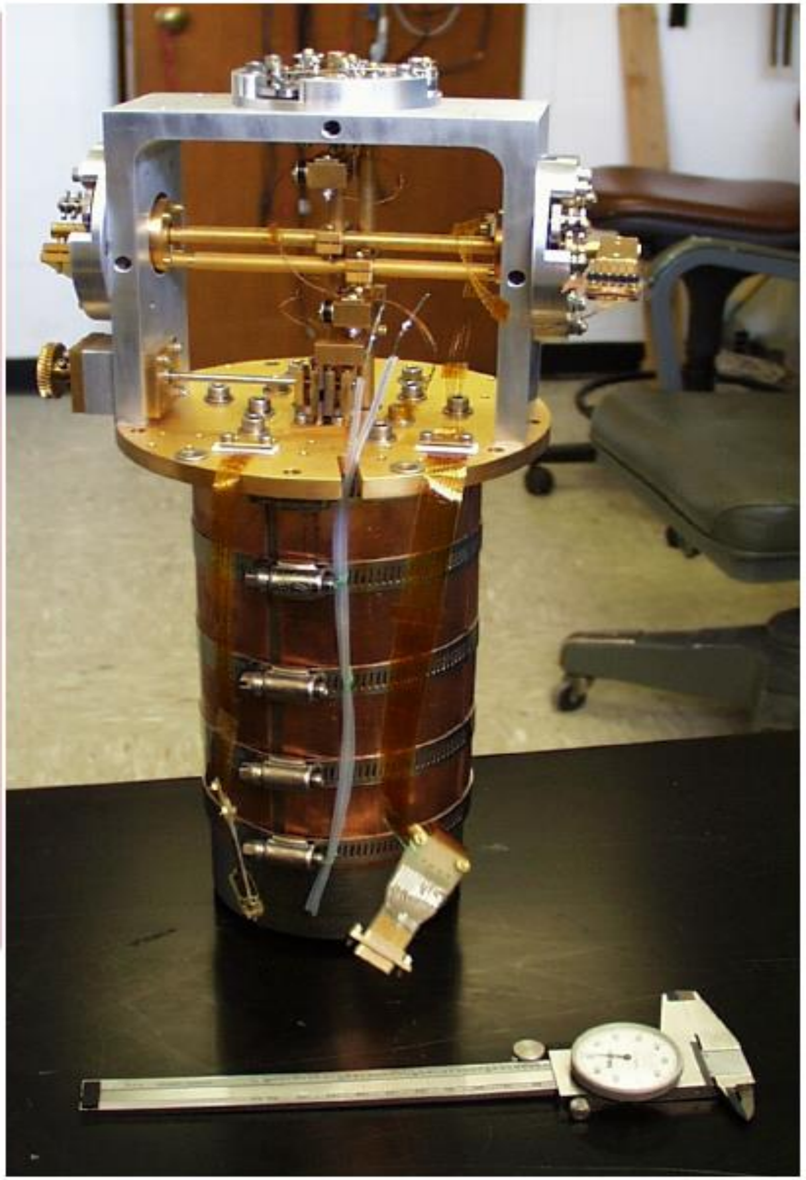

NIST 2-stage ADR -